INSIGHTS INTO THE MOLECULAR MECHANISM OF AXON OUTGROWTH BY MYELIN ASSOCIATED INHIBITORS

by

Heather M. Giebink

A dissertation submitted in partial fulfillment
of the requirements for the degree of
Doctor of Philosophy
(Biological Chemistry)
in The University of Michigan
2012

Doctoral Committee:

Associate Professor Anne B. Vojtek, Chair
Professor Christin Carter-Su
Professor Robert S. Fuller
Professor Daniel J. Goldman
Professor Benjamin L. Margolis

Acknowledgements

I would to take this opportunity to thank the multitude of people who have helped me achieve this milestone in my life. First and most importantly, I would like to thank my mentor, Anne Vojtek. There has been no one more important and influential than Anne in my development as a scientist. Her constant enthusiasm and dedication to my success has been a major motivation throughout my time in her lab. Anne allowed me to develop ideas and hypotheses on my own, to trouble shoot my failures, and was there to cheer me on as I figured them out. Not only did she provide quality scientific discussions, she was willing to listen and provide advice for non-scientific matters as well. I am forever grateful to Anne and thankful that I chose her laboratory to pursue my dissertation research.

I would also like to thank the various Vojtek laboratory members I have had the pleasure of interacting with over the years, especially Jennifer Taylor, Jonathan Zurawski, and Amanda Wilbur. I was under Jennifer Taylor's mentorship as a new member in the laboratory, and not only did she teach me valuable scientific techniques but she increased my crafting skills. Jennifer also constructed and tested many of the RNAi vectors in this dissertation. Jonathan Zurawski trained me in the delicate dissections and primary mouse work that encompasses a substantial piece of this dissertation. He also was always enthusiastic and created a work environment that was both productive and fun. Amanda Wilbur has provided valuable technical assistance and these last few years would not have been as entertaining or productive without her.

I would like to thank the members of my dissertation committee, namely Christin Carter-Su, Daniel Goldman, Robert Fuller, Benjamin Margolis and Matthew Young. The advice and guidance that I received from you from the very

beginning has proved indispensible. I would also like to thank my various collaborators whose contributions to this dissertation are cited at the end of the appropriate chapters. I would especially like to thank Lawrence Argetsinger for his technical advice and helpful discussions throughout my research. He could always provide a trick or an antibody that would work in pinch.

I would like to thank the Biological Chemistry department. The reason I chose Michigan was the familial environment and enthusiasm for science I felt at recruitment and I was not disappointed when I arrived here. I would also like to thank the departmental staff for their support, especially Beth Goodwin. I do not know what the department or students would do without Beth. I would especially like to thank the fantastic and brilliant women I have had a privilege to call my peers: Ashley Reinke, Corissa Lamphear, Katie Carr, Cherisse Loucks, Diane Calinski, and Lily Mancour.

I would not be the person that I am without the love and support of my husband, Chris. We met on the very first day of graduate school and I cannot imagine how this journey would have been without you. Our combination of an engineer and a biochemist has provided numerous laughs and discussions over the most interesting things. Thanks to you I now know that a Dalton is equal to the mass of a proton and you know that the gestational period for a mouse is 18-23 days. Last, but not least, I would like to thank my family. My parents and my brother who shaped me into the person I am and are always there for me. Since the very first chemical experiment I carried out in our washing machine with a load of dark clothes and bleach at the age of 10 to the last mouse experiment of my dissertation work, you have been there cheering me on and I am forever grateful.

Table of Contents

List of Figures

Abstract

Repair after injury to the adult mammalian central nervous system (CNS) is hindered by inhibitory proteins, including the myelin associated inhibitors (MAIs): NogoA, MAG, and OMgp. Blocking the function of MAIs and their receptors enhances axon regrowth following injury. These findings suggest that therapeutic control of these inhibitors may be a strategy for regulating axon outgrowth and plasticity, leading to restoration of neuronal connections lost in response to injury or disease. Thus, functional recovery after CNS injury is limited by MAIs, and small molecule compounds that can circumvent MAI inhibition are likely to enhance functional recovery after stroke or spinal cord injury.

The precise intracellular molecular signaling mechanisms of MAIs are not well understood. Toward this goal, it is demonstrated here that the multi-domain scaffold protein POSH assembles a distinct signaling module composed of the mixed-lineage kinase LZK, the actin-myosin regulatory protein Shroom3, and Rho-associated kinase, ROCK. Through the receptor PirB, the POSH complex mediates growth inhibitory signals from extracellular NogoA and MAG, as well as cell autonomous NogoA signaling. PirB associates with the protein tyrosine phosphatase, Shp2, and we show that phosphatase activity of Shp2 is required for axonal growth inhibition. In addition, NogoA stimulation promotes trapping of LZK with Shp2, suggesting LZK is a potential substrate for dephosphorylation by Shp2.

Lastly, interference with the function of any member of the POSH complex results in enhanced growth on MAIs, suggesting that chemicals that target protein-protein interactions within the POSH complex will reduce the inhibitory action of MAIs, facilitating axon outgrowth in the CNS. Towards this

goal, high-throughput screening in the Center for Chemical Genomics at the University of Michigan has identified potential inhibitors of the Shroom3-ROCK interaction. Collectively, these studies delineate an intracellular signaling pathway emanating from MAIs through the receptor PirB to the POSH complex. Further insight into the molecular signaling mechanisms of this pathway may provide novel therapeutic targets for axonal repair following CNS injury.

Chapter 1

Introduction

1.1 Development and wiring of the nervous system

The mammalian nervous system with its billions of nerve cells and unimaginably complex network of nerve fibers and connections is unlike any other organ in the body. During embryogenesis, the brain generates 50-100 thousand new cells per second derived from the neural tube [1]. Newborn neurons migrate to their designated destinations where they mature, projecting axons and dendrites to form neuronal connections. The correct formation of neuronal connections is crucial for higher order function of the nervous system; therefore nature has developed an extensive and complex system to mediate axonal growth and pathfinding.

The nervous system is patterned with molecular guidance cues which create a road map for developing axons, leading them to their synaptic targets (Figure 1.1). Guidance molecules can be located on the cell surface of neighboring neuronal or glial cells or secreted into the extracellular space acting as chemical signals [2]. These cues can be either repulsive or attractive and function as short-range or long-range signals. Moreover, some guidance cues are bifunctional, being attractive to some axons and repulsive to others [2, 3]. The semaphorins, which are a large family of both secreted and membrane-associated proteins, are an excellent example of bifunctional guidance cues. Members of the semaphorin family are capable of mediating both repulsive and attractive guidance events in the developing nervous system and it is believed their function is regulated by expression of distinct receptors on the cell surface [2-4].

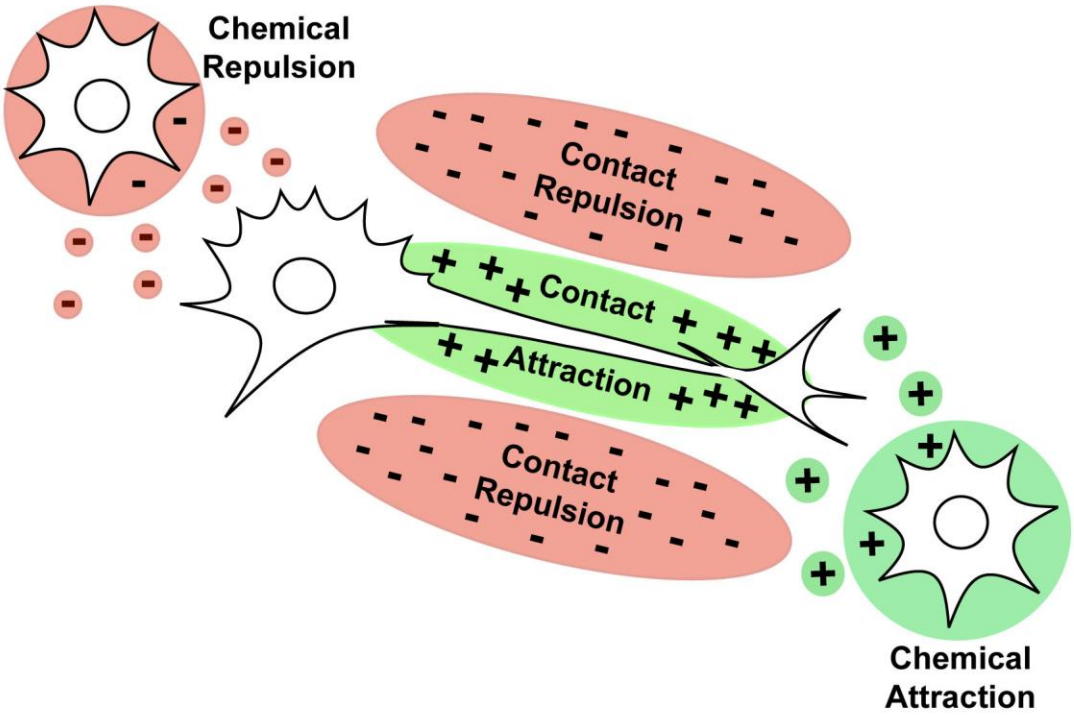

Figure 1.1 Guidance cues regulate axonal pathfinding

Neurons project their axons through the extracellular space to make their final neuronal connections. The tip of the axon contains the growth cone which responds to guidance cues. Guidance cues can be diffusible (chemical) that are released from other neuronal or glial cells, or associated with the extracelluar matrix or attached to neighboring cell membranes (contact). Guidance cues can be attractive or repulsive.

Guidance molecules influence axonal growth through modulating cytoskeleton dynamics, which is made up of actin, microtubule, or myosin molecules. Each axon extended by a differentiated neuron contains a growth cone at its leading edge. The growth cone detects molecular guidance cues and signaling events at the growth cone mediate the appropriate response. For example, inhibitory signals can cause the growth cone to collapse, facilitating axon retraction [2-4].

1.2 Plasticity of the nervous system

After the establishment and refinement of the nervous system during embryonic and early post-natal periods, the mammalian central nervous system undergoes stabilization, moving away from being highly fluidic towards a more structured environment to maintain neuronal connections [5]. Synaptic remodeling and dendritic pruning occurs to allow for learning and functional adaptation. However, long distance changes in axon length, greater than several millimeters or more, are rarely seen [6]. The umbrella term “neuronal plasticity” is used to define changes that culminate in rewiring or reorganization of neuronal networks. Examples of plastic changes include: synaptic remodeling and axonal sprouting leads to new neuronal connections [7].

Extensive research has gone into determining the intrinsic and extrinsic differences in gene expression, protein localization, and the extracellular environment responsible for the shift from rapid growth and re-arrangement to a more conservative structure and plasticity [5, 8, 9]. It is now known that intrinsic neuronal growth potential decreases as neurons mature and one hypothesis for this phenomenon is down-regulation of growth-promoting genes. Additionally, select guidance cues that influenced axonal pathfinding persist into adulthood, maintaining connections and directing secondary branching of axons and dendrites. There are also additional proteins that are expressed in the mature CNS which regulate neuronal plasticity [5, 8, 9]. Therefore, it may be more correct to refer to these molecules as “guidance cues” during development and

“regulatory cues” in adulthood. Regardless, the understanding of the function of regulatory cues throughout all stages of life provides a valuable tool and is particularly relevant for the development of therapeutic strategies to promote regeneration of damaged neuronal connections in the CNS after traumatic injury or disease.

1.3 Lack of regeneration of the central nervous system after injury or disease

Spontaneous and functionally relevant regeneration or replacement of lost neuronal tissue is limited and often absent following injury or disease of the CNS. In 1927, Ramon y Cajal was the first to observe that axons of the CNS fail to regenerate [10]. This is in stark contrast to the axons of the peripheral nervous system (PNS) whose axons regenerate after injury. Subsequently, Aguayo and colleagues demonstrated in a series of experiments that damaged CNS axons can regenerate if provided with a permissive substrate [11-13]. Sciatic nerve grafts were used as bridges between regions of the CNS, for example in a midthoracic spinal cord lesion and between the medulla oblongata and the upper thoracic spinal cord. They showed that transected axons from the adult rat CNS were able to grow into PNS tissue grafts to distances upwards of 1cm. Additionally, axon growth terminated at the edge of the graft where the CNS tissue resumed. These studies indicated that CNS neurons retain the intrinsic ability to regenerate when presented with the growth-permissive PNS environment. Conversely, PNS axons navigated around, not through CNS implants, suggesting the presence of inhibitory molecules in the CNS that both PNS and CNS neurons are responsive towards. This result was critical in establishing that CNS neurons retain the capability to grow and the lack of regeneration is due to the presence of inhibitory molecules and/or receptors/ligands, not present in the PNS. Working off this hypothesis, much effort began to identify CNS inhibitory molecules and characterize their mechanism of axon growth inhibition in the hope that manipulation of their activity will restore the permissive extrinsic growth environment of the developing CNS.

1.4 The role of myelin and its associated proteins on axon outgrowth

A prominent difference between the embryonic brain and the adult brain is the presence of myelin, which is visualized as the white matter of the brain. In humans, myelination begins in late fetal development and proceeds, although slower, into adulthood [14]. The brain myelinates in a wave like fashion from the back of the head to the frontal lobe, which is the last portion of the brain to myelinate [1, 15]. The onset of myelination coincides with a decrease in neuronal plasticity [16]. However, development of white matter structure in children correlates with enhanced motor skills, reading ability, and cognitive development, suggesting the stabilization of the brain by myelination is necessary for higher order function [16].

Myelin forms a layer called the myelin sheath around the axons of a subset of neurons (Figure 1.2A). The sheath is a greatly extended and modified plasma membrane. Myelin membranes originate from oligodendrocytes in the CNS and the Schwann cells in the PNS [17]. The main purpose of the myelin sheath is to enhance the transmission of electrical impulses along the axon. The presence of myelin increases the speed at which the signal travels as well as insulates the axon preventing the loss of the electrical current [1, 15]. In the PNS, when an axon is severed the myelin sheath can function as a track along which regrowth can occur [18]. However, CNS myelin does not support regeneration. Martin E Schwab first demonstrated this by culturing neurons on dissociated CNS glial cells. Neurons were unable to extend axons on cultured oligodendrocytes or isolated myelin from the CNS, but were able to grow on myelin from the sciatic nerve of the PNS [19]. This and work by other groups indicated that one of the differences between the regenerative capacity of the PNS, versus the CNS, was due to extrinsic molecules present in myelin originating from oligodendrocytes. Consistent with this hypothesis, three molecules isolated from CNS myelin have been shown to highly inhibit axonal

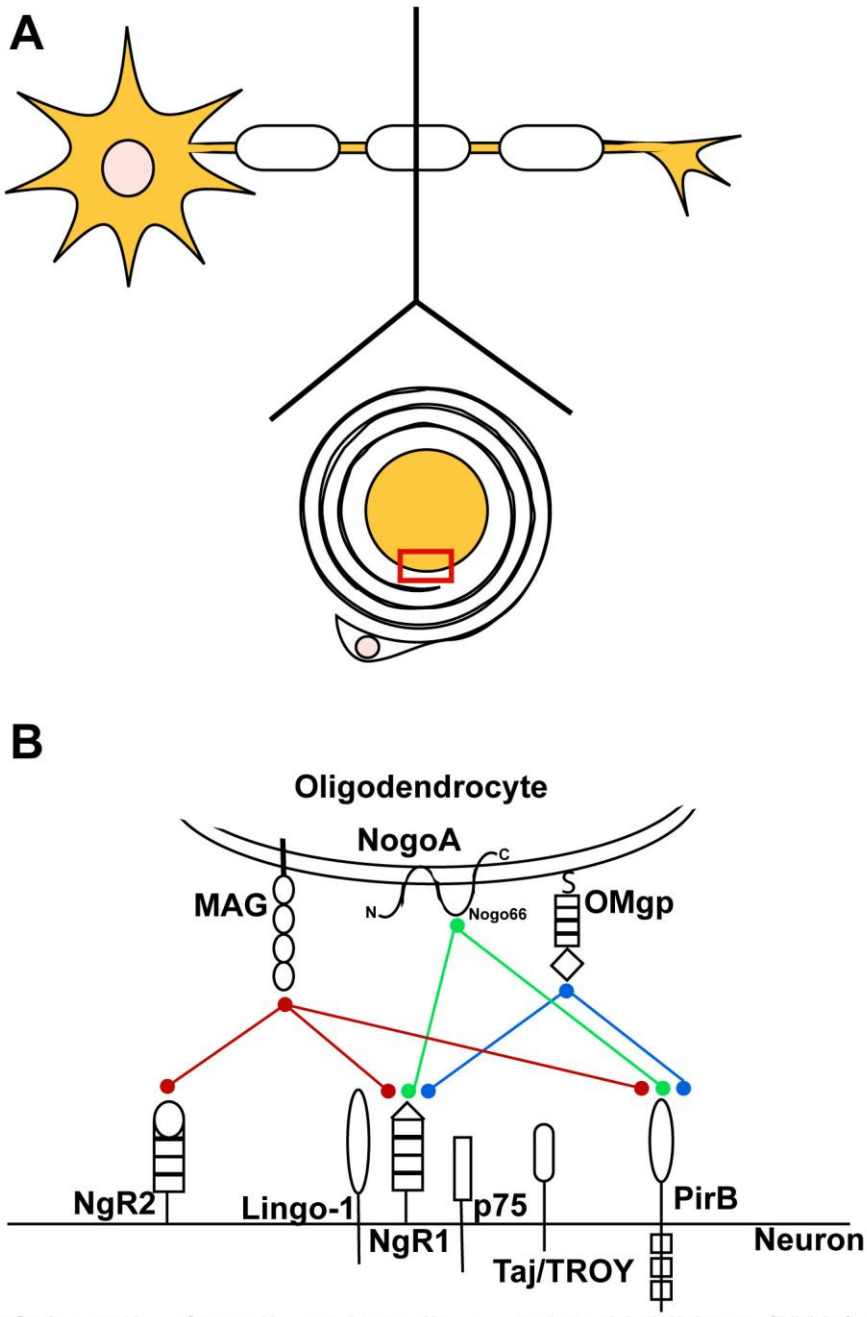

Figure 1.2 Schematic of myelin and myelin associated inhibitors (MAIs) present at the myelin-axon interface

(A) Oligodendrocytes form the myelin sheath around the axons of specific neurons. The sheath is a greatly extended and modified plasma membrane. A cross section reveals where myelin (white) makes contact with the axon (orange). The red box highlights the myelin-axon interface shown in detail in (B).
(B) A closer view of myelin-axon interface (red box in A). MAIs on the oligodendrocyte surface make contact with receptors on the axon. NogoA, MAG, and OMgp bind to NgR1 and PirB, while only MAG associates with NgR2. NgR1 interacts with co-receptors to mediate intracellular signaling (Lingo-1, p75, Taj/TROY).

growth in vitro: NogoA, myelin associated glycoprotein (MAG), and oligodendrocyte myelin glycoprotein (OMgp) (Figure 1.2B).

1.4.1 NogoA

The inhibitory activity of NogoA was discovered by Martin E Schwab and colleagues over 20 years ago. First, extraction of myelin with 4M guanidinium chloride provided conditions that removed peripheral membrane proteins, and resulted in myelin that maintained a non-permissive growth environment for neurons in vitro. Second, lipid extraction resulted in a growth-permissive lipid fraction and a non-permissive protein fraction that had to be maintained in liposomes to function. Finally, trypsin treatment of CNS myelin removed axonal growth inhibition [20]. Collectively, these studies show that a membrane-bound protein is facilitating the non-permissive growth of myelin. Separation of myelin proteins by SDS-PAGE identified two proteins of 35 and 250kDa, termed NI-35/250, that maintained a non-permissive substrate [20]. Removal of NI-35/250 from CNS myelin resulted in a growth permissive substrate, while addition of NI-35/250 to PNS membrane fractions caused a shift from permissive to non-permissive. Antibodies developed against NI-250 allowed for the isolation of a cDNA encoding a protein that was growth inhibitory and was designated NogoA [21-24].

NogoA is a member of the Reticulon family, also known as Reticulon 4-A [23]. Reticulons are membrane bound proteins and are named due to their high expression on smooth endoplasmic reticulum [25]. In mammals there are four genes, *rtn 1-4*, encoding multiple splice variants of the reticulon proteins [26]. The reticulon proteins contain a conserved structural motif, called the reticulon homology domain (RHD), which contains a hydrophilic loop of 60-70 amino acids flanked by two putative transmembrane domains [27]. The three splice variants of the reticulon 4 gene, NogoA, NogoB, and NogoC, contain 188 amino acids in their C-terminus which correspond to the RHD. NogoA and NogoB share the first 172 amino acids; however NogoA contains a unique 800 amino acids stretch in

between the N-terminus and the RHD. NogoC is made up of an extremely short N-terminus followed directly by the RHD [26, 27]. NogoA contains an endoplasmic reticulum retention motif, resulting in high ER expression and recent evidence suggests that NogoA may regulate the tubular morphology of the ER [28].

Three axonal growth inhibitory domains of NogoA have been identified. First, the loop between the two transmembrane domains, termed Nogo66, has been shown to be present on the extracellular surface of oligodendrocytes and has potent axon growth inhibitory effects in vitro [23, 29]. Nogo-66 binds to multiple receptors, including Nogo-66 receptor (NgR) and PirB (discussed in detail below) [30, 31]. The amino-terminal domain of NogoA contains a unique sequence called amino-Nogo that also inhibits axon outgrowth and the adhesion of non-neuronal cells; however the receptor mediating these actions has yet to be discovered [20, 29]. Amino-Nogo has been shown to bind and inhibit some integrin signaling, suggesting Amino-Nogo may inhibit axon growth through blocking growth-promoting integrin signaling [32]. A third, NogoA specific region, NiG-Δ20, also strongly inhibits neurite outgrowth [29].

Attempts to determine the membrane topology of NogoA have proven difficult. Computer modeling predicts two transmembrane domains in the RHD, which are long enough (28-36 amino acids) to loop back through the membrane. Immunofluorescence studies have shown the most common topology in the ER places the N- and C-terminals in the cytoplasm. However, studies with antibodies against the N-terminus of NogoA and Nogo66 show that both regions are localized on the cell surface of oligodendrocytes [23, 33]. These studies indicate that the first transmembrane domain may adopt a flexible mechanism to either extend across the membrane or to flip back to adopt a horseshoe-like orientation. Additionally, NogoA, expressed intracellularly on the endoplasmic reticulum, may only be exposed when there is injury or death of the oligodendrocyte.

NogoA is highly expressed on oligodendrocytes and only minimally on PNS Schwann cells consistent with a role in mediating axonal growth inhibition specifically in the CNS [34, 35]. On the oligodendrocyte surface, NogoA is

expressed on the innermost loop of myelin, where it could make contact with the axon (Figure 1.2). Interestingly, NogoA is also expressed in the neuron, albeit at lower levels. NogoA was found in the growth cone of growing olfactory bulb axons and in the projection neurons of the cortex and cerebellum [34-37]. In the developing forebrain cortex, NogoA expressing neurons migrate along NogoA positive radial glia and cells that will become part of the cortical plate pass between these NogoA expressing neurons. Interestingly, in NogoA knock-out mice, this migration is enhanced, while migration of cortical interneurons was delayed in NogoA deficient mice [38]. Additionally, removal of NogoA function in embryonic cortical neurons results in enhanced axonal branching in culture, while dorsal root ganglion neurons show increased fasciculation and decreased branching[39, 40]. Lastly, NogoA expressing radial glia in the ventral midline inhibit growing optic nerve axons and spinal cord commissural axons and blocking NogoA function leads to misprojected axons [41, 42]. Combined these studies suggest that NogoA can exert multiple guidance effects in the developing CNS in addition to its role as a myelin-associated inhibitory protein.

1.4.2 Myelin-associated glycoprotein

Myelin-associated glycoprotein (MAG) was identified through purification and separation of molecules present in myelin. It is a potent inhibitor of neurite outgrowth and immunodepletion of MAG from CNS myelin allows for permissive growth [43, 44]. MAG is expressed by both CNS and PNS glial cells and has been shown to participate in the formation and maintenance of the myelin sheath [45]. It is highly expressed in myelin membranes adjacent to the axon. Interestingly, MAG is a bifunctional molecule and can regulate neurite outgrowth in an age-dependent manner. MAG promotes the growth of specific types of young neurons, while in the mature CNS MAG strongly inhibits neurite outgrowth [9, 46]. The molecular mechanism of the switch is unknown; however it appears to be dependent on the neuronal cell type and developmental stage. For example, late embryonic rat cortical neurons show a growth inhibitory response

toward MAG, while post-natal day 1 dorsal root ganglion neurons are able to extend processes on MAG [44, 47-49].

MAG is a member of the immunoglobulin (Ig) super family and its extracellular domain contains five Ig domains [9]. It is also a sialic acid-binding protein with its first four Ig domains being homologous to those of other sialic acid-binding lectins. Following the Ig domains, MAG has a single transmembrane domain and a cytoplasmic domain. In rodents, MAG exists in two splice forms, L-MAG and S-MAG, corresponding to variable cytoplasmic domain length [50]. To exert axon-inhibitory activity, MAG, like Nogo-66, interacts with the Nogo-66 receptor and PirB [30, 51, 52]. It also interacts with Nogo receptor 2 (NgR2) [53, 54]. The sialic acid binding activity of MAG is not required for neurite growth inhibition; however it has been observed that under certain conditions sialic acid binding can potentiate inhibitory signals[55].

1.4.3 Oligodendrocyte myelin glycoprotein

A third myelin-associated protein, Oligodendrocyte myelin glycoprotein (OMgp), is a glycosylphosphatidylinositol (GPI)-linked protein that is expressed on oligodendrocytes, peripheral neurons, and in high levels on various CNS neurons [56, 57]. OMgp is a 110-kDa glycoprotein with five tandem leucine-rich repeats followed by a C-terminus with serine/threonine repeats. Similar to NogoA and MAG, OMgp expression induces growth cone collapse and inhibits neurite outgrowth[56]. The Nogo66 receptor and PirB both have been shown to bind OMgp to initiate signal transduction to inhibit axonal outgrowth [30, 58].

1.4.4 Additional inhibitory proteins in the CNS

In addition to MAIs, there are other proteins present in the CNS that mediate growth-inhibitory effects. Chrondroitin sulphate proteoglycans (CSPGs) are released by astrocytes at sites of CNS injury or disease along with other inhibitory extracellular matrix proteins[59]. CSPGs are potent inhibitors of axon

growth both in vitro and in vivo, and similar to MAG they have also been shown to promote growth in the correct cellular context. Canonical axon guidance molecules such as the semaphorin, netrin, and ephrin families are expressed through development and in the adult CNS. There is evidence that these proteins contribute to the inhibitory environment and upon injury the expression levels of these proteins often change [60-63]. For example, EphrinB3 is highly expressed in CNS myelin and is a potent inhibitor of neurite outgrowth in vitro, while Semaphorin 3A causes growth cone collapse. Through the identification of more and more inhibitory cues, it appears likely that robust regeneration of axon growth will require strategies that neutralize multiple inhibitory cues simultaneously, or a common downstream component.

1.5 Receptors mediating myelin-associated growth inhibition

There are several known receptors for MAIs and some receptors are able to associate with multiple MAIs. Additionally, several MAI receptors do not have intracellular domains, but rather require a co-receptor to relay signaling and depending on the neuronal cell type, the co-receptor can vary. A select group of receptors are described in greater detail below (Figure 1.2B).

1.5.1 Nogo-66 receptor 1

Nogo-66 receptor 1 (NgR1) was the first Nogo-66 receptor to be identified[31]. It is a GPI-linked leucine rich repeat protein that is expressed on the surface of neurons. Direct interaction of Nogo66 with NgR1 induces growth cone collapse, and transfection of Nogo66 unresponsive neurons with NgR1 converts them to responsive [31]. NgR1 does not bind Amino-Nogo and blocking NgR function does not alleviate growth cone collapse induced with Amino-Nogo, suggesting the presence of an additional receptor for Amino-Nogo that has yet to be identified. There are multiple NgR family members in addition to NgR1, NgR2 and NgR3. The NgR family shares 55% identity in the leucine-rich repeat region;

however only NgR1 binds Nogo66. Interestingly, MAG and OMgp also bind NgR1, although MAG has been shown to bind NgR2 with greater affinity [51, 56].

NgR1 does not have a transmembrane domain, and therefore it must associate with a co-receptor to mediate intracellular signaling (Figure 1.2B). The low affinity neurotrophin receptor p75 ($p75^{NTR}$) interacts with NgR1 through its extracellular domain [64]. The intracellular domain of $p75^{NTR}$ is required for signal transduction as a truncated receptor is no longer able to activate the small GTPase, Rho, in a MAG dependent manner [64-66]. LINGO1 (LRR and Ig domain containing Nogo Receptor interacting protein) has also been identified as a component of the NgR1/ $p75^{NTR}$ complex [67]. The fact that $p75^{NTR}$ is detectable on only a subset of mature neurons led to the discovery that TAJ/TROY, an orphan tumor necrosis factor receptor family member can substitute for p75 as an alternative co-receptor for NgR1/LINGO1[68].

1.5.2 Paired immunoglobulin-like receptor B (PirB)

Paired immunoglobulin-like receptor B (PirB) is a receptor for all three MAIs: NogoA, MAG, and OMgp (Figure 1.2B) [30]. PirB was first described in the immune system [69, 70]. PirB is a MHC-1 class I receptor, contains a single transmembrane domain, and its intracellular domain has three potential immunoreceptor tyrosine based inhibitory motifs (ITIMs). Phosphorylation of these sites promotes the association of the protein tyrosine phosphatases, Shp1 and Shp2 [71-73]. In immune cells, PirB acts as an inhibitory receptor and it is the recruitment of Shp1/Shp2 that leads to termination of signaling cascades initiated by activating receptors[74, 75]. In neurons, PirB has also been shown to associate with Shp2 through its intracellular domain, and this domain is crucial for relaying growth inhibition from myelin-associated proteins [30, 76]. Neutralization of PirB function by antibody treatment is sufficient to partially relieve growth inhibition by Nogo66 and myelin extracts and appears to be a more substantial mediator of MAI growth inhibition than NgR. Interestingly, studies with cerebellar granule neurons from NgR null mice suggest that the two

receptors work together to relay signals from myelin, but PirB is the more potent receptor of Nogo66 [30]. Recent studies have also shown that PirB together with p75 negatively regulate TrkB signaling to modulate axon outgrowth [77, 78]. Additionally, a transgenic mouse expressing a truncated form of PirB displays increased ocular-dominance plasticity suggesting that PirB acts as a negative regulator of neuronal stability/plasticity [30, 76]. Combined these studies define a role for PirB as a negative regulator of axon outgrowth in the CNS and also highlight the complexity of myelin-inhibitory events at the cellular surface of the neuron.

1.6 From animal models to clinical trials: targeting MAIs for regeneration

Myelin associated inhibitors are abundant in the adult mammalian central nervous system. They are expressed on the surface of oligodendrocytes, a subset of neurons, and are released after injury to limit axon outgrowth and plasticity. Much work has gone into the identification of MAIs and characterization of their inhibitory mechanism in cell culture. However, even though in vitro neurite growth assays are a powerful tool for studying inhibitory mechanisms, studies in animal models allow researchers to evaluate the significance and relative contribution of individual inhibitor molecules to regenerative failure in vivo.

Several knock-out animals have been engineered looking at functional recovery after CNS injury following removal of inhibitory proteins. Three separate laboratories generated Nogo knockouts. However, only two saw enhanced sprouting and axonal regeneration after spinal cord injury (SCI), while the third group did not observe any difference in regeneration in Nogo knockout animals after SCI [79-81]. It was found that differences in the genetic background of the mice played a role in the conflicting results as Nogo-A knockout animals generated in two different pure background strains confirmed the initial results, enhanced regenerative fiber growth[82]. Interestingly, studies looking at regeneration in p75, NgR, and PirB knockout animals did not see enhanced growth after SCI, although there was some mild sprouting[83-86]. These studies

highlight the redundancy of MAI receptors in the CNS, indicating that simply targeting one inhibitory molecule will not be sufficient to promote robust and functional regeneration.

Antibody-based strategies, soluble function-blocking NgR ectodomain (NgR (310)-Fc), and an NgR1 antagonistic peptide (NEP1-40) have been successful in achieving anatomical and functional recovery following CNS injury [87-89]. The antibody IN-1 binds NogoA and inhibits NogoA function and delivery of IN-1 via implanted hybridoma cells into rats that had undergone a unilateral stroke, induced branching of the intact axons and the establishment of compensatory circuits. This resulted in an improvement in fine motor movement of paw which was lost due to stroke injury [90-92]. Treatment with IN-1 antibody in adult rats that had undergone spinal cord injury resulted in several millimeters of regrowth of the injured axon. Application of peptides blocking NgR function also promoted growth after injury. Studies in macaque monkeys that had been subjected to a unilateral spinal cord transection showed recovery of hand function [6, 93, 94]. Due to these promising results, a human anti-human NogoA antibody (ATI 355) has entered into clinical trials both in Europe and in North America. Phase I clinical trials have progressed positively and Phase II clinical trials began in 2010 to test the efficacy of the antibody on spinal cord treatment in acute paraplegic and tetraplegic patients [6].

1.7 Decline of intrinsic growth-promoting signals in the adult CNS also contributes to the lack of regeneration after injury

Much effort has gone into the identification and characterization of extrinsic inhibitory proteins in the CNS. As described previously, inhibition of MAIs and other inhibitory cues can lead to functional regeneration after injury or disease. However, there are additional factors blocking regeneration. It has become clear that neurons in the adult CNS display a decreased intrinsic ability to regenerate when compared to embryonic neurons. For example, cerebellar slices taken from post-natal day 10 rats survive in cell culture and maintain cellular composition resembling the mature cerebellum. Mature Purkinje cell axons do not regenerate

after axotomy even when provided with permissive substrates from the sciatic nerve or embryonic slices. However, embryonic Purkinje cells readily regenerate after axotomy and extend axons robustly into adult cerebellar slices [95, 96]. Similar developmental declines have been observed with retinal ganglion cells and tissue explants from the brainstem [97, 98]. In addition, some embryonic neurons, such as dorsal root ganglion (DRG) neurons, are able to grow on MAG, while DRGs isolated from postnatal mice are not [47, 99]. This has been observed for several of the myelin inhibitory cues and from these results, two hypotheses have arisen. First, that the expression of receptors for inhibitory ligands is lower in the embryonic versus the adult CNS, and secondly, that the adult CNS lacks the intrinsic growth properties of the embryonic CNS [100]. However, it is more likely that both hypotheses contribute to the lack of regeneration in the CNS, and therefore the molecular mechanism of the switch decreasing intrinsic growth properties in the adult CNS will need to be elucidated. To this end, roles for cyclic AMP and the PTEN/mTOR pathway have been implicated in the lack of intrinsic growth-promoting signals in the adult CNS.

A direct correlation between cAMP levels and inhibition of neurite outgrowth by myelin and MAG was demonstrated. Intracellular cAMP levels are high in post-natal day 1 DRGs which are not inhibited by MAG or myelin. However, as the DRGs matured cAMP levels decreased, and the neurons became responsive to myelin inhibition [47]. Interestingly, a conditioning lesion on DRGs elevates cAMP levels and can relieve growth inhibition of MAIs [47, 100, 101]. The addition of pharmacological agents to elevate cAMP levels also relieves growth inhibition by MAIs. For example, injection of DRGs in vivo with a non-hydrolyzable cAMP analogue induces regeneration of lesioned dorsal column axons[101]. The ability of cAMP to overcome MAI inhibition is protein kinase A (PKA) dependent and links to the activation of the transcription factor cAMP response element binding protein (CREB)[102]. Consistent with the initiation of transcription, several cAMP-regulated genes have been linked to MAIs and research is ongoing to determine the molecular mechanism of cAMP-mediated inhibition of MAIs.

Recently, it was shown that deletion of PTEN enhances survival of axotomized retinal ganglion cells and promotes regeneration of injured optic nerve fibers through the induction of sprouting, formation of new synapses, and regeneration of injured corticospinal tract axons[103, 104]. Loss of PTEN function leads to the activation of Akt and subsequently, mTOR, a critical regulator of protein translation initiation and cell growth [105]. It has been shown that mTOR signaling is downregulated in the mature CNS and axotomy further decreases mTOR activity [104]. mTOR is a critical regulator of protein translation initiation and cell growth. This suggests that the injured axon is further crippled by an inability to effectively synthesize new protein to promote regeneration[106].

In summary, the lack of axonal regeneration in the CNS cannot only be attributed to the presence of extrinsic factors, such as myelin associated proteins. The loss of intrinsic growth capability of mature neurons also provides a large obstacle to promote regeneration in the injured CNS. Thus, these studies suggest that a dual approach, blocking MAI function and enhancing intrinsic neuronal growth, may be a more efficacious strategy to regenerate the injured CNS.

1.8 Intracellular axon growth inhibitory signaling pathways

Due to the complexity and redundancy of inhibitory signals at the neuronal cell surface, it is advantageous to understand the intracellular signaling pathways, as a more potent therapeutic strategy to enhance axonal regeneration could be developed. Currently, there is a lack of knowledge of the molecular mechanisms of MAIs and only a few signaling pathways have been linked to MAIs (Figure 1.3). MAG has been shown to increase calcium levels in neurons and this is dependent on the presence of both p75 and NgR [107, 108]. MAG enhances calcium levels by activating protein kinase C (PKC) in a phospholipase C (PLC) dependent manner. Inhibitors of PKC function relieve growth inhibition on MAG, NogoA, and myelin in cell culture [109, 110]. Additionally, epidermal

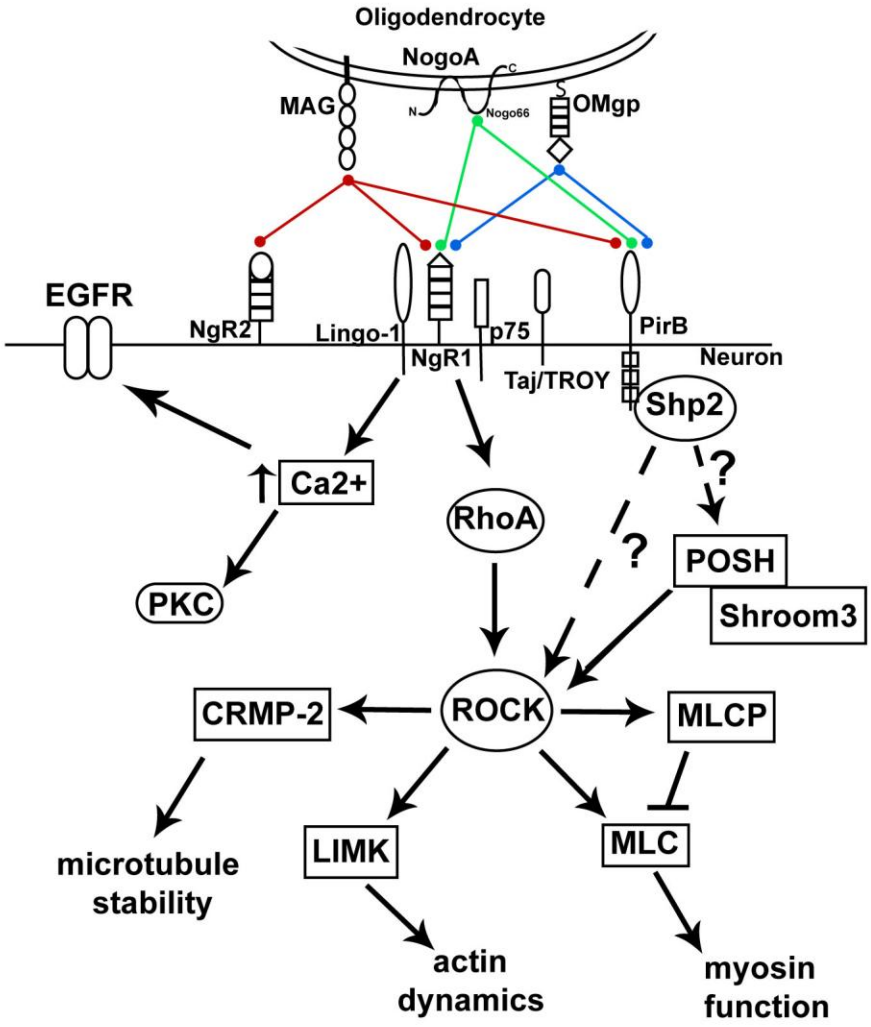

Figure 1.3 Signaling pathways mediated by MAIs

MAIs signal through Ca+dependent activation of PKC, the activation of epidermal growth factor receptor (EGFR), RhoA, and the activation of ROCK. NgR1, through its co-receptors activates Rho to inhibit axon outgrowth through remodeling of the cytoskeleton. Rho mediates inhibition through activation of ROCK, which in turn acts on multiple cytoskeletal regulatory proteins. PirB associates with the protein tyrosine phosphatase, Shp2, to mediate growth inhibition through an unknown mechanism. Our studies place the POSH-Shroom3 complex downstream of PirB signaling and potentially mediated by Shp2 phosphatase activity.

growth factor receptor (EGFR) is transactivated in response to Nogo66 and MAG, and it is suggested that this is due to increases in calcium levels [111].

MAIs must signal to the cytoskeleton to cause growth cone collapse and inhibition of axon growth, and the Rho family of small GTPases is well characterized as modulators of the actin-myosin cytoskeleton. The Rho family of GTPases includes RhoA, Rac1, and Cdc42. The GTPases cycle between being in an active GTP-bound state and an inactive GDP-bound state, and nucleotide exchange is controlled by several distinct inactivating GTPase-activating proteins (GAPs), activating guanine nucleotide exchange factors (GEFs) and guanine nucleotide dissociation inhibitors (GDIs) that maintain GTPases in an inactive state[112]. RhoA activation has been implicated as an essential component of MAI downstream signaling; the involvement of Rac1 or Cdc42 is unknown. However, Rac1 activity has been linked to growth cone collapse downstream of ephrin-A2 and semaphorin 3A, suggesting it may promote growth inhibition through a MAI-independent pathway [113-115]. Inhibition of RhoA activity releases inhibition by MAG or myelin in cell culture and promotes regeneration of the optic nerve in mice [116-118]. It was also found that the receptor p75 upon MAG or Nogo stimulation associates with a RHO-GDI, releasing its inhibitory association with RhoA, and resulting in RhoA activation [65, 66]. Downstream of RhoA activation, Rho-associated kinase (ROCK) is an important relay point for signal transduction to the cytoskeleton. Our laboratory has discovered that Plenty of Src Homology 3s (POSH), a scaffold protein for the Rho GTPase, Rac, negatively regulates axon outgrowth. Additionally, POSH forms a signaling complex with the actin-myosin regulatory protein Shroom3 and its associated protein ROCK to negatively regulate axon outgrowth, potentially linking POSH to changes in cytoskeletal dynamics to regulate axon outgrowth[119].

1.9 Plenty of Src Homology 3s (POSH)

Plenty of SH3s (POSH) is a multidomain scaffold protein compromised of four Src homology 3 (SH3) domains, a Rac binding domain (RBD), and a really

interesting new gene (RING) domain[120]. SH3 domains facilitate protein-protein interactions (PPIs) through proline rich regions (Figure 1.4). The presence of four SH3 domains highlights the role of POSH as a scaffold protein, as POSH could potentially associate with four distinct proteins through each SH3 domain. The RING domain classifies POSH as an ubiquitin E3 ligase. The E3 ubiquitin ligase family is large and structurally diverse, and specifies ubiquitin conjugation through their substrate recognition and the recruitment of a cognate E2 ubiquitin conjugating enzyme [121]. POSH levels are regulated by self-ubiquitination, however there remains minimal knowledge of additional substrates for ubiquitination by POSH.

POSH was discovered through a yeast two hybrid screen for Rac interacting proteins that facilitate Rac-mediated activation of c-Jun N-terminal kinase (JNK)[120]. POSH is ubiquitously expressed with highest expression levels in the kidney, lung, and brain[120]. Through its RBD, POSH binds the GTP-loaded (active) form of Rac but not the GDP-loaded (inactive), facilitating the activation of a mitogen-activated protein kinase (MAPK) signaling pathway including: mixed-lineage kinase 1 (MLK1), mitogen-activated protein (MAP) kinase kinases (MKKs) 4 and 7, and JNK [120, 122]. POSH also associated with the mixed-lineage kinases, dual leucine zipper (DLK) and leucine zipper kinase (LZK) to facilitate JNK interaction. However, DLK and LZK do not contain a canonical CRIB (Cdc42/Rac interactive binding) motif, thus their activation of JNK may be Rac independent [123, 124]. POSH forms a multiprotein complex with the scaffold protein JIP (JNK interacting protein) to activate JNK and promote apoptosis, leading to the complex being termed PJAC (POSH-JIP apoptotic complex). In the PJAC, POSH binds members of the MLK family and GTP-Rac, while JIP associates with MKK4/7 and JNK (Figure 1.5A). The formation of the complex promotes JNK activation, and is stabilized by a feed-forward loop enhancing JNK-mediated cellular events [125, 126]. The PJAC complex is regulated by Akt. Akt2 associates with POSH and phosphorylates MLK3, destabilizing the complex and causing it to disassemble[127]. Additionally, Akt1 binds JIP1 and inhibits its interaction with JNK [128].

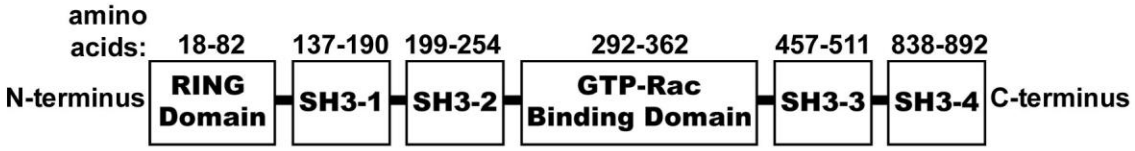

Figure 1.4 Domain structure of Plenty of Src Homology 3s (POSH)

POSH contains 6 potential protein-protein interaction domains including: (1) a RING domain in its N-terminus (amino acids 18-82) classifying POSH as an E3 ubiquitin ligase; (2) four Src Homology 3 (SH3) domains which associate with proline rich regions of proteins and (3) a centrally located, activated Rac (GTP loaded Rac) binding domain (amino acids 292-362).

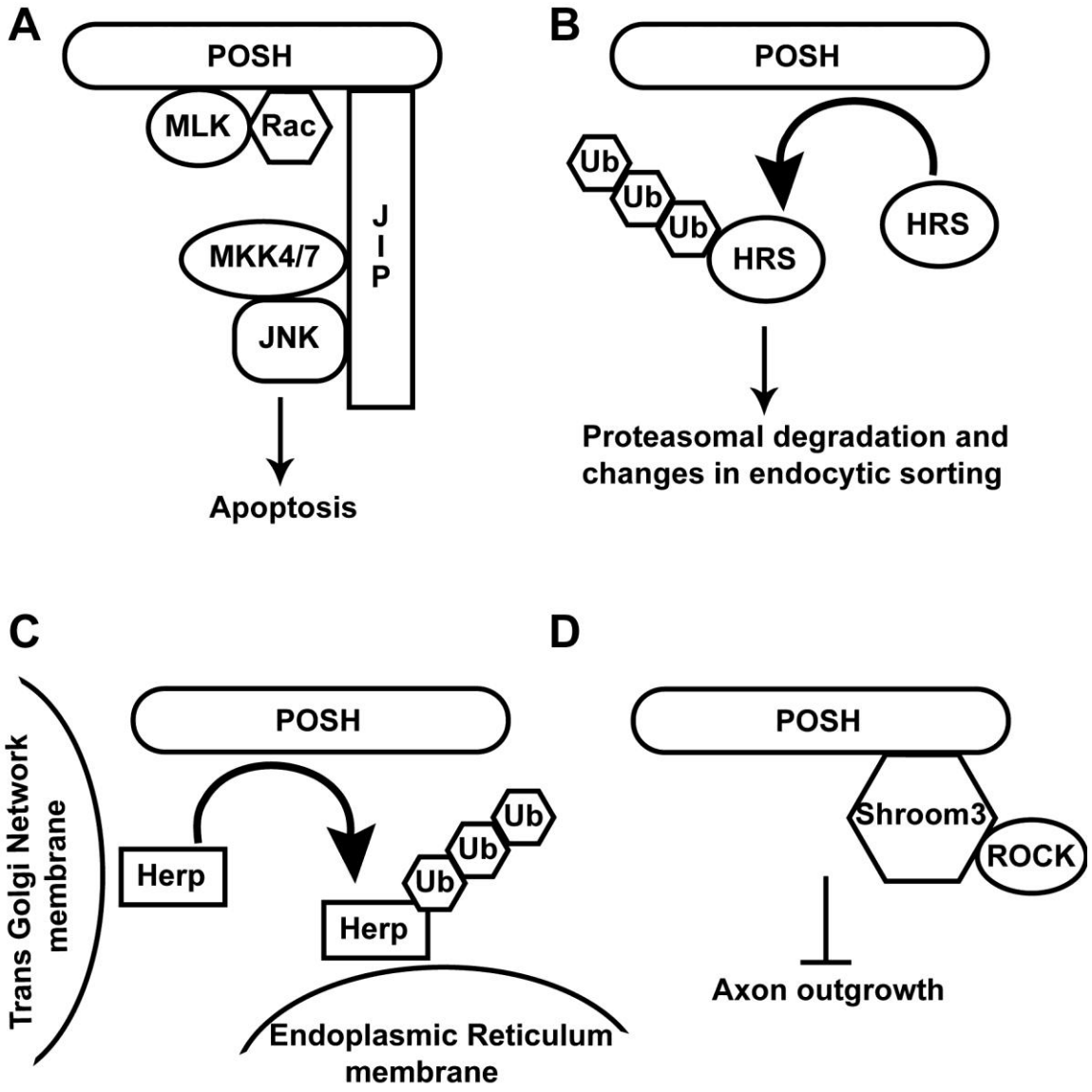

Figure 1.5 POSH regulates diverse biological functions through the assembly of distinct protein complexes

(A) In response to stress stimuli, POSH assembles a complex composed of Rac-GTP, MLKs, JIP, MKK4/7 and JNK, resulting in apoptosis.
(B) POSH ubiquitinates and promotes proteasomal degradation of Hrs leading to changes in endocytic sorting of membrane receptors.
(C) Elevation of intracelluar calcium promotes POSH-mediated poly-ubiquitination of Herp causing Herp to translocate from the *trans* Golgi network to the endoplasmic reticulum.
(D) The assembly of the POSH-Shroom3-ROCK complex results in axon growth inhibition.

In the nervous system, the JNK pathway regulates neuronal cell death evoked by stress stimuli, such as: withdrawal of trophic support, DNA damage, and oxidative stress. Overexpression of POSH, MLKs, MKK4/7, or constitutively active JNK has been reported to be sufficient to cause cell death in neuronal and non-neuronal cells, however our laboratory has not observed this phenotype [120, 122, 129]. Neuronal apoptotic death induced by trophic support withdrawal can be reversed through the removal of POSH function by POSH siRNA and JNK activation by MLKs is enhanced by overexpression of POSH [122]. These results highlight the importance of the scaffold in mediating apoptosis through JNK activation. Additionally, ischaemic stress, the loss of blood supply to the brain, induces JNK pathway activation and this is followed closely by neuronal cell death [130]. Removal of POSH function results in decreased neuronal cell death after ischemia in rats, indicating that manipulation of POSH function is neuroprotective in this context. POSH's role in apoptosis and neuronal cell death has also been characterized in *Xenopus* during early embryogenesis. Loss of POSH function resulted in neural tube defects that were similar to phenotypes seen with JNK deficient mice and MLK2 knockdown in *Xenopus* [131]. The above studies highlight a crucial role for POSH in JNK activation leading to apoptosis. However the POSH-JNK pathway and POSH itself have additional roles distinct from programmed cell death.

As a scaffold protein, POSH interacts with or regulates the function of many distinct proteins allowing POSH to affect diverse biological processes. In Drosophila, the dorsal appendages on eggshells serves as a breathing tube for the developing embryo and provides a mechanism for air exchange if the embryo becomes submerged [132]. Ras signaling is important for synthesis of dorsal appendages and loss of Ras signaling results in eggs with a single dorsal appendage [133]. POSH was identified in a screen for enhanced loss of Ras phenotypes in the dorsal appendage, suggesting that POSH regulates cell shape changes during development [133]. On endosomes, POSH has been shown to regulate hepatocyte growth factor-regulated tyrosine kinase substrate (Hrs), which is involved in receptor down-regulation and multivesicular body biogenesis.

POSH targets Hrs for ubiquitination and subsequent degradation, potentially affecting normal cell morphology (Figure 1.5B) [134]. The E3 ligase function of POSH and its association with the endosome is also involved in the production of infectious HIV-1. POSH facilitates the sorting of HIV Gag viral polyprotein to the inner leaflet of the plasma membrane, where GAG induces virus-like particle budding and release [135]. Furthermore, the E3 ligase activity of POSH in the *Drosophila* immune system leads to degradation of the JNK activator, transforming-growth factor β (TGFβ)-activated kinase (TAK1), and subsequent termination of the immune response[136]. POSH has a role in calcium homeostasis through its association with the homocysteine-inducible ER protein, Herp. POSH-Herp binding increases the levels of Herp in the endoplasmic reticulum (ER), where Herp protects the cell after ER stress by controlling calcium homeostasis (Figure 1.5C) [137]. Lastly, our laboratory has reported a novel role for POSH as a negative regulator of axon outgrowth [119]. POSH assembles a signaling complex composed of Shroom3 and ROCK to inhibit axon length (Figure 1.5D). It was found that the RING domain is required for POSH-mediated regulation of process outgrowth, suggesting a role for E3 ligase activity [119]. Through these collective studies, it is clear that POSH is able to regulate many diverse functions through the assembly of distinct protein complexes.

1.10 Shroom3

Shroom3, an f-actin and myosin binding protein, was first identified as a critical player in neural tube closure. Shroom3 deficient mice exhibit neural tube closure defects where the neural folds fail to converge at the dorsal midline and “mushroom” outward [138]. Exencephaly, where the brain is located outside the skull, was observed in all homozygous mutant embryos. Additional neural tube defect phenotypes, such as craniofacial clefting and spina bifida were observed in a smaller percentage of the mutants, 87% (68/78) and 23% (21/93) respectively[138]. Shroom3 contains two highly conserved domains termed ASDs (Apx/Shroom domains). Proteins which contain an ASD domain have been

classified into the Shroom family and renamed: Shroom1 (APX), Shroom2 (APXL), Shoom3, and Shroom4 (Kiaa1202) [139]. All four members of the Shroom family associate with cytoskeletal elements, and therefore are suggested to be involved in the control of cellular architecture. For example, Shroom1, Shroom2, and Shroom3 regulate the cellular distribution of γ-tubulin, linking the Shroom family to coordinating microtubule dynamics [140-142]. Shroom4 has also been shown to play a role in neural development and mutations have been linked to mental retardation[143].

Shroom3 is a key player in apical constriction, the process in which contraction of the apical side of a cell causes the cell to become wedge shaped. Apical constriction occurs during embryonic development where epithelial cells are undergoing morphological changes, including folding, invagination, and elongation. Correct formation of the neural tube requires these morphological changes to occur. Overexpression of Shroom3 in epithelial cells induces apical constriction as well as the recruitment of myosin II to the apical surface where it is hypothesized to elicit cell shape changes or maintain tension required for constriction [139, 144]. Both ASD domains of Shroom3 play a role in regulating actin-myosin dynamics to modulate cytoskeletal events. The ASD1 domain is involved in F-actin association, while the ASD2 domain recruits ROCK to regulate myosin II [145, 146]. The N-terminus of Shroom3 contains a post synaptic density 95/disclarge/zona occludens (PDZ) domain, providing an additional site for protein-protein interactions.

Shroom3 is widely expressed during embryonic development, suggesting roles in addition to apical constriction. Studies from our laboratory revealed that Shroom3 associates with POSH through the third SH3 domain of POSH [119]. The POSH binding region (PBD) of Shroom3 is located upstream of the ASD1 and ASD2 domains, and downstream of the PDZ domain. Removal of Shroom3 function by RNA interference (RNAi) in primary cortical neurons leads to enhanced axon length that is similar to the phenotype seen with POSH RNAi. The ASD1 and ASD2 domains are required for Shroom-mediated regulation of

axon length [119]. These results indicate a role for POSH, through Shroom3, as a modulator of the actin-myosin cytoskeleton.

1.11 ROCK

ROCK was first identified as an effector of the small GTPase Rho, facilitating Rho-induced formation of stress fibers and focal adhesions through the phosphorylation of myosin light chain (MLC) [147, 148]. There are two known isoforms, ROCKI and ROCKII, and both are ubiquitously expressed in rodents, although there is increased expression of ROCK II in muscle tissue and brain. ROCKs are serine/threonine kinases consisting of an amino-terminal kinase domain followed by a potential coiled-coil region, a Rho binding domain (RBD), and a C-terminal pleckstrin homology (PH) domain. ROCK is primarily located in the cytoplasm, however it can translocate to the cellular membrane when provided the proper stimuli [149].

The kinase activity of ROCKI and ROCKII is regulated in distinct mechanisms. The PH domain and the RBD function in the autoinhibition of enzymatic activity by interacting with the amino-terminal kinase domain [150]. Binding of activated GTP-bound Rho to the RBD is thought to open up the kinase, removing autoinhibition. ROCKII can also be activated in a Rho-independent manner by association with arachidonic acid treatment in smooth muscle [151]. In vivo, ROCKI is truncated by caspase-3 in the c-terminus resulting in a constitutively active kinase [152, 153]. There is also evidence that ROCK can associate with additional small GTPases which can bind and selectively inhibit ROCK function. For example, the small GTPase, Gem, binds to ROCKII in a region adjacent to the Rho binding domain and expression of Gem inhibits ROCK from activating its downstream substrates [154]. This finding is interesting as it suggests that ROCK may have additional unknown roles downstream of other small GTPases independent of Rho.

Following activation by Rho, ROCK regulates multiple signaling pathways that all have potential to modulate cytoskeletal functions downstream [149]. A

well studied target of ROCK phosphorylation is the light chain of myosin, also referred to as myosin light chain (MLC). Phosphorylation of MLC regulates myosin II function by promoting its interaction with actin, thereby activating myosin ATPase and enhancing cell contractility [155-157]. ROCK also phosphorylates myosin binding subunit (MBS) [157, 158]. MBS is one of three subunits of myosin light chain phosphatase (MLCP), a negative regulator of actomyosin contractility. Phosphorylation of MBS by ROCK causes MLCP to dissociate from myosin retaining myosin activity. Therefore, ROCK regulates contractility on multiple levels: activating contractility and inhibiting deactivation. Additionally, ROCK can regulate actin dynamics and microtubule stability through activation of LIM kinases and collapsing response mediator protein-2 (CRMP2), a neuronal protein that is involved in growth cone collapse [159, 160].

ROCK's regulation of actin-myosin function is crucial to modulating axon outgrowth. Recently, ROCK function has been shown to mediate neuronal responses to myelin-associated inhibitory proteins (MAIs) [161]. The ROCK antagonist, Y-27632, can promote neurite growth on MAI substrates in vitro and enhanced regeneration in rats subjected to corticospinal tract transection. Four independent studies showed that Y-27632 treatment allows outgrowth on MAG, NogoA, and crude myelin in cerebellar granule neurons, cortical neurons, and dorsal root ganglion cells [58, 116, 118]. Y-27632 treatment in rodents subjected to corticospinal tract transection yielded enhanced sprouting of cortical spinal tract fibers and accelerated locomoter recovery, visualized by recovery of hind limb function [116, 118]. This was also observed in ROCKII knock-out mice [162]. Investigation into the molecular mechanism of ROCK signaling downstream of MAIs revealed that upon NogoA stimulation ROCK translocates to the cellular membrane and phosphorylation of myosin light chain is enhanced [161]. However, further characterization of known ROCK effectors, such as LIMK and CRMP2, were not performed, therefore, the complete downstream signaling mechanism of MAIs through ROCK is unknown.

The ASD2 domain of Shroom3 binds Rho associated kinase (ROCK) to localize ROCK to the epithelial apical junction where ROCK contributes to apical

constriction [145]. Our laboratory has shown that Shroom3 also recruits ROCK to the POSH complex where ROCK mediates axon outgrowth [119]. Interference with ROCK activity with the inhibitor Y-27632 or expression of a dominant negative domain of ROCK, which disrupts the Shroom3-ROCK interaction, leads to enhanced axon length. Our data suggests that ROCK is involved in the POSH pathway as a negative regulator of axon length.

1.12 Mixed-lineage kinases: Dual leucine zipper kinase (DLK) and Leucine zipper kinase (LZK)

The mixed-lineage kinases (MLKs) are a family of serine/threonine protein kinases that act in a mitogen-activated protein kinase (MAPK) signaling pathway. The name mixed-lineage comes from their kinase domain where the conserved subdomains contain homology with both serine/threonine and tyrosine kinases [163]. However, there is no evidence for MLKs having tyrosine kinase activity. There are three subfamilies of MLKs, classified on the basis of their domain arrangements and sequence similarities: the MLKs, the dual-leucine-zipper-bearing kinase (DLK and LZK), and the zipper-sterile-α-motif kinases (ZAK). The MLKs (MLK1-4) are characterized by an amino-terminal src-homology-3 (SH3) domain, followed by a kinase domain, a leucine zipper region, and a Cdc42/Rac-interactive binding (CRIB) motif, which promotes activation via Rac or Cdc42 [164]. The MLK subgroup contains 75% sequence identity within their kinase domain and 65% identity from their SH3 domain to their CRIB motif. The c-terminal ends are less homologous, potentially serving as regulatory sites for distinct cellular functions.

DLK was identified using degenerative oligonucleotide-based PCR cloning in a screen to identify novel protein kinases[165]. LZK was isolated soon after from the human cerebellum[166]. DLK is an 888 amino acid protein, while LZK contains 966 amino acids. The proteins possess a kinase domain in their N-terminus followed by two leucine zipper domains with 86.4% homology [165, 166]. DLK and LZK lack the CRIB motif present in other MLK family members, and they are activated by dimerization rather than association of small GTPases.

DLK and LZK can form homo- and heterodimers, however there is evidence that only homodimers occur through the zipper domains, while heterodimers occur through additional binding regions in the N-terminus [124, 167]. DLK and LZK bind and phosphorylate MKK7 to activate JNK, and DLK has been shown to activate p38 through the phosphorylation of MKK4 [167, 168]. Additionally both proteins associate with the scaffold proteins POSH and JIP (JNK-interacting protein) to facilitate JNK activation [124, 169]. However, DLK is also held in an inactive, monomer state by JIP. Phosphorylation of JIP by JNK releases DLK and facilitates its dimerization, subsequent activation, and leads to further activation of JNK [170, 171]. This model suggests a feed forward mechanism of regulation for the DLK-JIP-JNK signaling pathway. Additionally, JIP tyrosine-phosphorylation by Src family members increases the affinity of JIP for DLK, preventing the activation of JNK [172].

In vitro, LZK is primarily known for inducing JNK activation and apoptosis, and its in vivo role is not well characterized. On the other hand, DLK has several roles defined in the nervous system. In *Caenorhabditis elegans*, a DLK homolog is required for axon regeneration by initiating the formation of new growth cones on severed axons through the activation of MKK4 and p38 [173]. In *Drosophila melanogaster*, DLK regulates synaptic growth through activation of JNK. Interestingly in both systems, DLK is negatively regulated by an E3 ubiquitin ligase protein family denoted PHR (human Pam, mouse Phr1, zebrafish Esrom, *Drosophila* Highwire, and *C.elegans* RPM-1)[174]. In a collection of studies using DLK knockout mice, researchers found that loss of DLK lead to defects in neuronal migration and axon outgrowth resulting in reduced size of the anterior commisure and corpus callosum[175]. Further studies revealed that DLK regulates axon outgrowth through JNK activation, followed by downstream activation of doublecortin (DCX) and microtubule-associated protein 1b (MAP1B) [175-177]. Collectively these studies highlight a role for DLK/LZK as regulators of axonal development and outgrowth upstream of JNK activation.

1.13 POSH is a negative regulator of axon outgrowth

Our laboratory identified a novel role for POSH as a negative regulator of axon length [119]. Removal of POSH function by RNA interference (RNAi) in differentiated P19 cells or primary cortical neurons from mice results in enhanced axon length. The enhancement in axon length was not due to a increase in cell survival, which suggested that the signaling pathway mediating axon outgrowth is independent from its role in apoptosis[120, 122, 131, 178]. Consistent with this hypothesis, POSH binds the actin-myosin regulatory protein, Shroom3, through its third SH3 domain. RNAi-mediated interference of Shroom3 expression also results in long axons suggesting that POSH and Shroom3 work in concert to negatively regulate axon outgrowth.

Shroom3 regulates the actin-myosin cytoskeleton through its ASD1/2 domains and we found that both domains are required for regulation of process length. Expression of the ASD1 domain in cortical neurons acts as a dominant negative to block the binding of endogenous Shroom3 to actin, and results in neurons with enhanced process length. Additionally, a Shroom3 mutant lacking the ASD2 domain is no longer able to regulate axon outgrowth. The ASD2 domain regulates myosin II activity or localization through the recruitment of ROCK and interference with the ability of Shroom3 to bind ROCK results in enhanced process growth, indicating that interaction with ROCK is critical for Shroom3-POSH to regulate axon length [119, 144, 145]. Interestingly, loss of myosin IIA function reverses the POSH and Shroom3 long process phenotype, indicating that increased myosin II function may be the driving force in the POSH/Shroom3 phenotypes. As stated previously, ROCK regulates myosin II activity by phosphorylating myosin light chain and myosin light chain phosphatase[149]. However, it is unknown as to whether the POSH-Shroom3-ROCK complex is directly regulating myosin II function or if enhanced myosin II activity is an effect of a shift in the balance of cytoskeletal forces due to loss of POSH/Shroom3 function.

Collectively the research from our laboratory suggests that POSH assembles an axon growth inhibitory complex that links through Shroom3 and ROCK, directly or indirectly, to the actin-myosin network. However, the upstream signaling components relaying growth inhibition through the POSH complex remain unknown. Thus, this thesis aims to characterize the upstream molecular mechanism of axon growth inhibition mediated by the POSH complex. The elucidation of this signaling pathway will increase the knowledge of downstream inhibitory events and provide novel targets for therapeutic strategies to overcome neurite growth inhibition during development, and also in the adult CNS where the regenerative capacity is severely limited.

1.14 References

1. Purves, D., Neuroscience. 2012, Sunderland, MA: Sinauer Associates. xvi, 759, [60] p.
2. TessierLavigne, M. and C.S. Goodman, The molecular biology of axon guidance. Science, 1996. 274(5290): p. 1123-1133.
3. Huber, A.B., et al., Signaling at the growth cone: Ligand-receptor complexes and the control of axon growth and guidance. Annual Review of Neuroscience, 2003. 26: p. 509-563.
4. Gallo, G. and P.C. Letourneau, Regulation of growth cone actin filaments by guidance cues. Journal of Neurobiology, 2004. 58(1): p. 92-102.
5. Liu, B.P., et al., Extracellular regulators of axonal growth in the adult central nervous system. Philosophical Transactions of the Royal Society B-Biological Sciences, 2006. 361(1473): p. 1593-1610.
6. Zorner, B., M.E. Schwab, and Nyas, Anti-Nogo on the go: from animal models to a clinical trial, in Discoveries in Spinal Cord Injury Research: From Bench to Bedside. 2010, Wiley-Blackwell: Malden. p. E22-E34.
7. Nudo, R.J., Plasticity. NeuroRX, 2006. 3(4): p. 420-427.
8. Giger, R.J., E.R. Hollis, and M.H. Tuszynski, Guidance Molecules in Axon Regeneration. Cold Spring Harbor Perspectives in Biology, 2010. 2(7).
9. Giger, R.J., et al., Mechanisms of CNS myelin inhibition: Evidence for distinct and neuronal cell type specific receptor systems. Restorative Neurology and Neuroscience, 2008. 26(2-3): p. 97-115.
10. Ramón y Cajal, S. and R.M. May, Degeneration & regeneration of the nervous system. Estudios sobre la degeneración y regeneración del sistema nervioso.English. 1928, London: Oxford University Press, Humphrey Milford. 2 v.
11. Richardson, P.M., U.M. McGuinness, and A.J. Aguayo, AXONS FROM CNS NEURONS REGENERATE INTO PNS GRAFTS. Nature, 1980. 284(5753): p. 264-265.
12. Benfey, M. and A.J. Aguayo, EXTENSIVE ELONGATION OF AXONS FROM RAT-BRAIN INTO PERIPHERAL-NERVE GRAFTS. Nature, 1982. 296(5853): p. 150-152.
13. David, S. and A.J. Aguayo, AXONAL ELONGATION INTO PERIPHERAL NERVOUS-SYSTEM BRIDGES AFTER CENTRAL NERVOUS-SYSTEM INJURY IN ADULT-RATS. Science, 1981. 214(4523): p. 931-933.
14. Giedd, J.N., Structural magnetic resonance imaging of the adolescent brain, in Adolescent Brain Development: Vulnerabilities and Opportunities, R.E. Dahl and L.P. Spear, Editors. 2004. p. 77-85.
15. Siegel, G.J., et al., Basic neurochemistry: molecular, cellular, and medical aspects. 2006, Burlington ; London: Elsevier Academic. xxiv, 992 p.
16. Fields, R.D., Myelination: an overlooked mechanism of synaptic plasticity? Neuroscientist, 2005. 11(6): p. 528-31.
17. Webster, H.D., GEOMETRY OF PERIPHERAL MYELIN SHEATHS DURING THEIR FORMATION AND GROWTH IN RAT SCIATIC NERVES. Journal of Cell Biology, 1971. 48(2): p. 348-&.
18. Huebner, E.A. and S.M. Strittmatter, Axon Regeneration in the Peripheral and Central Nervous Systems, in Cell Biology of the Axon, E. Koenig, Editor. 2009. p. 339-351.
19. Schwab, M.E. and P. Caroni, OLIGODENDROCYTES AND CNS MYELIN ARE NONPERMISSIVE SUBSTRATES FOR NEURITE GROWTH AND

FIBROBLAST SPREADING INVITRO. Journal of Neuroscience, 1988. 8(7): p. 2381-2393.
20. Caroni, P. and M.E. Schwab, 2 MEMBRANE-PROTEIN FRACTIONS FROM RAT CENTRAL MYELIN WITH INHIBITORY PROPERTIES FOR NEURITE GROWTH AND FIBROBLAST SPREADING. Journal of Cell Biology, 1988. 106(4): p. 1281-1288.
21. Caroni, P. and M.E. Schwab, ANTIBODY AGAINST MYELIN-ASSOCIATED INHIBITOR OF NEURITE GROWTH NEUTRALIZES NONPERMISSIVE SUBSTRATE PROPERTIES OF CNS WHITE MATTER. Neuron, 1988. 1(1): p. 85-96.
22. Chen, M.S., et al., Nogo-A is a myelin-associated neurite outgrowth inhibitor and an antigen for monoclonal antibody IN-1. Nature, 2000. 403(6768): p. 434-439.
23. GrandPre, T., et al., Identification of the Nogo inhibitor of axon regeneration as a Reticulon protein. Nature, 2000. 403(6768): p. 439-444.
24. Prinjha, R., et al., Neurobiology - Inhibitor of neurite outgrowth in humans. Nature, 2000. 403(6768): p. 383-384.
25. Vandevelde, H.J.K., et al., NSP-ENCODED RETICULONS, NEUROENDOCRINE PROTEINS OF A NOVEL GENE FAMILY ASSOCIATED WITH MEMBRANES OF THE ENDOPLASMIC-RETICULUM. Journal of Cell Science, 1994. 107: p. 2403-2416.
26. Yan, R., et al., Reticulon proteins: emerging players in neurodegenerative diseases. Cellular and Molecular Life Sciences, 2006. 63(7-8): p. 877-889.
27. Yang, Y.S. and S.M. Strittmatter, The reticulons: a family of proteins with diverse functions. Genome Biology, 2007. 8(12).
28. Voeltz, G.K., et al., A class of membrane proteins shaping the tubular endoplasmic reticulum. Cell, 2006. 124(3): p. 573-586.
29. Oertle, T., et al., Nogo-A inhibits neurite outgrowth and cell spreading with three discrete regions. Journal of Neuroscience, 2003. 23(13): p. 5393-5406.
30. Atwal, J.K., et al., PirB is a Functional Receptor for Myelin Inhibitors of Axonal Regeneration. Science, 2008. 322(5903): p. 967-970.
31. Fournier, A.E., T. GrandPre, and S.M. Strittmatter, Identification of a receptor mediating Nogo-66 inhibition of axonal regeneration. Nature, 2001. 409(6818): p. 341-346.
32. Hu, F.H. and S.M. Strittmatter, The N-terminal domain of Nogo-A inhibits cell adhesion and axonal outgrowth by an integrin-specific mechanism. Journal of Neuroscience, 2008. 28(5): p. 1262-1269.
33. Hamada, N., et al., Molecular cloning and characterization of the mouse reticulon 3 cDNA. Cellular and Molecular Biology, 2002. 48(2): p. 163-172.
34. Huber, A.B., et al., Patterns of Nogo mRNA and protein expression in the developing and adult rat and after CNS lesions. Journal of Neuroscience, 2002. 22(9): p. 3553-3567.
35. Wang, X.X., et al., Localization of Nogo-A and Nogo-66 receptor proteins at sites of axon-myelin and synaptic contact. Journal of Neuroscience, 2002. 22(13): p. 5505-5515.
36. Liu, H.P., C.E.L. Ng, and B.L. Tang, Nogo-A expression in mouse central nervous system neurons. Neuroscience Letters, 2002. 328(3): p. 257-260.
37. Tozaki, H., et al., Expression of Nogo protein by growing axons in the developing nervous system. Molecular Brain Research, 2002. 104(2): p. 111-119.
38. Mathis, C., et al., Nogo-A Regulates Neural Precursor Migration in the Embryonic Mouse Cortex. Cerebral Cortex, 2010. 20(10): p. 2380-2390.

39. Mingorance-Le Meur, A., et al., Involvement of the Myelin-Associated Inhibitor Nogo-A in Early Cortical Development and Neuronal Maturation. Cerebral Cortex, 2007. 17(10): p. 2375-2386.
40. Petrinovic, M.M., et al., Neuronal Nogo-A regulates neurite fasciculation, branching and extension in the developing nervous system. Development, 2010. 137(15): p. 2539-2550.
41. Wang, J., et al., The growth-inhibitory protein Nogo is involved in midline routing of axons in the mouse optic chiasm. Journal of Neuroscience Research, 2008. 86(12): p. 2581-2590.
42. Wang, J., et al., Localization of an axon growth inhibitory molecule Nogo and its receptor in the spinal cord of mouse embryos. Brain Research, 2010. 1306: p. 8-17.
43. McKerracher, L., et al., IDENTIFICATION OF MYELIN-ASSOCIATED GLYCOPROTEIN AS A MAJOR MYELIN-DERIVED INHIBITOR OF NEURITE GROWTH. Neuron, 1994. 13(4): p. 805-811.
44. Mukhopadhyay, G., et al., A NOVEL ROLE FOR MYELIN-ASSOCIATED GLYCOPROTEIN AS AN INHIBITOR OF AXONAL REGENERATION. Neuron, 1994. 13(3): p. 757-767.
45. Quarles, R.H., Myelin sheaths: glycoproteins involved in their formation, maintenance and degeneration. Cellular and Molecular Life Sciences, 2002. 59(11): p. 1851-1871.
46. Filbin, M.T., Myelin-associated inhibitors of axonal regeneration in the adult mammalian CNS. Nature Reviews Neuroscience, 2003. 4(9): p. 703-713.
47. Cai, D., et al., Neuronal cyclic AMP controls the developmental loss in ability of axons to regenerate. Journal of Neuroscience, 2001. 21(13): p. 4731-4739.
48. Chivatakarn, O., et al., The Nogo-66 receptor NgR1 is required only for the acute growth cone-collapsing but not the chronic growth-inhibitory actions of myelin inhibitors. Journal of Neuroscience, 2007. 27(27): p. 7117-7124.
49. Vinson, M., et al., Characterization of the sialic acid-binding site in sialoadhesin by site-directed mutagenesis. Journal of Biological Chemistry, 1996. 271(16): p. 9267-9272.
50. Crocker, P.R. and A. Varki, Siglecs, sialic acids and innate immunity. Trends in Immunology, 2001. 22(6): p. 337-342.
51. Domeniconi, M., et al., Myelin-associated glycoprotein interacts with the Nogo66 receptor to inhibit neurite outgrowth. Neuron, 2002. 35(2): p. 283-290.
52. Liu, B.P., et al., Myelin-associated glycoprotein as a functional ligand for the Nogo-66 receptor. Science, 2002. 297(5584): p. 1190-1193.
53. Lauren, J., et al., Characterization of myelin ligand complexes with neuronal Nogo-66 receptor family members. Journal of Biological Chemistry, 2007. 282(8): p. 5715-5725.
54. Venkatesh, K., et al., The Nogo-66 receptor homolog NgR2 is a sialic acid-dependent receptor selective for myelin-associated glycoprotein. Journal of Neuroscience, 2005. 25(4): p. 808-822.
55. Tang, S., et al., Myelin-associated glycoprotein interacts with neurons via a sialic acid binding site at ARG118 and a distinct neurite inhibition site. Journal of Cell Biology, 1997. 138(6): p. 1355-1366.
56. Wang, K.C., et al., Oligodendrocyte-myelin glycoprotein is a Nogo receptor ligand that inhibits neurite outgrowth. Nature, 2002. 417(6892): p. 941-944.
57. Habib, A.A., et al., Expression of the oligodendrocyte-myelin glycoprotein by neurons in the mouse central nervous system. Journal of Neurochemistry, 1998. 70(4): p. 1704-1711.

58. Dergham, P., et al., Rho signaling pathway targeted to promote spinal cord repair. Journal of Neuroscience, 2002. 22(15): p. 6570-6577.
59. McKeon, R.J., A. Hoke, and J. Silver, INJURY-INDUCED PROTEOGLYCANS INHIBIT THE POTENTIAL FOR LAMININ-MEDIATED AXON GROWTH ON ASTROCYTIC SCARS. Experimental Neurology, 1995. 136(1): p. 32-43.
60. Benson, M.D., et al., Ephrin-B3 is a myelin-based inhibitor of neurite outgrowth. Proceedings of the National Academy of Sciences of the United States of America, 2005. 102(30): p. 10694-10699.
61. Kaneko, S., et al., A selective Sema3A inhibitor enhances regenerative responses and functional recovery of the injured spinal cord. Nature Medicine, 2006. 12(12): p. 1380-1389.
62. Low, K., et al., Netrin-1 is a novel myelin-associated inhibitor to axon growth. Journal of Neuroscience, 2008. 28(5): p. 1099-1108.
63. Moreau-Fauvarque, C., et al., The transmembrane semaphorin Sema4D/CD100, an inhibitor of axonal growth, is expressed on oligodendrocytes and upregulated after CNS lesion. Journal of Neuroscience, 2003. 23(27): p. 9229-9239.
64. Wang, K.C., et al., p75 interacts with the Nogo receptor as a co-receptor for Nogo, MAG and OMgp. Nature, 2002. 420(6911): p. 74-78.
65. Yamashita, T., H. Higuchi, and M. Tohyama, The p75 receptor transduces the signal from myelin-associated glycoprotein to Rho. Journal of Cell Biology, 2002. 157(4): p. 565-570.
66. Yamashita, T., K.L. Tucker, and Y.A. Barde, Neurotrophin binding to the p75 receptor modulates Rho activity and axonal outgrowth. Neuron, 1999. 24(3): p. 585-593.
67. Mi, S., et al., LINGO-1 is a component of the Nogo-66 receptor/p75 signaling complex. Nature Neuroscience, 2004. 7(3): p. 221-228.
68. Park, J.B., et al., A TNF receptor family member, TROY, is a coreceptor with Nogo receptor in mediating the inhibitory activity of myelin inhibitors. Neuron, 2005. 45(3): p. 345-351.
69. Chen, H.E., et al., Regulation of colony-stimulating factor 1 receptor signaling by the SH2 domain-containing tyrosine phosphatase SHPTP1. Molecular and Cellular Biology, 1996. 16(7): p. 3685-3697.
70. Timms, J.F., et al., Identification of major binding proteins and substrates for the SH2-containing protein tyrosine phosphatase SHP-1 in macrophages. Molecular and Cellular Biology, 1998. 18(7): p. 3838-3850.
71. Kubagawa, H., P.D. Burrows, and M.D. Coopers, A novel pair of immunoglobulin-like receptors expressed by B cells and myeloid cells. Proceedings of the National Academy of Sciences of the United States of America, 1997. 94(10): p. 5261-5266.
72. Burshtyn, D.N., et al., A novel phosphotyrosine motif with a critical amino acid at position-2 for the SH2 domain-mediated activation of the tyrosine phosphatase SHP-1. Journal of Biological Chemistry, 1997. 272(20): p. 13066-13072.
73. Vivier, E. and M. Daeron, Immunoreceptor tyrosine-based inhibition motifs. Immunology Today, 1997. 18(6): p. 286-291.
74. Blery, M., et al., The paired Ig-like receptor PIR-B is an inhibitory receptor that recruits the protein-tyrosine phosphatase SHP-1. Proceedings of the National Academy of Sciences of the United States of America, 1998. 95(5): p. 2446-2451.
75. Maeda, A., et al., Requirement of SH2-containing protein tyrosine phosphatases SHP-1 and SHP-2 for paired immunoglobulin-like receptor B (PIR-B)-mediated inhibitory signal. Journal of Experimental Medicine, 1998. 187(8): p. 1355-1360.

76. Syken, J., et al., PirB restricts ocular-dominance plasticity in visual cortex. Science, 2006. 313(5794): p. 1795-800.
77. Fujita, Y., et al., Myelin suppresses axon regeneration by PIR-B/SHP-mediated inhibition of Trk activity. Embo Journal, 2011. 30(7): p. 1389-1401.
78. Fujita, Y., et al., The p75 receptor mediates axon growth inhibition through an association with PIR-B. Cell Death & Disease, 2011. 2.
79. Kim, J.E., et al., Axon regeneration in young adult mice lacking Nogo-A/B. Neuron, 2003. 38(2): p. 187-199.
80. Simonen, M., et al., Systemic deletion of the myelin-associated outgrowth inhibitor Nogo-A improves regenerative and plastic responses after spinal cord injury. Neuron, 2003. 38(2): p. 201-211.
81. Zheng, B.H., et al., Lack of enhanced spinal regeneration in Nogo-deficient mice. Neuron, 2003. 38(2): p. 213-224.
82. Dimou, L., et al., Nogo-A-deficient mice reveal strain-dependent differences in axonal regeneration. Journal of Neuroscience, 2006. 26(21): p. 5591-5603.
83. Kim, J.E., et al., Nogo-66 receptor prevents raphespinal and rubrospinal axon regeneration and limits functional recovery from spinal cord injury. Neuron, 2004. 44(3): p. 439-451.
84. Nakamura, Y., et al., Paired Immunoglobulin-like Receptor B Knockout Does Not Enhance Axonal Regeneration or Locomotor Recovery after Spinal Cord Injury. Journal of Biological Chemistry, 2011. 286(3): p. 1876-1883.
85. Song, X.Y., et al., Suppression of p75NTR does not promote regeneration of injured spinal cord in mice. Journal of Neuroscience, 2004. 24(2): p. 542-546.
86. Zheng, B.H., et al., Genetic deletion of the Nogo receptor does not reduce neurite inhibition in vitro or promote corticospinal tract regeneration in vivo. Proceedings of the National Academy of Sciences of the United States of America, 2005. 102(4): p. 1205-1210.
87. GrandPre, T., S.X. Li, and S.M. Strittmatter, Nogo-66 receptor antagonist peptide promotes axonal regeneration. Nature, 2002. 417(6888): p. 547-551.
88. Li, S.X., et al., Blockade of Nogo-66, myelin-associated glycoprotein, and oligodendrocyte myelin glycoprotein by soluble Nogo-66 receptor promotes axonal sprouting and recovery after spinal injury. Journal of Neuroscience, 2004. 24(46): p. 10511-10520.
89. MacDermid, V.E., et al., A soluble Nogo receptor differentially affects plasticity of spinally projecting axons. European Journal of Neuroscience, 2004. 20(10): p. 2567-2579.
90. Benowitz, L.I. and S.T. Carmichael, Promoting axonal rewiring to improve outcome after stroke. Neurobiology of Disease, 2010. 37(2): p. 259-266.
91. Papadopoulos, C.M., et al., Functional recovery and neuroanatomical plasticity following middle cerebral artery occlusion and IN-1 antibody treatment in the adult rat. Annals of Neurology, 2002. 51(4): p. 433-441.
92. Papadopoulos, C.M., et al., Dendritic plasticity in the adult rat following middle cerebral artery occlusion and Nogo-A neutralization. Cerebral Cortex, 2006. 16(4): p. 529-536.
93. Freund, P., et al., Nogo-A-specific antibody treatment enhances sprouting and functional recovery after cervical lesion in adult primates. Nature Medicine, 2006. 12(7): p. 790-792.
94. Freund, P., et al., Anti-Nogo-A antibody treatment promotes recovery of manual dexterity after unilateral cervical lesion in adult primates - re-examination and extension of behavioral data. European Journal of Neuroscience, 2009. 29(5): p. 983-996.

95. Bouslama-Oueghlani, L., et al., The developmental loss of the ability of Purkinje cells to regenerate their axons occurs in the absence of myelin: An in vitro model to prevent myelination. Journal of Neuroscience, 2003. 23(23): p. 8318-8329.
96. Dusart, I., M.S. Airaksinen, and C. Sotelo, Purkinje cell survival and axonal regeneration are age dependent: An in vitro study. Journal of Neuroscience, 1997. 17(10): p. 3710-3726.
97. Blackmore, M. and P.C. Letourneau, Changes within maturing neurons limit axonal regeneration in the developing spinal cord. Journal of Neurobiology, 2006. 66(4): p. 348-360.
98. Goldberg, J.L., et al., Amacrine-signaled loss of intrinsic axon growth ability by retinal ganglion cells. Science, 2002. 296(5574): p. 1860-1864.
99. Johnson, P.W., et al., RECOMBINANT MYELIN-ASSOCIATED GLYCOPROTEIN CONFERS NEURAL ADHESION AND NEURITE OUTGROWTH FUNCTION. Neuron, 1989. 3(3): p. 377-385.
100. Hannila, S.S. and M.T. Filbin, The role of cyclic AMP signaling in promoting axonal regeneration after spinal cord injury. Experimental Neurology, 2008. 209(2): p. 321-332.
101. Qiu, J., et al., Spinal axon regeneration induced by elevation of cyclic AMP. Neuron, 2002. 34(6): p. 895-903.
102. Gao, Y., et al., Activated CREB is sufficient to overcome inhibitors in myelin and promote spinal axon regeneration in vivo. Neuron, 2004. 44(4): p. 609-621.
103. Park, K.K., et al., PTEN/mTOR and axon regeneration. Experimental Neurology, 2010. 223(1): p. 45-50.
104. Park, K.K., et al., Promoting Axon Regeneration in the Adult CNS by Modulation of the PTEN/mTOR Pathway. Science, 2008. 322(5903): p. 963-966.
105. Maehama, T. and J.E. Dixon, The tumor suppressor, PTEN/MMAC1, dephosphorylates the lipid second messenger, phosphatidylinositol 3,4,5-trisphosphate. Journal of Biological Chemistry, 1998. 273(22): p. 13375-13378.
106. Verma, P., et al., Axonal protein synthesis and degradation are necessary for efficient growth cone regeneration. Journal of Neuroscience, 2005. 25(2): p. 331-342.
107. Loschinger, J., et al., Retinal axon growth cone responses to different environmental cues are mediated by different second-messenger systems. Journal of Neurobiology, 1997. 33(6): p. 825-834.
108. Wong, S.T., et al., A p75(NTR) and Nogo receptor complex mediates repulsive signaling by myelin-associated glycoprotein. Nature Neuroscience, 2002. 5(12): p. 1302-1308.
109. Hasegawa, Y., et al., Promotion of axon regeneration by myelin-associated glycoprotein and Nogo through divergent signals downstream of G(i)/G. Journal of Neuroscience, 2004. 24(30): p. 6826-6832.
110. Sivasankaran, R., et al., PKC mediates inhibitory effects of myelin and chondroitin sulfate proteoglycans on axonal regeneration. Nature Neuroscience, 2004. 7(3): p. 261-268.
111. Koprivica, V., et al., EGFR activation mediates inhibition of axon regeneration by myelin and chondroitin sulfate proteoglycans. Science, 2005. 310(5745): p. 106-110.
112. Etienne-Manneville, S. and A. Hall, Rho GTPases in cell biology. Nature, 2002. 420(6916): p. 629-635.
113. Jin, Z. and S.M. Strittmatter, Rad mediates collapsin-1-induced growth cone collapse. Journal of Neuroscience, 1997. 17(16): p. 6256-6263.

114. Jurney, W.M., et al., Rac1-mediated endocytosis during ephrin-A2-and semaphorin 3A-induced growth cone collapse. Journal of Neuroscience, 2002. 22(14): p. 6019-6028.
115. Kuhn, T.B., et al., Myelin and collapsin-1 induce motor neuron growth cone collapse through different pathways: Inhibition of collapse by opposing mutants of Rac1. Journal of Neuroscience, 1999. 19(6): p. 1965-1975.
116. Fournier, A.E., B.T. Takizawa, and S.M. Strittmatter, Rho kinase inhibition enhances axonal regeneration in the injured CNS. Journal of Neuroscience, 2003. 23(4): p. 1416-1423.
117. Lehmann, M., et al., Inactivation of Rho signaling pathway promotes CNS axon regeneration. Journal of Neuroscience, 1999. 19(17): p. 7537-7547.
118. Niederost, B., et al., Nogo-A and myelin-associated glycoprotein mediate neurite growth inhibition by antagonistic regulation of RhoA and Rac1. Journal of Neuroscience, 2002. 22(23): p. 10368-10376.
119. Taylor, J., et al., The scaffold protein POSH regulates axon outgrowth. Mol Biol Cell, 2008. 19(12): p. 5181-92.
120. Tapon, N., et al., A new Rac target POSH is an SHS-containing scaffold protein involved in the JNK and NF-kappa B signalling pathways. Embo Journal, 1998. 17(5): p. 1395-1404.
121. Fang, S. and A.M. Weissman, Ubiquitin-proteasome system. Cellular and Molecular Life Sciences, 2004. 61(13): p. 1546-1561.
122. Xu, Z.H., N.V. Kukekov, and L.A. Greene, POSH acts as a scaffold for a multiprotein complex that mediates JNK activation in apoptosis. Embo Journal, 2003. 22(2): p. 252-261.
123. Burbelo, P.D., D. Drechsel, and A. Hall, A Conserved Binding Motif Defines Numerous Candidate Target Proteins for Both Cdc42 and Rac GTPases. Journal of Biological Chemistry, 1995. 270(49): p. 29071-29074.
124. Nihalani, D., S. Merritt, and L.B. Holzman, Identification of structural and functional domains in mixed lineage kinase dual leucine zipper-bearing kinase required for complex formation and stress-activated protein kinase activation. Journal of Biological Chemistry, 2000. 275(10): p. 7273-7279.
125. Wang, C., et al., Regulation of the protein stability of POSH and MLK family. Protein & Cell, 2010. 1(9): p. 871-878.
126. Xu, Z.H., N.V. Kukekov, and L.A. Greene, Regulation of apoptotic c-Jun N-terminal kinase signaling by a stabilization-based feed-forward loop. Molecular and Cellular Biology, 2005. 25(22): p. 9949-9959.
127. Figueroa, C., et al., Akt2 negatively regulates assembly of the POSH-MLK-JNK signaling complex. Journal of Biological Chemistry, 2003. 278(48): p. 47922-47927.
128. Kim, A.H., et al., Akt1 regulates a JNK scaffold during excitotoxic apoptosis. Neuron, 2002. 35(4): p. 697-709.
129. Xu, Z.H., et al., The MLK family mediates c-Jun N-terminal kinase activation in neuronal apoptosis. Molecular and Cellular Biology, 2001. 21(14): p. 4713-4724.
130. Irving, E.A. and M. Bamford, Role of mitogen- and stress-activated kinases in ischemic injury. Journal of Cerebral Blood Flow and Metabolism, 2002. 22(6): p. 631-647.
131. Kim, G.H., E. Park, and J.K. Han, The assembly of POSH-JNK regulates Xenopus anterior neural development. Developmental Biology, 2005. 286(1): p. 256-269.
132. Berg, C.A., The Drosophila shell game: patterning genes and morphological change. Trends in Genetics, 2005. 21(6): p. 346-355.

133. Schnorr, J.D., et al., Ras1 interacts with multiple new signaling and cytoskeletal loci in Drosophila eggshell patterning and morphogenesis. Genetics, 2001. 159(2): p. 609-622.
134. Kim, G.H., et al., Novel function of POSH, a JNK scaffold, as an E3 ubiquitin ligase for the Hrs stability on early endosornes. Cellular Signalling, 2006. 18(4): p. 553-563.
135. Alroy, I., et al., The trans-Golgi network-associated human ubiquitin-protein ligase POSH is essential for HIV Woe 1 production. Proceedings of the National Academy of Sciences of the United States of America, 2005. 102(5): p. 1478-1483.
136. Tsuda, M., et al., The RING-finger scaffold protein Plenty of SH3s targets TAK1 to control immunity signalling in Drosophila. Embo Reports, 2005. 6(11): p. 1082-1087.
137. Tuvia, S., et al., The ubiquitin E3 ligase POSH regulates calcium homeostasis through spatial control of Herp. Journal of Cell Biology, 2007. 177(1): p. 51-61.
138. Hildebrand, J.D. and P. Soriano, Shroom, a PDZ domain-containing actin-binding protein, is required for neural tube morphogenesis in mice. Cell, 1999. 99(5): p. 485-497.
139. Hagens, O., et al., A new standard nomenclature for proteins related to Apx and Shroom. Bmc Cell Biology, 2006. 7.
140. Lee, C., M.P. Le, and J.B. Wallingford, The Shroom Family Proteins Play Broad Roles in the Morphogenesis of Thickened Epithelial Sheets. Developmental Dynamics, 2009. 238(6): p. 1480-1491.
141. Lee, C., H.M. Scherr, and J.B. Wallingford, Shroom family proteins regulate gamma-tubulin distribution and microtubule architecture during epithelial cell shape change. Development, 2007. 134(7): p. 1431-1441.
142. Zuckerman, J.B., et al., Association of the epithelial sodium channel with Apx and alpha-spectrin in A6 renal epithelial cells. Journal of Biological Chemistry, 1999. 274(33): p. 23286-23295.
143. Hagens, O., et al., Disruptions of the novel KIAA1202 gene are associated with X-linked mental retardation. Human Genetics, 2006. 118(5): p. 578-590.
144. Hildebrand, J.D., Shroom regulates epithelial cell shape via the apical positioning of an actomyosin network. Journal of Cell Science, 2005. 118(22): p. 5191-5203.
145. Nishimura, T. and M. Takeichi, Shroom3-mediated recruitment of Rho kinases to the apical cell junctions regulates epithelial and neuroepithelial planar remodeling. Development, 2008. 135(8): p. 1493-1502.
146. Yoder, M. and J.D. Hildebrand, Shroom4 (Kiaa1202) is an actin-associated protein implicated in cytoskeletal organization. Cell Motility and the Cytoskeleton, 2007. 64(1): p. 49-63.
147. Leung, T., et al., The p160 RhoA-binding kinase ROK alpha is a member of a kinase family and is involved in the reorganization of the cytoskeleton. Molecular and Cellular Biology, 1996. 16(10): p. 5313-5327.
148. Leung, T., et al., A NOVEL SERINE/THREONINE KINASE BINDING THE RAS-RELATED RHOA GTPASE WHICH TRANSLOCATES THE KINASE TO PERIPHERAL MEMBRANES. Journal of Biological Chemistry, 1995. 270(49): p. 29051-29054.
149. Riento, K. and A.J. Ridley, Rocks: Multifunctional kinases in cell behaviour. Nature Reviews Molecular Cell Biology, 2003. 4(6): p. 446-456.
150. Chen, X.Q., et al., Characterization of RhoA-binding kinase ROK alpha implication of the pleckstrin homology domain in ROK alpha function using

region-specific antibodies. Journal of Biological Chemistry, 2002. 277(15): p. 12680-12688.
151. Feng, J.H., et al., Rho-associated kinase of chicken gizzard smooth muscle. Journal of Biological Chemistry, 1999. 274(6): p. 3744-3752.
152. Coleman, M.L., et al., Membrane blebbing during apoptosis results from caspase-mediated activation of ROCK I. Nature Cell Biology, 2001. 3(4): p. 339-345.
153. Sebbagh, M., et al., Caspase-3-mediated cleavage of ROCK I induces MLC phosphorylation and apoptotic membrane blebbing. Nature Cell Biology, 2001. 3(4): p. 346-352.
154. Ward, Y., et al., The GTP binding proteins Gem and Rad are negative regulators of the Rho-Rho kinase pathway. Journal of Cell Biology, 2002. 157(2): p. 291-302.
155. Amano, M., et al., Myosin II activation promotes neurite retraction during the action of Rho and Rho-kinase. Genes to Cells, 1998. 3(3): p. 177-188.
156. Amano, M., et al., Phosphorylation and activation of myosin by Rho-associated kinase (Rho-kinase). Journal of Biological Chemistry, 1996. 271(34): p. 20246-20249.
157. Chihara, K., et al., Cytoskeletal rearrangements and transcriptional activation of c-fos serum response element by Rho-kinase. Journal of Biological Chemistry, 1997. 272(40): p. 25121-25127.
158. Kimura, K., et al., Regulation of myosin phosphatase by Rho and Rho-Associated kinase (Rho-kinase). Science, 1996. 273(5272): p. 245-248.
159. Arimura, N., et al., Phosphorylation of collapsin response mediator protein-2 by Rho-kinase - Evidence for two separate signaling pathways for growth cone collapse. Journal of Biological Chemistry, 2000. 275(31): p. 23973-23980.
160. Goshima, Y., et al., COLLAPSIN-INDUCED GROWTH CONE COLLAPSE MEDIATED BY AN INTRACELLULAR PROTEIN RELATED TO UNC-33. Nature, 1995. 376(6540): p. 509-514.
161. Alabed, Y.Z., et al., Neuronal responses to myelin are mediated by rho kinase. Journal of Neurochemistry, 2006. 96(6): p. 1616-1625.
162. Duffy, P., et al., Rho-Associated Kinase II (ROCKII) Limits Axonal Growth after Trauma within the Adult Mouse Spinal Cord. Journal of Neuroscience, 2009. 29(48): p. 15266-15276.
163. Gallo, K.A. and G.L. Johnson, Mixed-lineage kinase control of JNK and p38 MAPK pathways. Nature Reviews Molecular Cell Biology, 2002. 3(9): p. 663-672.
164. Teramoto, H., et al., Signaling from the small GTP-binding proteins Rac1 and Cdc42 to the c-Jun N-terminal kinase stress-activated protein kinase pathway - A role for mixed lineage kinase 3 protein-tyrosine kinase 1, a novel member of the mixed lineage kinase family. Journal of Biological Chemistry, 1996. 271(44): p. 27225-27228.
165. Holzman, L.B., S.E. Merritt, and G. Fan, IDENTIFICATION, MOLECULAR-CLONING, AND CHARACTERIZATION OF DUAL LEUCINE-ZIPPER BEARING KINASE - NOVEL SERINE/THREONINE PROTEIN-KINASE THAT DEFINES A 2ND SUBFAMILY OF MIXED LINEAGE KINASES. Journal of Biological Chemistry, 1994. 269(49): p. 30808-30817.
166. Sakuma, H., et al., Molecular cloning and functional expression of a cDNA encoding a new member of mixed lineage protein kinase from human brain. Journal of Biological Chemistry, 1997. 272(45): p. 28622-28629.
167. Ikeda, A., et al., Identification and characterization of functional domains in a mixed lineage kinase LZK. Febs Letters, 2001. 488(3): p. 190-195.

168. Merritt, S.E., et al., The mixed lineage kinase DLK utilizes MKK7 and not MKK4 as substrate. Journal of Biological Chemistry, 1999. 274(15): p. 10195-10202.
169. Ikeda, A., et al., Mixed lineage kinase LZK forms a functional signaling complex with JIP-1, a scaffold protein of the c-Jun NH2-terminal kinase pathway. Journal of Biochemistry, 2001. 130(6): p. 773-781.
170. Nihalani, D., et al., Mixed lineage kinase-dependent JNK activation is governed by interactions of scaffold protein JIP with MAPK module components. Embo Journal, 2001. 20(13): p. 3447-3458.
171. Nihalani, D., H.N. Wong, and L.B. Holzman, Recruitment of JNK to JIP1 and JNK-dependent JIP1 phosphorylation regulates JNK module dynamics and activation. Journal of Biological Chemistry, 2003. 278(31): p. 28694-28702.
172. Nihalani, D., et al., Src family kinases directly regulate JIP1 module dynamics and activation. Molecular and Cellular Biology, 2007. 27(7): p. 2431-2441.
173. Hammarlund, M., et al., Axon Regeneration Requires a Conserved MAP Kinase Pathway. Science, 2009. 323(5915): p. 802-806.
174. Po, M.D., C. Hwang, and M. Zhen, PHRs: bridging axon guidance, outgrowth and synapse development. Current Opinion in Neurobiology, 2010. 20(1): p. 100-107.
175. Hirai, S., et al., The c-Jun N-terminal kinase activator dual leucine zipper kinase regulates axon growth and neuronal migration in the developing cerebral cortex. Journal of Neuroscience, 2006. 26(46): p. 11992-12002.
176. Eto, K., et al., Role of dual leucine zipper-bearing kinase (DLK/MUK/ZPK) in axonal growth. Neuroscience Research, 2010. 66(1): p. 37-45.
177. Hirai, S., et al., Axon Formation in Neocortical Neurons Depends on Stage-Specific Regulation of Microtubule Stability by the Dual Leucine Zipper Kinase-c-Jun N-Terminal Kinase Pathway. Journal of Neuroscience, 2011. 31(17): p. 6468-6480.
178. Zhang, Q.G., et al., Knock-down of POSH expression is neuroprotective through down-regulating activation of the MLK3-MKK4-JNK pathway following cerebral ischaemia in the rat hippocampal CA1 subfield. Journal of Neurochemistry, 2005. 95(3): p. 784-795.

Chapter 2

POSH is an intracellular signal transducer for the axon outgrowth inhibitor Nogo66

2.1 Introduction

The regenerative and plastic capacity of the adult mammalian CNS is limited, contributing to poor functional recovery after injury or disease. CNS axons are capable of regenerating but fail to do so, in part because factors present in the CNS actively prevent axon outgrowth [1-4]. Factors that limit axon outgrowth and plasticity have been purified from CNS myelin and include myelin associated glycoprotein (MAG), oligodendrocyte myelin glycoprotein (OMgp), and NogoA [1, 4-6]. In addition to limiting axon outgrowth and plasticity in the adult CNS, NogoA also regulates axon outgrowth and plasticity during development [6-13].

Nogo66, an axon outgrowth inhibitory domain of NogoA, engages cell surface receptors, Nogo66 Receptor 1 (NgR1) and Paired Immunoglobulin-like Receptor B (PirB), to mediate intracellular signal transduction [7, 14-16]. NgR1 links to Rho and its downstream effector Rho kinase to regulate cytoskeletal dynamics associated with growth cone collapse and inhibition of axon outgrowth [1, 4]. PirB is a recently identified receptor for myelin-derived inhibitory substrates [7, 11]. The signaling pathway activated when myelin derived inhibitors engage PirB is not known. However, in hematopoietic cells, where PirB signaling has been more extensively studied, phosphorylation of the receptor at specific tyrosines by src family kinases recruits SH2-homology-containing protein tyrosine phosphatases SHP1 and SHP2 [17, 18].

Plenty of SH3s (POSH, also known as SH3rf1) is an intracellular multidomain scaffold protein that regulates diverse biological functions, including apoptosis, calcium homeostasis, morphogenesis, and neuronal process outgrowth [19-25]. POSH contains multiple protein-protein interaction domains, including an amino-terminal RING domain, four Src homology 3 (SH3) domains, and a Rac binding domain. As a scaffold protein, POSH exerts its function through interacting partners, which include the actin-myosin regulatory protein Shroom3, the small GTPase Rac, and mixed lineage kinases [21, 22, 24, 26]. Our laboratory previously reported that POSH limits axon growth through a Shroom3-ROCK-myosin signaling pathway [22]. Here, we demonstrate that the scaffold protein POSH, in association with Shroom3 and the mixed lineage kinase LZK, relays axon outgrowth inhibition downstream of NogoA and PirB.

2.2 Results

2.2.1 POSH RNAi neurons are refractory to myelin and Nogo66-mediated inhibition of axon outgrowth

In a previous report, we demonstrated that POSH limits axon outgrowth through a Shroom3-ROCK-myosin signaling pathway [22]. To determine whether myelin inhibitors signal to POSH to limit axon outgrowth, control neurons or neurons with RNAi mediated knockdown of POSH function were assessed for their ability to extend processes in the presence of CNS myelin. Mouse primary embryonic cortical neurons were nucleofected with control or POSH RNAi expression vectors and cultured on poly-L-lysine/laminin (PLL) with or without purified myelin. The UI4-SIBR RNAi vectors express a single vector derived transcript for RNAi and GFP expression, with GFP expression identifying the transfected neurons [22, 27]. Process outgrowth in GFP-labeled cortical neurons was analyzed 72 hours after nucleofection and plating. Myelin reduced average process length of control RNAi transfected neurons to 66% of the length on PLL only (Figure 2.1A-B, G). POSH RNAi neurons exhibited increased process length relative to control RNAi neurons, when plated on PLL, as we previously reported

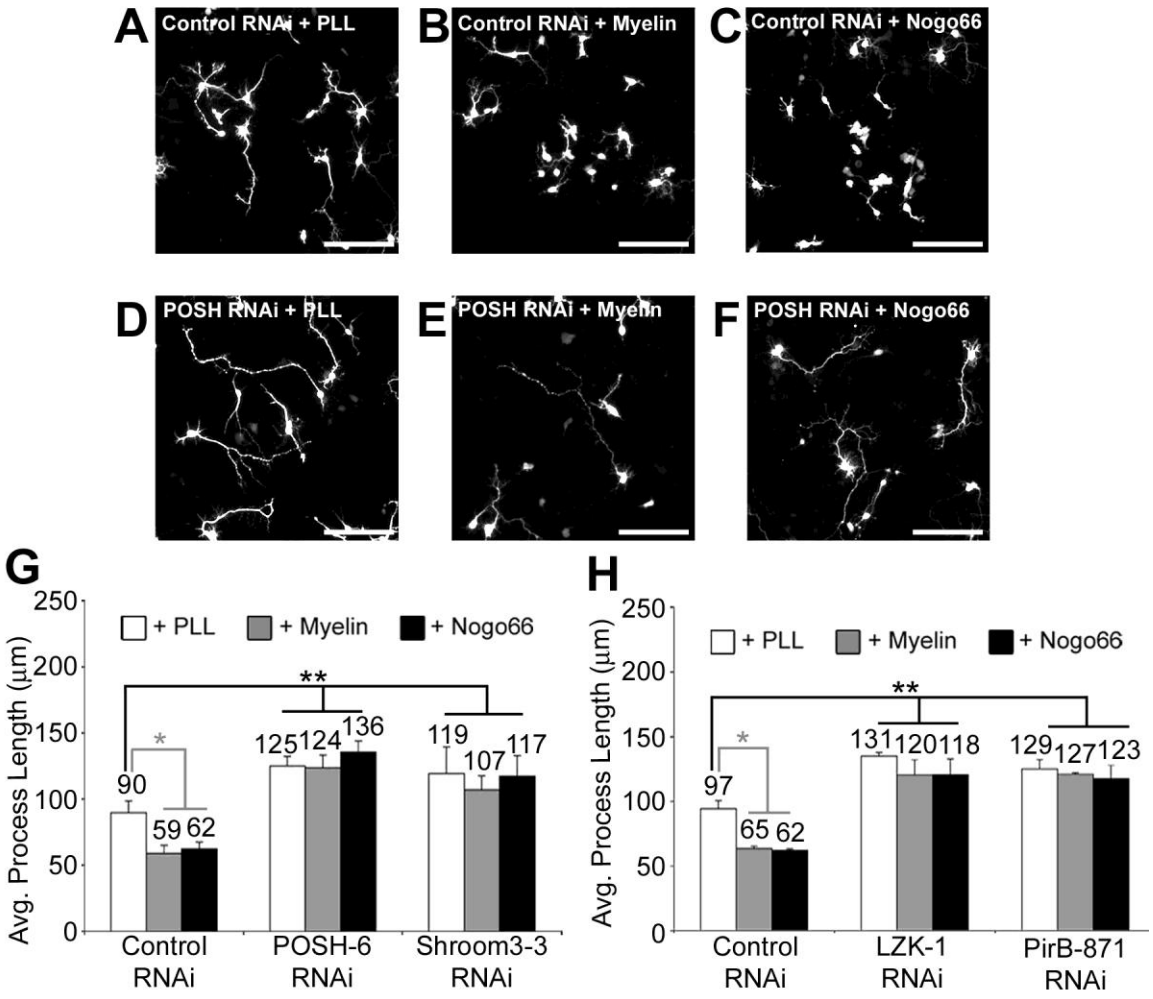

Figure 2.1 Primary cortical neurons with RNAi knockdown of POSH, POSH associated proteins, or the PirB receptor are refractory to myelin and Nogo66-mediated inhibition of axon outgrowth.

(A-H) Cortical neurons (embryonic day 14.5) were nucleofected with the indicated RNAi expression vectors and plated to poly-l-lysine/laminin (PLL) (A,D), PLL plus myelin (B,E), or PLL plus Nogo66 (C,F) coated dishes. Neurons were fixed 3 days after nucleofection, stained for GFP, and process length was determined. RNAi vectors express GFP and a specific siRNA from a single vector-derived transcript. The control RNAi vector expresses a functional siRNA that targets luciferase and serves as a control for non-specific effects. POSH-6, Shroom3-3, LZK-1 and PirB-871 RNAi vectors express specific siRNAs that target POSH, Shroom3, LZK, and PirB receptor mRNA sequences, respectively. Scale bars, 100μm.
(G, H) Average process length was determined from three independent experiments, with 551-810 neurons in total measured per condition. Myelin and Nogo66 reduced average process length of control neurons. In contrast, neither myelin nor Nogo66 reduced average process length of POSH, Shroom3, LZK or PirB-RNAi knockdown neurons. *p,**p<0.0001; Student's *t* test.

[22], indicating that POSH negatively regulates process outgrowth (Figure 2.1A, D, G). Strikingly, process length of POSH RNAi neurons was not reduced when plated on myelin (Figure 2.1D-E, G). The observation that POSH RNAi neurons are refractory to inhibition by myelin suggests that in primary cortical neurons myelin based inhibitors act through a signaling pathway that includes POSH.

Several proteins in myelin limit process outgrowth, including NogoA [1, 5]. We tested whether Nogo66, a soluble domain of the NogoA ligand, inhibits process outgrowth of control or POSH RNAi neurons. Primary cortical neurons were nucleofected with control or POSH RNAi expression vectors and cultured on bacterially expressed and purified Nogo66. Process length was assessed in fixed, GFP-stained neurons. Nogo66 inhibited process length of control RNAi neurons (Figure 2.1A, C, G). In contrast, POSH RNAi neurons were refractory to the inhibitory action of Nogo66 (Figure 2.1D, F-G). This result suggests that Nogo66 signals to POSH to inhibit process outgrowth and that the inhibitory action of myelin is mediated, at least in part, through a NogoA/POSH signaling pathway.

2.2.2 POSH associated proteins, Shroom3 and LZK, negatively regulate axon length and are intracellular signal transducers of myelin and Nogo66

POSH regulates biological outcomes by assembling a protein interaction network, which includes the actin-myosin regulatory protein Shroom3 and the mixed lineage kinase LZK [24, 28]. To determine whether these known binding partners for POSH mediate myelin inhibition, primary cortical neurons were nucleofected with control, Shroom3, or LZK RNAi vectors and process outgrowth was analyzed in the presence or absence of myelin. Inhibition of Shroom3 function by RNAi resulted in increased process length relative to control neurons when neurons were plated to PLL (Figure 2.1G), consistent with our previous study demonstrating that the POSH-Shroom3 complex inhibits process outgrowth [22]. Likewise, LZK RNAi cortical neurons exhibited increased process lengths when plated to PLL relative to control neurons (Figure 2.1H and Figure 2.2),

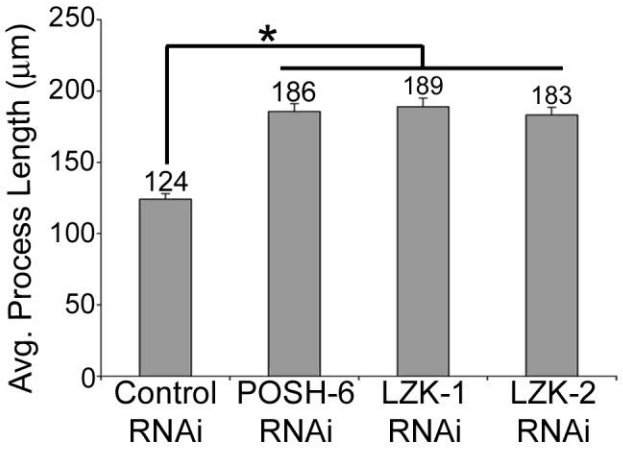

Figure 2.2 LZK negatively regulates axon outgrowth

(A) RNAi-mediated reduction in LZK function in primary cortical neurons results in an increase in process length. LZK-1 and LZK-2 are two independent RNAi constructs targeting different LZK mRNA sequences. A total of 394-437 neurons per condition from three independent experiments were measured for process length. *$p < 0.0001$, Student's *t* test.

consistent with a role for LZK as a negative regulator of process outgrowth. Plating to myelin did not inhibit process length of Shroom3 or LZK RNAi neurons (Figure 2.1G-H). In addition, process length was not decreased when Shroom3 or LZK RNAi neurons were plated to Nogo66 (Figure 2.1G-H). Thus, reducing Shroom3 or LZK function with RNAi results in neurons that are refractory to myelin and Nogo66 inhibition. Taken together, the observations that POSH and its binding partners Shroom3 and LZK modulate responsiveness to myelin and Nogo66 identify the POSH complex as an intracellular signal transducer for myelin-derived inhibitors.

2.2.3 POSH is required for Nogo66 inhibition of axon outgrowth in CGNs

Since different neuronal cell types could utilize different mechanisms for Nogo66 inhibition and Nogo66 also inhibits axon outgrowth in cerebellar granule neurons (CGNs), we investigated whether POSH mediates inhibition of axon outgrowth in response to Nogo66 in postnatal CGNs [7, 29]. Like cortical neurons, POSH RNAi CGNs were refractory to the inhibitory action of Nogo66 (Figure 2.3A-E), suggesting that a POSH-dependent mechanism operates in different neuronal cell types to inhibit axon outgrowth in response to Nogo66.

2.2.4 Nogo inhibits axon outgrowth in both a cell-autonomous and non-cell-autonomous fashion

Like NogoA, POSH is expressed in mouse embryonic cortical neurons in vitro (Figure 2.4A) [10, 30, 31]. Given this overlap in expression, RNAi mediated reduction of NogoA function was used to investigate the potential for signaling from endogenous NogoA to POSH. Cortical primary neurons were nucleofected with control or Nogo specific RNAi expression vectors to determine if Nogo expression in cortical neurons limits axon outgrowth. The Nogo gene encodes for three variants, NogoA-C that share a carboxyl terminal neurite outgrowth inhibitory domain, Nogo66 [1,[14, 15]. In addition, NogoA has a unique domain, not present in NogoB-C, which inhibits neurite outgrowth [15]. The Nogo-3 RNAi

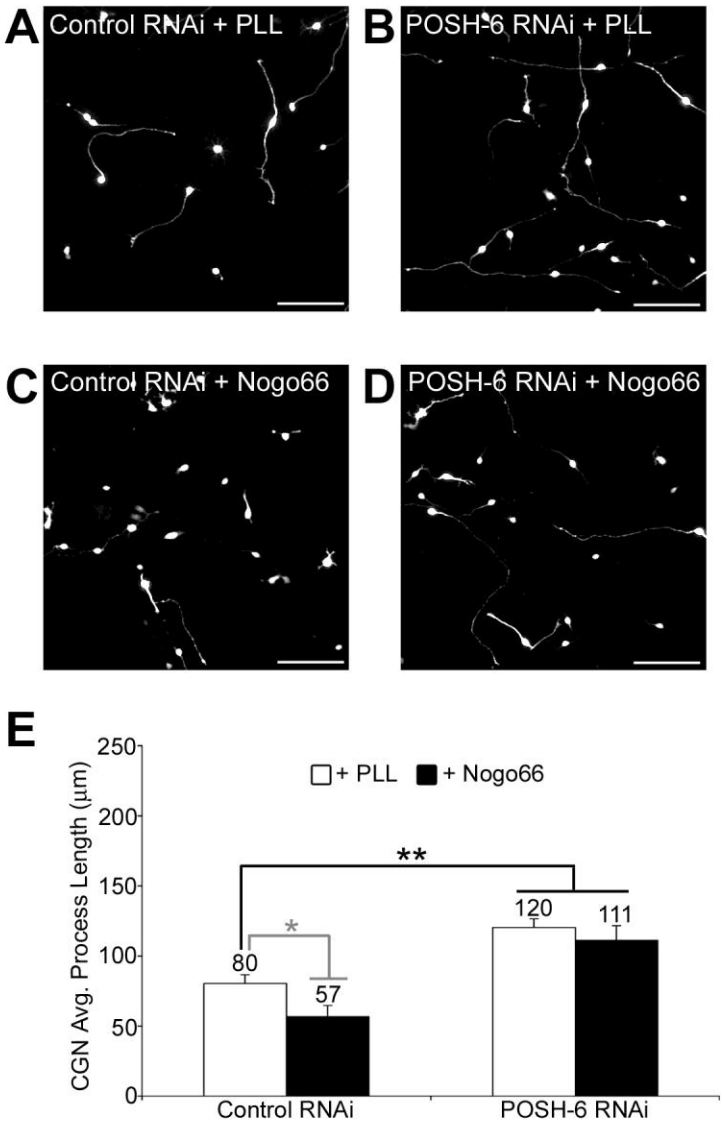

Figure 2.3 POSH is required for Nogo66 inhibition of axon outgrowth in primary mouse cerebellar granule neurons (CGNs)

(A-D) CGNs nucleofected with a control RNAi vector are inhibited by Nogo66 (A,C). CGNs transfected with a POSH RNAi vectors are refractory to Nogo66-mediated inhibition of axon outgrowth (B,D). CGNs were fixed and stained for GFP 36 hours after nucleofection and plated to poly-L-lysine/laminin (PLL) or PLL+Nogo66, upper panels.
(E) Average process length was determined in three independent experiments, resulting in a total of 347-404 neurons measured per condition.*p, ** $p<0.0001$ Students *t* test.

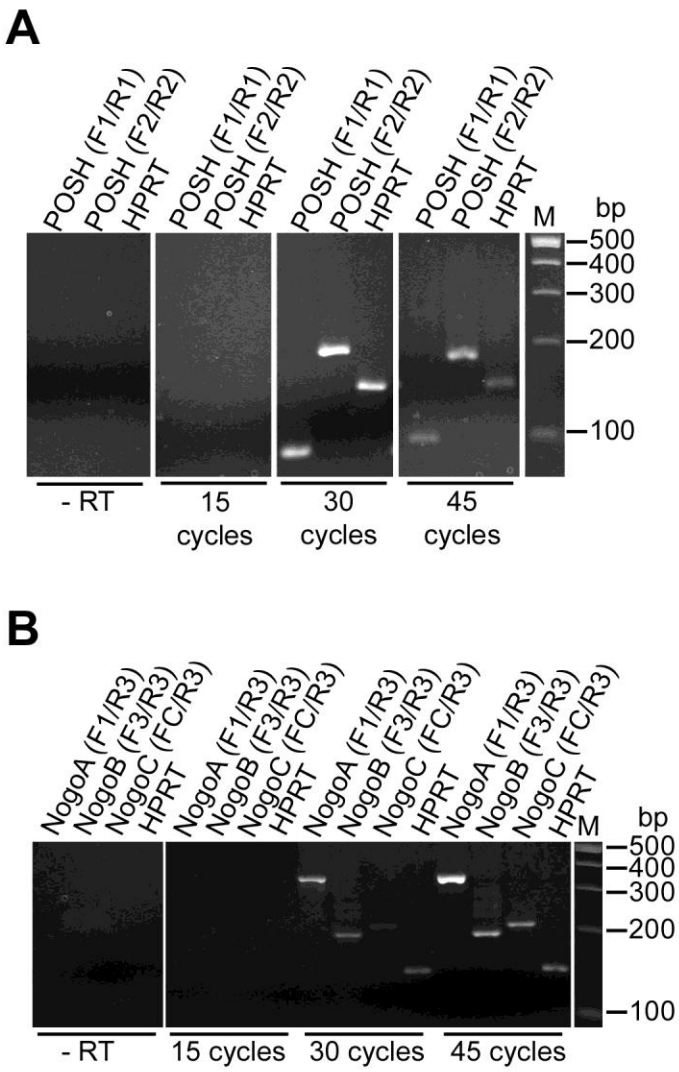

Figure 2.4 POSH and NogoA, B and C are expressed in cortical neurons

(A) RT-PCR analysis of POSH expression in cortical neurons. cDNA made from RNA isolated from cortical neurons was analyzed for POSH expression using two distinct primer pairs. POSH F1/R1 amplifies a 99bp fragment of POSH between nucleotides 1066 and 1165 in its coding region, while POSH F2/R2 amplifies 187bp fragment between nucleotides 40 and 227 of the POSH 3'UTR. HPRT was used as a reaction control. POSH mRNA is detected in cortical neurons.
(B) RT-PCR analysis of Nogo/Rtn4 expression in cortical neurons. cDNA from RNA isolated from cortical neurons was analyzed for Nogo A, B, or C expression with primers that recognize an exon unique to a specific mRNA spliced form (NogoA, F1/R3; NogoC, FC/R3) or with primers that produce a PCR fragment of a distinct, characteristic size (NogoB, F3/R3). HPRT was used as a RT-PCR control. Nogo A, B, and C are expressed in cultured cortical neurons.

construct targets the exon unique to NogoA, which is absent from NogoB and NogoC, and thus this construct specifically targets NogoA (Figure 2.5). Process length in Nogo-3 RNAi-depleted neurons was increased relative to control (Figure 2.6A), as expected if NogoA limits process outgrowth. Similar results were obtained with a second siRNA, Nogo-1, that targets the 3'UTR of the Nogo mRNA, reducing the expression of Nogo isoforms, NogoA/B (Figure 2.5). The Nogo-1 RNAi construct is also expected to reduce the expression of NogoC since the 3'UTR is conserved among the mRNAs for the three Nogo isoforms and RT-PCR analysis indicates that NogoC, along with NogoA/B, is expressed in cortical neurons (Figure 2.4B). Together, these results support a role for NogoA as an inhibitor of process outgrowth of cortical neurons grown in culture, and suggest that NogoB and C do not function redundantly with NogoA to regulate process outgrowth.

Since RNAi mediated reduction of NogoA function in neurons enhances process length, this result suggests that NogoA acts in a cell autonomous, intrinsic fashion to inhibit process outgrowth. In addition, NogoA can act in a non-cell autonomous fashion, as process outgrowth of control cortical neurons is inhibited when plated directly onto purified Nogo66 protein (Figure 2.1 and Figure 2.6B). Finally, purified Nogo66 protein, added externally, reverses the NogoA RNAi phenotype (Figure 2.6B), unlike the addition of Nogo66 to PirB RNAi neurons (compare Figures 2.6B and Figure 2.1H), indicating that cells in which NogoA is reduced can still respond to external Nogo66 as expected.

2.2.5 Suppression of Myosin IIA function reverses the Nogo RNAi phenotype

Myosin IIA RNAi reverses the increase in process length associated with RNAi-depletion of POSH or the POSH associated proteins, Shroom3 and LZK (Figure 2.7A and [22]). However, myosin IIA RNAi does not reverse the increase in process length resulting from RNAi-mediated reduction of the neurite outgrowth inhibitors Robo1 or Ephrin B2 [22]. The molecular mechanism by

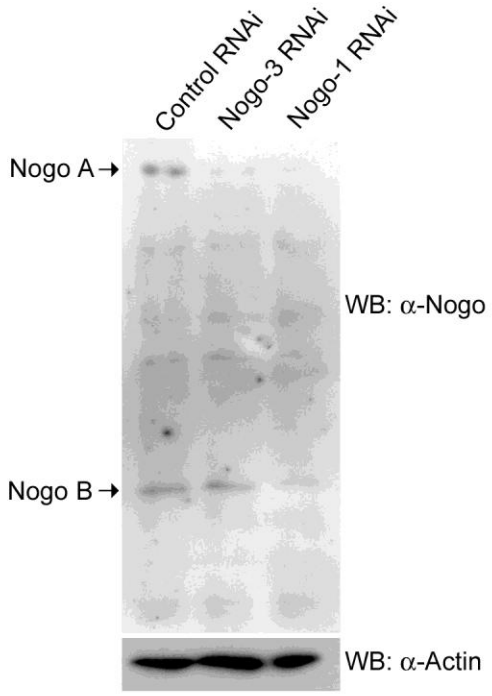

Figure 2.5 RNAi mediated reduction of Nogo

(A) RNAi-mediated reduction of Nogo. Extracts were prepared from puromycin selected P19 cells transiently transfected with the indicated UI4-SIBR-GFP RNAi expression vectors and a GFP/puromycin expression vector. The Nogo-3 RNAi vector, by targeting a unique exon in NogoA, specifically inhibits NogoA only. The Nogo-1 RNAi vector targets the Nogo 3'UTR and therefore reduces expression of all three Nogo isoforms (Nogo A-C). Endogenous Nogo protein was detected in extracts by western blot analysis with a NogoA/B specific antibody (upper panel). Western blot for actin, internal loading control (lower panel).

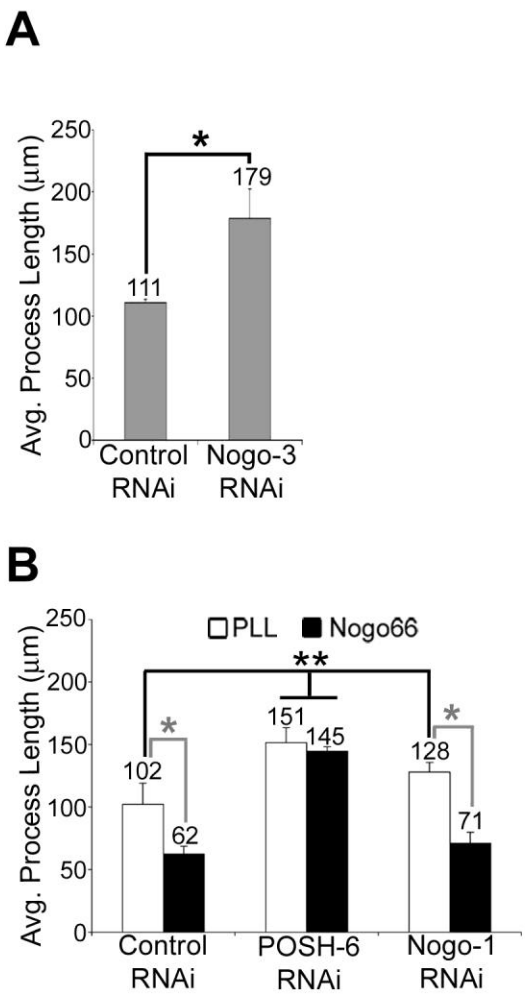

Figure 2.6 Nogo inhibits axon outgrowth in cortical neurons in both a cell autonomous and non-cell autonomous fashion

(A-B) Primary cortical neurons were nucleofected with the indicated RNAi constructs, plated to PLL (A-B) or PLL plus Nogo66 (B) and process length determined on fixed, GFP expressing neurons. Average process length was determined from three independent experiments, with a combined total of 364-521 neurons measured per condition.
(A) RNAi mediated reduction of NogoA function enhances axon outgrowth of primary cortical neurons. The Nogo-3 RNAi vector targets an exon unique to NogoA mRNA, selectively reducing the expression of NogoA but not NogoB or C. *$p < 0.0001$, Student's *t* test.
(B) External addition of purified Nogo66 reverses the Nogo RNAi phenotype. Process length was determined 3 days after nucleofection and plating to PLL or PLL plus Nogo66. *p,**$p < 0.0001$, Student's *t* test.

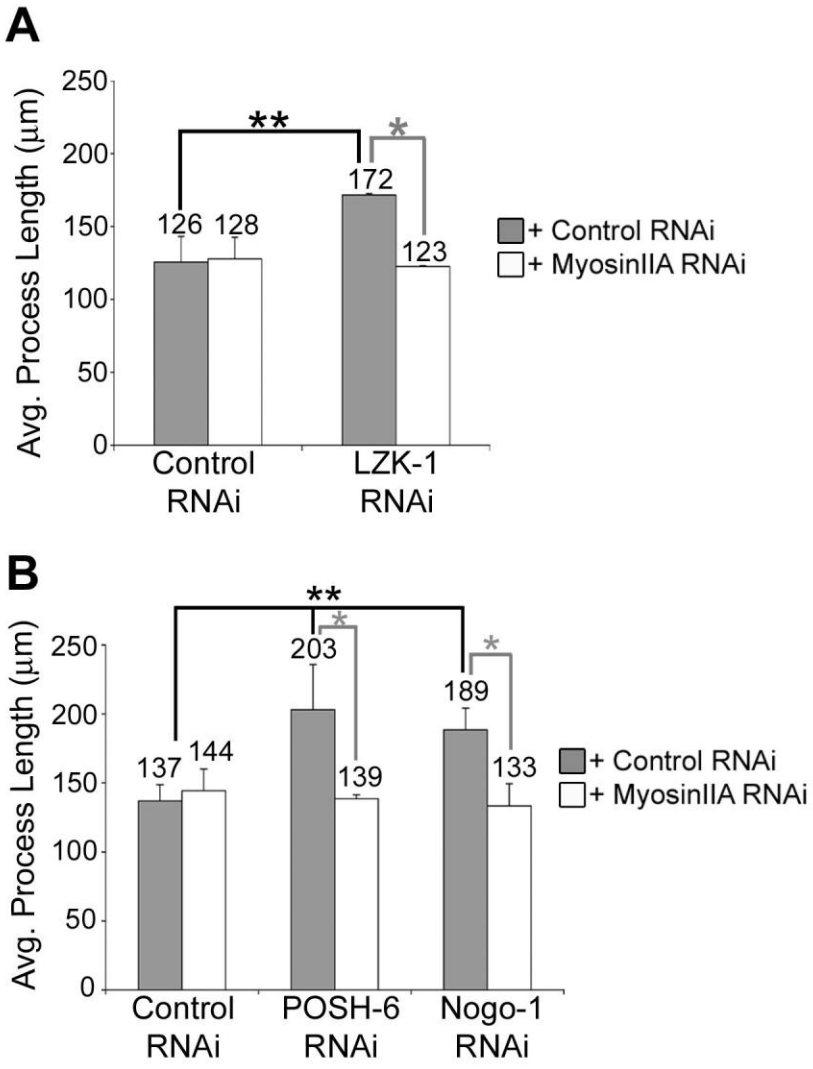

Figure 2.7 Myosin IIA reduction by RNAi reverses the POSH, LZK, and Nogo RNAi phenotype

(A) Attenuation of LZK RNAi enhanced process outgrowth phenotype by RNAi mediated reduction of myosin IIA. Primary cortical neurons were nucleofected with control or LZK RNAi expression vectors and either a control RNAi vector or an RNAi vector that reduces myosin IIA function. Average process length of fixed, GFP nucleofected neurons was determined from three independent experiments (395-477 neurons in total per condition). *p,**p < 0.0001, Student's *t* test.
(B) RNAi mediated reduction of NogoA-C enhances axon outgrowth. As observed for POSH RNAi, enhanced axon outgrowth from Nogo RNAi is reversed by a reduction in myosin IIA function. Nogo-1 RNAi targets the 3'UTR of the Nogo mRNA, reducing expression of NogoA-C. *p,**p < 0.0001, Student's *t* test.

which a reduction in myosin IIA function suppresses axon outgrowth in neurons deficient in POSH function, but not Ephrin B2 or Robo1, remains to be determined. Nonetheless, these observations suggest that myosin IIA reduction of function can distinguish among pathways that negatively regulate axon outgrowth, with some pathways sensitive to myosin IIA reduction of function (e.g. POSH) and others insensitive (Ephrin B2, Robo), and this provides a useful tool to assess whether specific components might be associated with a POSH signaling pathway for axon outgrowth inhibition.

The ability of myosin IIA RNAi to suppress axon outgrowth was used to test whether NogoA signals to POSH to regulate process outgrowth. Primary cortical neurons were nucleofected with control, POSH or Nogo RNAi expression vectors, together with a myosin IIA RNAi expression vector. As reported previously, control neuron process length was unaffected by myosin IIA RNAi, and POSH RNAi neuron process length was reduced by myosin IIA RNAi (Figure 2.7B). Process length of Nogo RNAi neurons was also reduced by myosin IIA RNAi (Figure 2.7B), consistent with the hypothesis that NogoA signals through a POSH dependent pathway to regulate process outgrowth.

2.2.6 LZK is a downstream effector of a Nogo/POSH signaling pathway

Next, suppression analysis was used to test the hypothesis that LZK is a functional effector for Nogo signaling and to order the genes in the signaling pathway. If increased expression of LZK can compensate for loss of Nogo function, then this observation would support a role for LZK as a downstream effector of Nogo signaling. Cortical neurons were nucleofected with a Nogo RNAi expression vector and a control vector or a vector that expresses catalytically active or inactive forms of LZK. The efficiency of nucleofection of both plasmids was 94% (data not shown). Ectopic expression of wild type, but not catalytically inactive, LZK suppressed the enhanced process length phenotype exhibited by Nogo RNAi nucleofected neurons (Figure 2.8A-E). Suppression of the Nogo

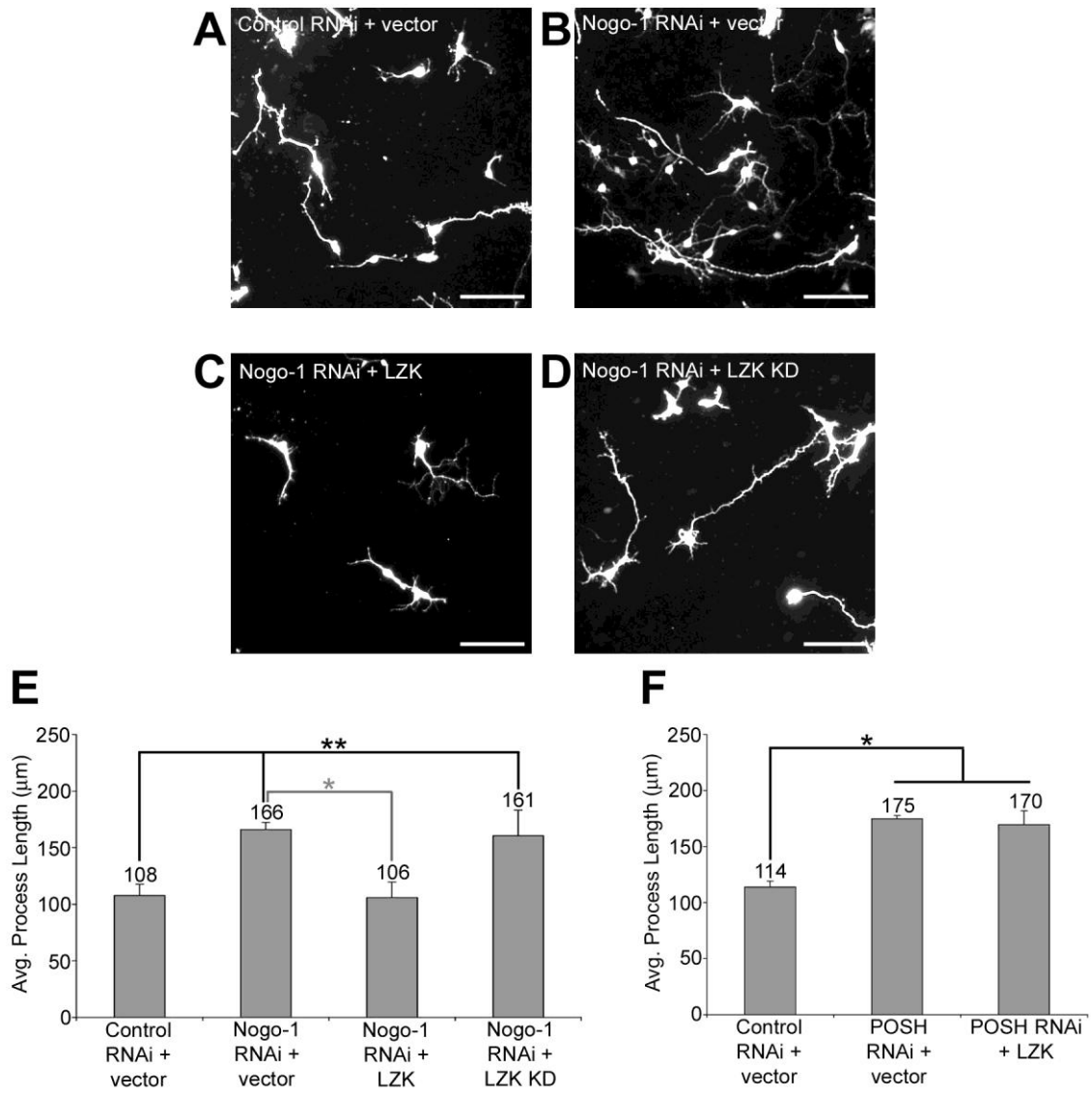

Figure 2.8 LZK is a downstream effector of a Nogo/POSH signaling pathway.

(A-E) LZK functions downstream of Nogo. Cortical neurons were nucleofected with the indicated RNAi vectors and expression vectors for wild-type LZK, kinase dead (K/D) LZK, or vector control. Nucleofected neurons were fixed and stained for GFP 72 hours after nucleofection. Measurements were made on 237-312 neurons per condition from three independent experiments. The increase in process length from Nogo RNAi is reversed by ectopic expression of catalytically active, but not kinase dead, LZK.*p,**p < 0.0001, Student's *t* test. Scale bar, 100μm

(F) LZK suppression is POSH-dependent. Primary neurons were nucleofected with control or POSH RNAi vectors and an expression vector for wild type LZK or vector control. In total, 325-414 neurons were measured per condition from three independent experiments. Ectopic expression of catalytically active LZK fails to reverse the POSH RNAi-mediated increase in process length. *p < 0.0001, Student's *t* test.

RNAi knockdown phenotype by increased expression of LZK is consistent with a model in which Nogo/POSH signaling is mediated, at least in part, by LZK. It is also possible that increased LZK activity suppresses by activating a compensatory signaling pathway, not directly linked to NogoA function. However, this is unlikely because increased expression of LZK did not suppress process outgrowth of POSH RNAi neurons (Figure 2.8F), indicating that LZK suppression of process outgrowth requires the POSH scaffold. Together, these observations indicate that LZK regulates process outgrowth inhibition in a POSH-dependent manner downstream of NogoA.

2.2.7 The PirB receptor transmits inhibitory signal from myelin and Nogo66 to the LZK-POSH complex

PirB is a functional receptor for Nogo and MAG in CGNs and dorsal root ganglion neurons [7]. If PirB transmits axon outgrowth inhibitory signals in cortical neurons, then reducing PirB function with RNAi should lead to increased process length. Cortical neurons with an RNAi mediated reduction in PirB function exhibited an increase in process length (Figure 2.9A), consistent with PirB functioning as a negative regulator of process outgrowth. A second RNAi construct, targeting a different PirB sequence, gave a similar result (data not shown and Figure 2.9B). Further, if PirB is acting as a receptor to transmit inhibitory signals from myelin and NogoA in cortical neurons, then PirB RNAi neurons should be refractory to myelin and Nogo66 inhibition. Process length of PirB RNAi neurons was unaffected by myelin and Nogo66 (Figure 2.1H), supporting a role for PirB in myelin/Nogo mediated inhibition in cortical neurons. Moreover, if PirB acts through POSH to inhibit process outgrowth, then myosin IIA RNAi is expected to reverse the PirB RNAi phenotype. Indeed, PirB RNAi neuronal process length was decreased by RNAi mediated reduction in myosin IIA (Figure 2.9C). Finally, if PirB signals to the POSH complex, then ectopic expression of LZK is expected to reverse the PirB RNAi phenotype. Overexpression of LZK in PirB RNAi-depleted cortical neurons reduced process length to control levels (Figure 2.9A), supporting a role for the PirB receptor in

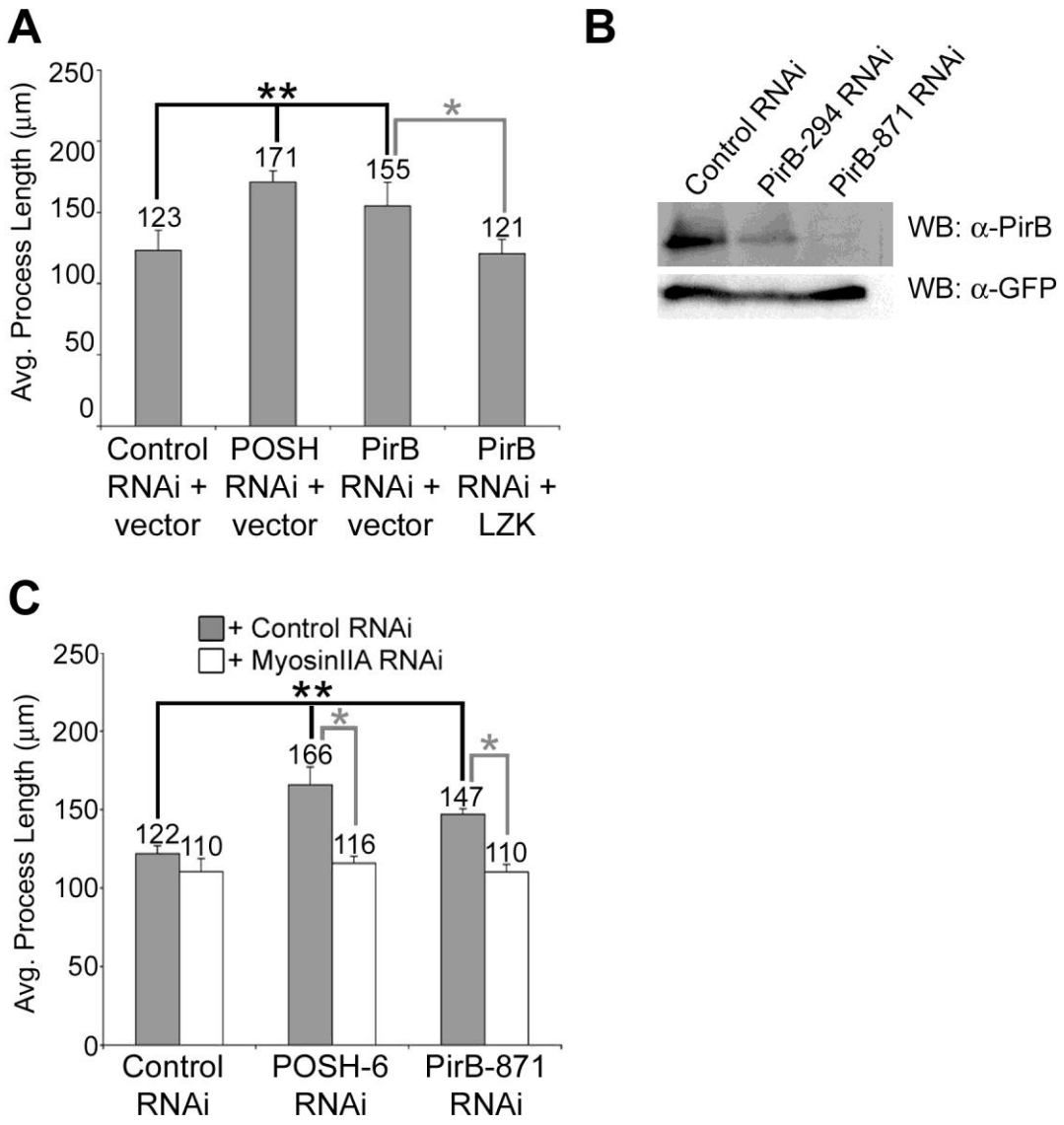

Figure 2.9 The PirB receptor transmits inhibitory signals from myelin and Nogo66 to the LZK-POSH scaffold complex

(A,C) Primary cortical neurons were nucleofected with the indicated RNAi vectors, plated to PLL, and process length scored 72 hours after nucleofection. In total, 359-627 neurons were measured per condition from three independent experiments.
(A) LZK functions downstream of PirB. The PirB RNAi-mediated increase in process length is reversed by ectopic expression of LZK. *p,**p < 0.0001, Student's *t* test.
(B) RNAi-mediated reduction of PirB. HEK293 cells were transiently transfected with a PirB expression construct and the indicated PirB RNAi construct, which also expresses GFP. PirB-294 and PirB-871 target different sequences in the PirB coding region. PirB was detected in extracts by western blot analysis with a PirB specific antibody (upper panel). Western blot for GFP, loading control (lower panel).
(C) As observed for POSH RNAi, reduction of myosin IIA function reverses the PirB RNAi phenotype. *p,**p < 0.0001, Student's *t* test.

transmitting inhibitory cues to the POSH/LZK complex to regulate process outgrowth.

2.3 Discussion

Together, these results define a central role for the POSH complex in relaying process outgrowth inhibition downstream of NogoA and PirB (Figure 2.10). Supporting a role for POSH as a downstream effector of myelin-based inhibitory signals, RNAi-mediated reduction in POSH function results in primary cortical neurons that robustly extend processes in the presence of CNS myelin, in contrast to control neurons, which are inhibited by myelin. As a scaffold protein, POSH operates through co-associating binding partners. POSH interacts with the actin-myosin regulatory protein Shroom3 to regulate process outgrowth inhibition and we demonstrate here that neurons with RNAi-knockdown of Shroom3 function are refractory to the inhibitory action of CNS myelin, supporting a role for the POSH/Shroom3 complex in process outgrowth inhibition downstream of myelin [22]. Neurons with an RNAi-mediated reduction in a second POSH interacting protein, the mixed lineage kinase LZK, are also refractory to the inhibitory action of myelin, providing further support for a key role for the POSH complex in transmitting axon outgrowth inhibitory cues from CNS myelin-derived inhibitors.

PirB is a receptor for Nogo66, and our observations are consistent with PirB signaling to POSH to mediate process outgrowth inhibition in cortical neurons [7, 32]. First, RNAi-mediated reduction of PirB in primary cortical neurons results in increased neuronal process length and prevents inhibition by myelin or Nogo66, indicating that PirB, like POSH RNAi, negatively regulates process length in cortical neurons. Second, overexpression of the POSH-associated effector protein LZK suppresses the PirB RNAi-mediated increase in process length. Similarly, LZK suppresses increased process outgrowth from

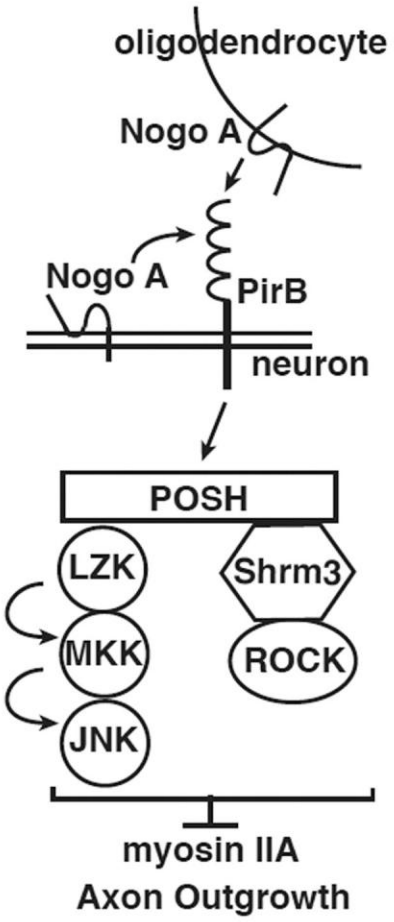

Figure 2.10 Model for process outgrowth inhibition by NogoA

The POSH scaffold protein couples to the mixed lineage kinase LZK and the actin-myosin regulatory protein Shroom3 to relay process outgrowth inhibitory signals from NogoA. PirB, a receptor for NogoA, relays signals to the POSH complex. External NogoA can inhibit axon outgrowth. In addition, NogoA on the neuron can self-limit axon outgrowth in a cell autonomous manner.

Nogo RNAi neurons. However, increased expression of LZK does not suppress the POSH RNAi enhanced process outgrowth phenotype, arguing that LZK does not suppress by simply activating a compensatory signaling pathway unlinked to PirB and POSH, but instead requires the POSH scaffold.

Finally, inhibition of myosin IIA function reverses the PirB phenotype, as well as the Nogo RNAi-mediated enhancement of process outgrowth. MyosinIIA RNAi reverses the increase in process length under some conditions but not others [22]. The mechanism by which loss of myosin IIA function is able to shorten process length under some conditions but not others remains to be determined. Nonetheless, that reduction of both ligand and receptor (Nogo/PirB) can be reversed by reduction of myosin IIA function, matching what is observed for POSH and POSH-associated proteins, further supports the proposed pathway of NogoA-PirB-POSH. Collectively, these observations implicate the PirB receptor as a critical component in signaling process outgrowth inhibition reliant on POSH function. In hematopoietic cells, PirB signals by recruitment of the tyrosine phosphatases SHP1/2 [17, 18]. Likewise, in neurons responding to myelin inhibition, PirB may recruit SHP2 to signal to POSH, but the identity of potential SHP2 substrate(s) in this pathway remains to be determined.

Further, these studies suggest that neuronally expressed NogoA limits axon outgrowth in a cell autonomous, intrinsic fashion, as RNAi-mediated reduction in cortical neurons enhances axon outgrowth. In contrast to neurons in which PirB or POSH/Shroom3/LZK are inhibited by RNAi, external application of Nogo66 to Nogo RNAi knockdown neurons inhibits enhanced process outgrowth. This is consistent with the model that the NogoA RNAi phenotype represents a loss of an autocrine signal for PirB, whereas disruption of PirB or POSH complex function prevents inhibition by either extrinsic or autocrine NogoA. The existence of autocrine Nogo inhibition also suggests an explanation for increased process outgrowth from POSH RNAi neurons in the absence of external inhibitory molecules [22]. Intriguingly, multiple inhibitory domains reside within Nogo, yet Nogo66 alone is sufficient to suppress the Nogo RNAi phenotype, highlighting the important role of this domain in mediating process outgrowth inhibition. The

ability of NogoA to limit process outgrowth in *cis* may function to limit axon outgrowth and plasticity during development [6-13]. Collectively, these results indicate that extrinsic and intrinsic mechanisms for impeding axon outgrowth converge on the POSH scaffold complex. Whether POSH signaling is downstream of CNS axon outgrowth inhibitors, in addition to NogoA/Nogo66, is an important question to be addressed in future studies.

Several Nogo isoforms are expressed in neurons, NogoA-C. All three isoforms contain the Nogo66 C-terminal inhibitory domain and are reported to localize to the plasma membrane [33]. Surprisingly, RNAi-mediated reduction of NogoA function alone is indistinguishable from RNAi-mediated reduction of all three Nogo isoforms simultaneously, indicating that NogoB and C fail to compensate for NogoA deficiency. Perhaps unique sequences present in NogoA enable the protein to fold in a conformation that facilitates binding to a Nogo receptor residing in the same membrane (in *cis*).

Proteins present in CNS myelin, including NogoA, are a major impediment to the repair of the injured CNS. The results presented here demonstrate a novel function for the POSH scaffold in signaling process outgrowth inhibition in response to NogoA, and delineate a new signaling pathway for process outgrowth inhibition, comprised of NogoA, PirB, POSH and LZK.

Identification of intracellular signaling components mediating myelin inhibition provides potential new targets for the development of therapeutics aimed at restoring function in the injured CNS. Blockade of POSH scaffold function, or the function of POSH associated proteins, has the potential to enhance axon outgrowth and plasticity, and functional recovery in the injured CNS.

2.4 Acknowledgements

We would like to thank Jonathan Zurawski for myelin preparation, Nogo RNAi plasmid construction, LZK cloning, and optimization of primary cortical neuron experiments. Jonathan also contributed data to Figures 2.2 and 2.7. Also, we

thank Huanqing Zhang for immunofluorescence studies which were not included in this chapter. Additionally, David Turner for assistance with RNAi design, helpful discussion, and critical editing of the manuscript. This chapter was previously published in the Journal of Neuroscience [40].

2.5 Materials and Methods

2.5.1 Antibodies

For axon outgrowth assays, cells were stained with anti-green fluorescent protein (GFP) rabbit primary antibody (Invitrogen) and Alexa Fluor 488 goat anti-rabbit secondary antibody (Molecular Probes). For western blots the following primary antibodies were used: goat anti-Nogo (N18) (Santa Cruz), anti-ILT-5/PirB (C-19) (Santa Cruz), rabbit anti-Actin (Sigma), and rabbit anti-GFP (Invitrogen). Secondary antibodies used were: Goat Anti-Rabbit IgG Horseradish Peroxidase (HRP) Conjugate (BioRad) and Bovine anti-goat IgG HRP (Santa Cruz).

2.5.2 Expression constructs and RNAi

pUI4-SIBR-GFP is a short interfering RNA (siRNA) expression vector that co-expresses the GFP protein and a siRNA from an intronic expression cassette (the SIBR cassette) based on the miR-155 microRNA precursor [22, 27]. For each siRNA, a pUI4-SIBR-GFP vector expressing one to four identical tandem copies of the siRNA SIBR cassette was constructed [22, 27]. POSH-6, luciferase (a functional control RNAi vector), Shroom3-3, and myosinIIA-1 are described in [22]. The sequences of LZK, Nogo and PirB siRNAs are: LZK-1, 5' UUCAUCGGGACUGUUCGAGUGG 3'; LZK-2, 5' AUCAAUGUUACAGUAGCCGGAG 3'; Nogo-1, 5' AAUCUUUGAAAUGACGGUUACG 3'; Nogo-3, 5' UAUACCGUCAUAACUAACUGGA 3'; PirB-294, 5' AACAAUAACAGCGAUAUUGCCC 3'; and, PirB-874 siRNA 5'

AACAUCGAUAUUGACCUGCAUU 3'. Western blot analysis confirmed knock-down of endogenous NogoA and PirB (Fig. S4). To construct CS2+NFLAG LZK, an N-terminally FLAG tagged construct, LZK was cloned by RT-PCR from RNA isolated from adult mouse brain. Kinase dead LZK was constructed by site-directed mutagenesis, AAG being converted to GCG, substituting lysine 195 to alanine. ATP fails to bind at the active site in the mutant protein, resulting in a catalytically defective kinase-dead mutant [28].

2.5.3 Preparation of myelin and recombinant proteins

Myelin extracts were prepared from adult rat brains, as described [34]. His-SUMO-conjugated Nogo66 (amino acids 1055-1079) or His-SUMO was expressed overnight at 25°C in Escherichia coli purified on Ni-NTA His Bind Resin (Qiagen). Briefly, E.coli were lysed by sonication in PBS+ (PBS, 0.1mM PMSF, 0.35mg aprotinin, 0.1% □-mercaptoethanol, 10mM imidazole, 2nM leupeptin). Triton X-100 was added to the lysate at 1% of the final volume. Lysates were incubated with Ni-NTA His Bind Resin for 1 hour at 4°C and washed three times in PBS+ with 300mM NaCl. Protein was eluted from the beads with elution buffer (50mM $NaHPO_4$, 300mM NaCl, 250mM imidazole) and 25% glycerol was added. Protein concentration was determined by Bradford assay (BioRad) and Coomassie gel with Bovine serum albumin (BSA) standards.

2.5.4 Axon outgrowth Assays

4-well chamber slides (Fisher Lab Tek II) were coated for 4 hours with 10 µg/ml poly-L-lysine then overnight with 2µg/ml laminin (Invitrogen) or overnight at 4°C with laminin+myelin, laminin+control His-SUMO (2.5µg /cm^2), or laminin+His-SUMO Nogo66 (2.5µg /cm^2). After overnight incubation, unbound substrates were removed by rinsing with PBS. Cortical primary progenitors were cultured as previously described [22]. Primary progenitors were nucleofected with a total of 6µg of DNA: 4.5µg of pUI4 vector and 1.5µg of empty vector control, pCS2-

NFLAG LZK, or pCS2-NFLAG LZK KD. In Fig. 2B, 4B, and S2B, cells were nucleofected with 6µg of DNA: 3µg of pUI4 vector and 3µg of pUI4-myosin IIA RNAi expression vector. Cells were fixed in 3.7% formaldehyde 72 hours post-nucleofection. Cells were stained with an anti-GFP primary antibody (Invitrogen) and Alexa Fluor 488 goat anti-rabbit secondary antibody (Molecular Probes). The efficiency of co-nucleofection of two different plasmids in primary cortical neurons is 94%. Co-nucleofection efficiency was determined by nucleofecting two plasmids expressing different markers (mCherry or GFP) and the percentage of cells expressing GFP, mCherry or both markers was determined in two independent experiments.

2.5.5 Measurement of Process Length

The length of the longest process per cell was measured in photographs of fixed, GFP stained neurons with the polyline function in MicroSuite imaging software version 5.0 (Olympus, Tokyo, Japan) [22]. For Fig. 2A-B, 3E-F, 4A-B, and S2, processes 50µm (3 times the length of the cell body) or greater were measured. In Fig. 1, 2C, and S1, using the box function in the MicroSuite imaging software, the longest process per cell for all the cells within the box was measured. Results are presented as average process length, determined from three independent nucleofections, with a total of 325-810 GFP-positive neurons measured per condition, except for Fig. 3E where the total number of neurons measured from the three independent nucleofections was 237-312. Statistical significance was assessed using the Students t-test. The data sets analyzed in the t-test were the measurements of the total number of GFP-positive neurons from three independent nucleofections.

2.5.6 Cerebellular Granule Neurons

Cerebellular Granule neurons (CGNs) were isolated from the cerebellum of post-natal day (P) 8 mice as described [35]. CGNs were nucleofected as

described [36, 37] with a total of 4µg of DNA: luciferase (control RNAi vector) or POSH-6 RNAi vector. Cells were plated onto 4-well chamber slides incubated for 4 hours with 10 µg/ml poly-L-lysine then overnight with 2µg/ml laminin or laminin+myelin at room temperature, laminin+control His-SUMO (2.5µg /cm^2) or laminin+His-SUMO Nogo66 (2.5µg /cm^2) at 4°C. 24 hours post-nucleofection cells were fixed with 3.7% formaldehyde. Cells were incubated with rabbit anti-GFP primary antibody (Invitrogen) and neuronal class III β-tubulin monoclonal antibody TuJ1 (Covance), followed by detection with Alexa Fluor 488 goat anti-rabbit (Molecular Probes) and Alexa Fluor 594 goat anti-mouse secondary antibodies (Molecular Probes). Average process length was quantified as described above and in [22].

2.5.7 Reverse Transcription-PCR

RNA was purified from untransfected cortical neuron cultures (RNeasy kits, QIAGEN) and genomic DNA was removed from RNA samples using RNase-Free DNase (QIAGEN), as recommended. Reverse transcription (RT) was performed using SuperScript II (Invitrogen) and Random Primer 12 (NEB) at 25°C for 10 min, 42°C for 1 hr, and 72°C for 15 min. cDNA samples were analyzed by PCR (Expand High Fidelity PCR system; Roche) with the following primers: POSH F1, 5’ CAGGTCCATATAAGCACCACTG 3’; POSH R1, 5’ GGTAGGGGACATCTGAAGGGA 3’; POSH F2, 5’ GTGACTAAAGAGCACAAAGCAG 3’; POSH R2, 5’ CAAGGCACACTTTACACATCAG 3’; Nogo F1, 5’ GTGCCCTTATTGCTTCCAAA 3’; Nogo R3, 5’ TCTGGATAGCTTGGATCACACCCTTA 3’; Nogo F3 5’ CAGGGGCTCGGGCTCAGT 3’; Nogo F-C 5’ ATGGACGATCAGAAGAAACGTTGGAA 3’; HPRT forward, 5’ CAAACTTTGCTTTCCCTGGT 3’; HPRT reverse, 5” CAAGGGCATATCCAACAACA 3’. Nogo F1, Nogo F3 and Nogo R3 have been previously described [38]. PCR products were analyzed by agarose gel

electrophoresis. Similar results were obtained with two independent RNA samples.

2.5.8 Western Blot Analysis to test efficacy of RNAi constructs

Western blot analysis was performed to test the ability of the siRNAs to target endogenous Nogo. Cellular extracts were prepared from transiently transfected, puromycin selected P19 cells, as previously described [22, 39]. To test the efficacy of the vector expressed PirB siRNAs, HEK 293 cells were transfected with a PirB expression construct together with a control or PirB RNAi vector. Western analysis was performed on the extracts prepared 36 hours after transfection.

2.6 References

1. Gonzenbach, R.R. and M.E. Schwab, Disinhibition of neurite growth to repair the injured adult CNS: focusing on Nogo. Cell Mol Life Sci, 2008. 65(1): p. 161-76.
2. Kubo, T., et al., Rho-ROCK inhibitors as emerging strategies to promote nerve regeneration. Curr Pharm Des, 2007. 13(24): p. 2493-9.
3. Schwab, M.E. and P. Caroni, Antibody against myelin-associated inhibitor of neurite growth neutralizes nonpermissive substrate properties of CNS white matter. Neuron, 2008. 60(3): p. 404-5.
4. Walmsley, A.R. and A.K. Mir, Targeting the Nogo-A signalling pathway to promote recovery following acute CNS injury. Curr Pharm Des, 2007. 13(24): p. 2470-84.
5. Giger, R.J., et al., Mechanisms of CNS myelin inhibition: evidence for distinct and neuronal cell type specific receptor systems. Restor Neurol Neurosci, 2008. 26(2-3): p. 97-115.
6. McGee, A.W., et al., Experience-driven plasticity of visual cortex limited by myelin and Nogo receptor. Science, 2005. 309(5744): p. 2222-6.
7. Atwal, J.K., et al., PirB is a Functional Receptor for Myelin Inhibitors of Axonal Regeneration. Science, 2008. 322(5903): p. 967-970.
8. Brosamle, C. and M.E. Halpern, Nogo-Nogo receptor signalling in PNS axon outgrowth and pathfinding. Mol Cell Neurosci, 2009. 40(4): p. 401-9.
9. Datwani, A., et al., Classical MHCI molecules regulate retinogeniculate refinement and limit ocular dominance plasticity. Neuron, 2009. 64(4): p. 463-70.
10. Mingorance-Le Meur, A., et al., Involvement of the myelin-associated inhibitor Nogo-A in early cortical development and neuronal maturation. Cereb Cortex, 2007. 17(10): p. 2375-86.
11. Syken, J., et al., PirB restricts ocular-dominance plasticity in visual cortex. Science, 2006. 313(5794): p. 1795-800.
12. Wang, J., et al., The growth-inhibitory protein Nogo is involved in midline routing of axons in the mouse optic chiasm. J Neurosci Res, 2008.
13. Petrinovic, M.M., et al., Neuronal Nogo-A regulates neurite fasciculation, branching and extension in the developing nervous system. Development. 137(15): p. 2539-50.
14. GrandPre, T., et al., Identification of the Nogo inhibitor of axon regeneration as a Reticulon protein. Nature, 2000. 403(6768): p. 439-444.
15. Oertle, T., et al., Nogo-A inhibits neurite outgrowth and cell spreading with three discrete regions. J Neurosci, 2003. 23(13): p. 5393-406.
16. Fournier, A.E., T. GrandPre, and S.M. Strittmatter, Identification of a receptor mediating Nogo-66 inhibition of axonal regeneration. Nature, 2001. 409(6818): p. 341-346.
17. Ho, L.H., et al., Constitutive tyrosine phosphorylation of the inhibitory paired Ig-like receptor PIR-B. Proc Natl Acad Sci U S A, 1999. 96(26): p. 15086-90.
18. Kubagawa, H., P.D. Burrows, and M.D. Cooper, A novel pair of immunoglobulin-like receptors expressed by B cells and myeloid cells. Proc Natl Acad Sci U S A, 1997. 94(10): p. 5261-6.
19. Figueroa, C., et al., Akt2 negatively regulates assembly of the POSH-MLK-JNK signaling complex. J Biol Chem, 2003. 278(48): p. 47922-7.
20. Schnorr, J.D., et al., Ras1 interacts with multiple new signaling and cytoskeletal loci in Drosophila eggshell patterning and morphogenesis. Genetics, 2001. 159(2): p. 609-622.

21. Tapon, N., et al., A new rac target POSH is an SH3-containing scaffold protein involved in the JNK and NF-kappaB signalling pathways. EMBO J, 1998. 17(5): p. 1395-404.
22. Taylor, J., et al., The scaffold protein POSH regulates axon outgrowth. Mol Biol Cell, 2008. 19(12): p. 5181-92.
23. Tuvia, S., et al., The ubiquitin E3 ligase POSH regulates calcium homeostasis through spatial control of Herp. J Cell Biol, 2007. 177(1): p. 51-61.
24. Xu, Z., N.V. Kukekov, and L.A. Greene, POSH acts as a scaffold for a multiprotein complex that mediates JNK activation in apoptosis. EMBO J, 2003. 22(2): p. 252-61.
25. Xu, Z., N.V. Kukekov, and L.A. Greene, Regulation of apoptotic c-Jun N-terminal kinase signaling by a stabilization-based feed-forward loop. Mol Cell Biol, 2005. 25(22): p. 9949-59.
26. Zhang, Q.G., et al., Role of Rac1 GTPase in JNK signaling and delayed neuronal cell death following global cerebral ischemia. Brain Res, 2009. 1265: p. 138-47.
27. Chung, K.H., et al., Polycistronic RNA polymerase II expression vectors for RNA interference based on BIC/miR-155. Nucleic Acids Res, 2006. 34(7): p. e53.
28. Ikeda, A., et al., Identification and characterization of functional domains in a mixed lineage kinase LZK. FEBS Lett, 2001. 488(3): p. 190-5.
29. Wang, K.C., et al., p75 interacts with the Nogo receptor as a co-receptor for Nogo, MAG and OMgp. Nature, 2002. 420(6911): p. 74-78.
30. Huber, A.B., et al., Patterns of Nogo mRNA and protein expression in the developing and adult rat and after CNS lesions. J Neurosci, 2002. 22(9): p. 3553-67.
31. Wang, X., et al., Localization of Nogo-A and Nogo-66 receptor proteins at sites of axon-myelin and synaptic contact. J Neurosci, 2002. 22(13): p. 5505-15.
32. Filbin, M.T., PirB, a second receptor for the myelin inhibitors of axonal regeneration Nogo66, MAG, and OMgp: implications for regeneration in vivo. Neuron, 2008. 60(5): p. 740-2.
33. Dodd, D.A., et al., Nogo-A, -B, and -C are found on the cell surface and interact together in many different cell types. J Biol Chem, 2005. 280(13): p. 12494-502.
34. Larocca, J.N. and W.T. Norton, Isolation of Myelin. Current Protocols in Cell Biology, 2006: p. 3.25.1-3.25.19.
35. Bilimoria, P.M. and A. Bonni Cultures of Cerebellar Granule Neurons. Cold Spring Harbor Protocols, 2008. doi:10.1101/pdb.prot5107.
36. Robak, L.A., et al., Molecular basis of the interactions of the Nogo-66 receptor and its homolog NgR2 with myelin-associated glycoprotein: development of NgROMNI-Fc, a novel antagonist of CNS myelin inhibition. J Neurosci, 2009. 29(18): p. 5768-83.
37. Venkatesh, K., et al., The Nogo-66 receptor homolog NgR2 is a sialic acid-dependent receptor selective for myelin-associated glycoprotein. J Neurosci, 2005. 25(4): p. 808-22.
38. Makeyev, E.V., et al., The MicroRNA miR-124 promotes neuronal differentiation by triggering brain-specific alternative pre-mRNA splicing. Mol Cell, 2007. 27(3): p. 435-48.
39. Vojtek, A.B., et al., Akt regulates basic helix-loop-helix transcription factor-coactivator complex formation and activity during neuronal differentiation. Mol Cell Biol, 2003. 23(13): p. 4417-27.
40. Dickson, H.M., et al., POSH is an intracellular signal transducer for the axon outgrowth inhibitor Nogo66. J Neurosci, 2010. 30(40): p. 13319-25.

Chapter 3

The Shp2 phosphatase suppresses axon outgrowth by regulating the function of the mixed lineage kinase LZK

3.1 Introduction

Traumatic injury or disease to the adult central nervous system (CNS) often results in severed neuronal axons, leading to cell death and a loss of neuronal signaling and connectivity. Deficits in functional connectivity between neurons can lead to severe physical and mental impairments. Recovery after these injuries is rare, due to the limited capacity of the CNS to regenerate damaged neurons and their axons [1, 2]. Myelin-associated inhibitors (MAIs) of axonal growth and regeneration play a crucial role in the inability of the adult central nervous system to recover after injury or disease. The three major MAIs are: MAG, NogoA, and OMgp [1-3]. Blocking the action of these proteins and/or their receptors leads to enhanced regeneration of axons after injury, suggesting that circumventing the action of these inhibitors could be a strategy to enhance axon outgrowth of injured neurons [3, 4]. Complicating therapeutic strategies is the presence of multiple receptors for the inhibitory proteins including the Nogo-66 receptor (NgR1) and paired immunoglobulin-like receptor B (PirB). Additionally, NgR1 and PirB receptors bind all three MAIs [3, 5-7]. The complexity at the neuronal cell surface suggests that blocking the intracellular signaling pathways regulated by MAIs may be a complementary and perhaps more efficacious strategy to enhance axon growth after injury.

Previous studies in our laboratory have revealed a novel role for the intracellular scaffold protein POSH as a regulator of axon outgrowth in neurons [8, 9]. POSH mediates this function by facilitating the assembly of a signaling

module composed of the actin myosin regulatory protein Shroom3, Rho-associated kinase (ROCK), and leucine zipper kinase (LZK) [8, 9]. Loss of function of any member of the complex or inhibition of complex assembly leads to an enhancement of axon length, indicating the POSH module negatively regulates axon length [8]. Through the receptor PirB, the POSH complex relays inhibitory signals from NogoA, specifically a 66-amino acid loop of NogoA termed Nogo66 [8]. These studies delineated a novel intracellular signaling pathway for process growth inhibition by Nogo66, comprised of NogoA, PirB, POSH, LZK, Shroom3, and ROCK. However, the molecular mechanism by which growth inhibitory signals are relayed from the receptor PirB to the POSH complex is unknown.

Shp2 is an ubiquitously expressed, mammalian, non-transmembrane, protein tyrosine phosphatase. Shp2 contains two N-terminally located src-homology 2 (N-SH2 and C-SH2) domains, a central phosphotyrosine phosphatase domain (PTP), a C-terminal tail with tyrosyl phosphorylation sites, and a proline-rich motif [10]. In the absence of a tyrosine-phosphorylated binding partner, the N-terminal SH2 domain binds the phosphatase domain blocking its active site [11, 12]. Shp2 is involved in many signaling pathways including Ras/ERK MAP kinase pathway and the JAK/Stat pathway [10, 13]. In macrophages, immunoprecipitation experiments using Shp1 (a Shp2 family member) discovered a 130-kDa phosphotyrosyl protein that was constitutively associated with Shp1 through its SH2 domains [14]. In further experiments, the identity of the 130-kDa protein was determined to be PirB and it was shown that Shp2 associates with PirB in a similar mechanism as Shp1 [15]. The cytoplasmic domain of PirB contains three potential immunoreceptor tyrosine based inhibitory motifs (ITIM), I/V-X-pY-X-X-L/V/I which are known binding sites for Shp1, Shp2, and SH2 domain-containing inositol phosphatase (SHIP) [16-18]. PirB's third and fourth ITIMs are important for recruitment of Shp2 and downstream signaling[19]. In immune cells, PirB has been classified as an inhibitory receptor; the recruitment and activation of Shp1/2 leads to disruption of signaling cascades initiated by the activating receptor PirA [20, 21].

In neurons, PirB and Shp2 associate and the interaction is dependent on the intracellular domain [22]. PirB is a receptor for myelin-derived inhibitory substrates and studies using a truncated mutant of PirB have shown that the intracellular domain is important for relaying myelin inhibitory cues [22]. Additionally, a transgenic mouse for the truncated form of PirB displays increased ocular-dominance plasticity suggesting that PirB acts as a negative regulator of neuronal stability/plasticity [5, 22]. Recent studies have also shown that PirB and Shp2 together with p75, a co-receptor for NgR1, negatively regulate TrkB signaling to modulate axon outgrowth [23, 24]. Together these studies highlight the role of PirB and Shp2 as regulators of signaling both in the nervous system and in the immune system.

In this study, we report that Shp2 relays Nogo66-growth inhibitory signals downstream from the receptor PirB and its activity as a phosphatase is required for this function. Nogo66 stimulation induces an enhancement in the association of tyrosine-phosphorylated proteins with Shp2. LZK is tyrosine phosphorylated and binds to a Shp2 substrate trap mutant, suggesting that LZK is a Shp2 substrate and its function is regulated by phosphorylation events. Interestingly, a close family member of LZK, DLK, is also a negative regulator of axon length and an intracellular signaling protein for Nogo66, suggesting functional redundancy of the kinases. However, DLK cannot compensate for the loss of PirB in CGNs and is not trapped by Shp2, suggesting that DLK and LZK undergo selective regulation. Finally, the POSH complex also relays inhibitory signals from MAG, indicating that the POSH complex may be a convergence point for MAIs. Collectively, this study places Shp2 in the NogoA-PirB-POSH complex signaling pathway.

3.2 Results

3.2.1 The Shp2 phosphatase is required for NogoA-mediated growth inhibition

In neurons and in immune cells, PirB and Shp2 associate and the interaction is required for downstream signaling of the myelin-inhibitory protein MAG [20-23]. PirB is a functional receptor for NogoA in cerebellar granule neurons (CGNs) as reducing PirB function by RNA interference (RNAi) leads to increased process length and the neurons are refractory to Nogo66 inhibition (Figure 3.1). To determine if PirB is facilitating Nogo66 growth inhibition through Shp2, the ability of Shp2 to compensate for the loss of PirB function was tested. Specifically, we tested whether overexpression of Shp2 would suppress the PirB long axon phenotype or restore growth inhibition to PirB RNAi neurons on Nogo66. To perform these suppression analysis experiments, constitutively active or catalytically inactive Shp2 was expressed in PirB RNAi CGNs. In the absence of a receptor or activating protein, Shp2 is held in an inactive, folded-conformation through the interaction of its N-terminal SH2 domain with the protein tyrosine phosphatase domain [12, 25]. Interaction of Shp2 with specific phosphorylated residues on activating proteins relieves this auto-inhibition [10, 11]. To mimic activation, a glutamate 76 to lysine mutation was made which disrupts the ability of the SH2 domain from interacting with its tail, resulting in a constitutively active or receptor independent Shp2 mutant [10-12]. Ectopic expression of Shp2 E76K in PirB RNAi neurons reduced process length to control levels and was able to restore growth inhibition on Nogo66 (Figure 3.1). These results indicate that Shp2 function is downstream of PirB and is involved in mediating inhibitory signals from Nogo66.

To extend this analysis, a phosphatase dead Shp2 mutant was constructed by mutating arginine 465 to methionine (RM). This invariant arginine is located in the active site of the phosphatase where it coordinates and stabilizes the phosphate group on the substrate [11, 12, 25]. The RM mutant was constructed in the E76K background to create a double mutant that resides in the open, active conformation but is phosphatase dead. Ectopic expression of

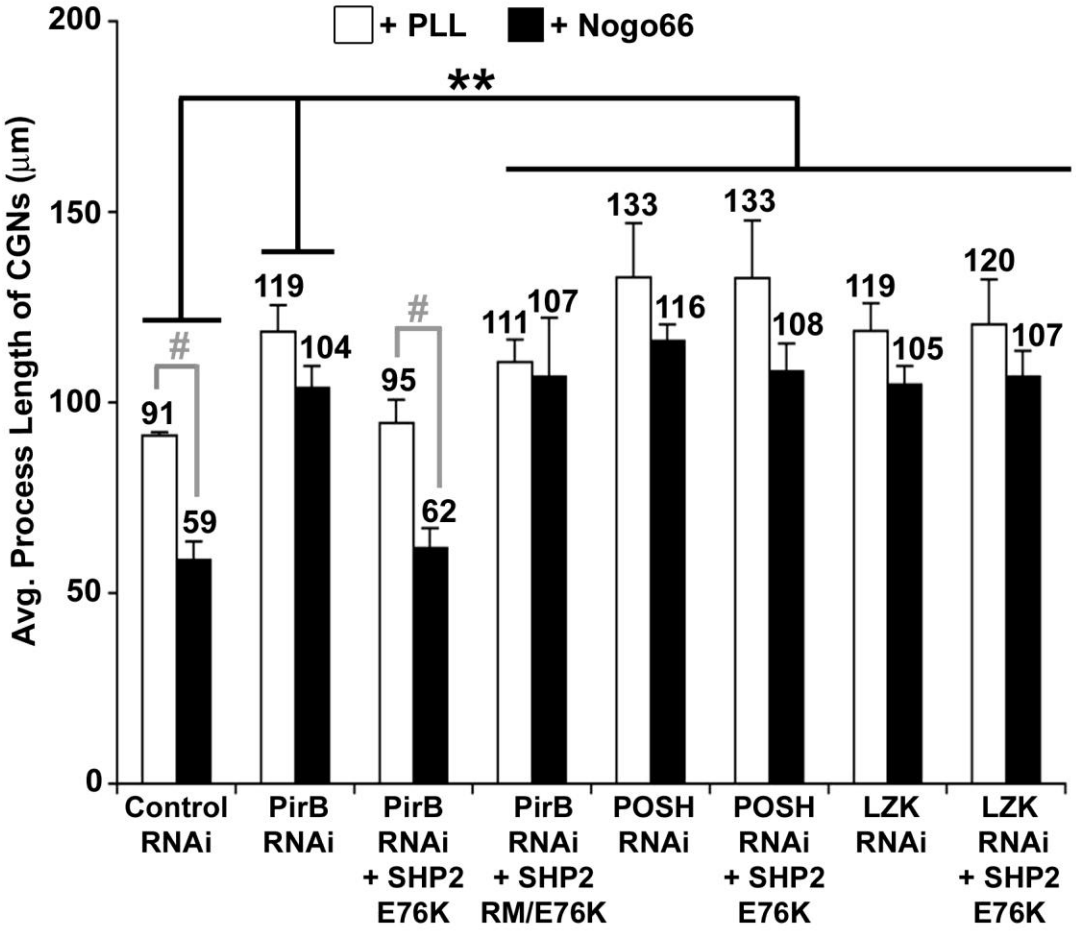

Figure 3.1 Shp2 phosphatase activity is required for transmission of Nogo66-mediated inhibitory signals through the POSH-LZK complex

CGNs were nucleofected with the indicated RNAi vectors and with either an empty control, Shp2 E76K, or Shp2 E76K/RM expressing vectors. CGNs were plated to poly-l-lysine/laminin (PLL) or PLL+Nogo66, and process length was scored 24 hr after nucleofection. Average process length was determined from three independent experiments, with 386-442 neurons in total measured per condition. Constitutively active Shp2 suppressed the PirB RNAi phenotype, but not POSH or LZK RNAi neurons. #p,** $p<0.0001$, Students *t* test.

Shp2 RM/E76K was not able to complement the loss of PirB by RNAi or restore Nogo66 growth-inhibition (Figure 3.1). Collectively, these results show that Shp2 is downstream of NogoA/PirB signaling and the phosphatase activity of Shp2 is necessary for mediation of NogoA/PirB growth inhibition in CGNs.

3.2.2 Regulation of axon outgrowth by Shp2 is dependent on the POSH complex

The assembly of the POSH complex, consisting of POSH, LZK, and Shroom3, is crucial for the regulation of axon outgrowth and NogoA mediated growth inhibition [8, 9]. To determine whether Shp2 relays growth inhibitory signals through the POSH module, the ability of Shp2 to compensate for the loss of POSH or LZK was tested. The loss of POSH or LZK function in CGNs by RNAi results in a long process phenotype (Figure 3.1 and [8, 9]). Overexpression of Shp2 E76K is not able to complement the loss of POSH or LZK function (Figure 3.1). Also, Nogo66-mediated growth inhibition is not restored by ectopic expression of activated Shp2, indicating Shp2 requires the presence of POSH and LZK to mediate inhibitory signals and is not functioning through a separate inhibitory pathway. Importantly, these results show that Shp2 signaling occurs upstream of or in concert with the POSH/LZK signaling module.

3.2.3 Nogo66 enhances Shp2 association with tyrosine-phosphorylated proteins

Since the phosphatase activity of Shp2 and the presence of the POSH complex members are required for Shp2 to relay NogoA mediated growth inhibition, we hypothesized that Shp2 is acting on a member of the POSH complex. A widely used method for identifying physiological substrates of protein tyrosine phosphatases (PTPs) is to create a “substrate trap” by mutating specific amino acids in the catalytic domain of PTPs [15, 26, 27]. The trapping mutants are able to bind substrates but cannot dephosphorylate them. Shp2 contains a conserved catalytic domain, which contains twenty-seven invariant residues, and

mutation of D425A and C459S has been reported as an effective substrate trap [15, 26, 27]. The cysteine residue acts as a nucleophile on the phosphorus atom of the substrate, followed by cleavage of the scissile P-O bond, which is facilitated by the aspartate [11, 12, 25]. The suppression of P-O cleavage is thought to stabilize and enhance the phosphatase-substrate interaction. To identify substrates of Shp2 downstream of NogoA, the DA/CS mutation was generated in the isolated PTP domain of Shp2, as well as in full-length Shp2.

Using the substrate trap method, Nogo66 dependent increases or decreases in tyrosine phosphorylated proteins were assessed. CGNs were stimulated with Nogo66 for 15 minutes followed by pull-down analysis with Shp2 Wild-type (WT) and DA/CS PTP domains purified from *E.coli* as GST fusion proteins. Western blot analysis was performed to examine levels of tyrosine phosphorylated proteins (Figure 3.2A). In the native assay, no interacting proteins were trapped or detected with or without Nogo66 treatment. To increase the pool of phosphorylated proteins in the cells and to enhance the sensitivity of the assay, CGNs were pretreated with the phosphatase inhibitor pervanadate and trapped Shp2 substrates were detected (Figure 3.2A). Shp2 PTP DA/CS trapped at least eight tyrosine-phosphorylated proteins of differing molecular weights. No phosphorylated proteins were detected using WT PTP, indicating that the substrate trap was functioning as expected. Upon Nogo66 treatment, there is enhanced trapping of the tyrosine-phosphorylated proteins, suggesting potential Shp2 substrates. Three bands which correspond with the molecular weights of 200kDa, 120kDa, and 80kDa could be Shroom3 (198kDa), LZK (100kDa), and/or POSH (89kDa). Endogenous POSH, Shroom3, or LZK were not detected using protein specific antibodies in either the pull downs or in cellular extracts, the latter suggesting endogenous protein levels may be below the level of detection for the available commercial antibodies (data not shown).

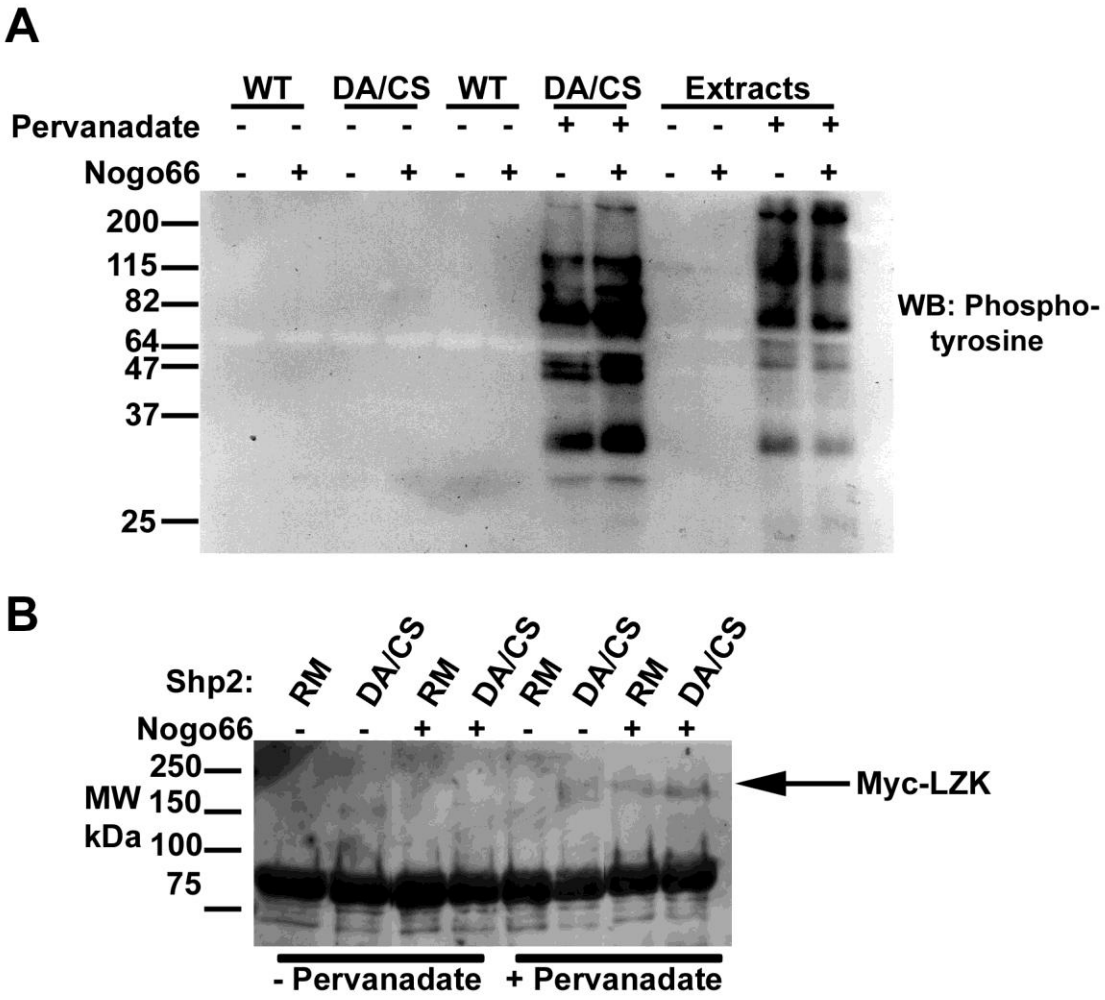

Figure 3.2 Nogo66 enhances Shp2 association with tyrosine-phosphorylated proteins (A) and LZK (B).

(A) CGNs were treated with or without pervanadate and with or without Nogo66. Neuronal cellular lysates were subjected to GST-Shp2 PTP WT or GST-Shp2 PTP DA/CS pull down analysis. Western blot analysis was performed to detect tyrosine-phosphorylated proteins. Nogo66 treatment induced enhanced trapping of tyrosine-phosphorylated proteins. Western blot is a representative image from three independent experiments.
(B) CGNs, nucleofected with Myc-LZK plasmids, were plated onto HisSUMO (-) or immobilized Nogo66 (+). Prior to harvest, CGNs were treated with or without pervanadate and trapping experiments were performed with full length GST-Shp2 RM or GST-Shp2 DA/CS, followed by western blot analysis for myc-tagged LZK. Nogo66 treatment results in loss of LZK association with Shp2, indicating dephosphorylation following Nogo66 treatment. Pervanadate treatment to inhibit endogenous tyrosine phosphatases results in enhanced Shp2 trapping of LZK. Nogo66 treatment further enhances LZK trapping by Shp2 in pervanadate treated CGNs.Western blot is a representative image from two independent experiments.

3.2.4 LZK is a novel Shp2 interacting protein

To test the hypothesis that a POSH complex member is a substrate of Shp2, a candidate approach using the trapping method was taken. CGNs were nucleofected with expression constructs for myc-tagged LZK. To examine the effects of Nogo66 stimulation on phosphorylation status of LZK, CGNs were plated to PLL or Nogo66. 24 hours after transfection, CGNs were treated with or without pervanadate for 30 minutes prior to harvest. Preliminary results of pull downs with full length Shp2 RM (catalytically inactive, but non-trapping) or Shp2 DA/CS (catalytically inactive trapping) showed that stimulation with Nogo66 results in decreased trapping of LZK (Figure 3.2B, comparison of lane 2 to lane 4). This result suggests that in neurons LZK is phosphorylated, and upon Nogo66 stimulation, LZK is targeted for dephosphorylation by Shp2. Consistent with this hypothesis, inhibition of endogenous phosphatases with pervanadate treatment leads to enhanced Shp2 trapping of LZK upon Nogo66 stimulation, indicating that Nogo66 is promoting the association of LZK with Shp2 (Figure 3.2B, comparison of lane 6 to lane 8). Collectively, these results show that ectopically expressed LZK is trapped by Shp2 in a Nogo66 dependent manner.

3.2.5 In HEK 293 cells, LZK is trapped by Shp2 and is tyrosine phosphorylated

To confirm and extend the observations in primary neurons, Shp2 trapping experiments were performed in the immortalized and readily transfectable HEK 293 cell line. 293 cells were transfected with expression constructs for myc-tagged POSH or LZK and were treated with pervanadate for 30 minutes prior to harvest. Pull downs with full length Shp2 RM or Shp2 DA/CS showed that only LZK is trapped by inactive Shp2 (Figure 3.3A). These results confirm the results observed in CGNs and suggest that HEK 293 cells can be used to examine the molecular mechanism of Shp2 trapping of LZK.

To further analyze the Shp2-LZK interaction, the tyrosine-phosphorylation status of LZK was assessed. HEK 293 cells were transfected with Myc-LZK,

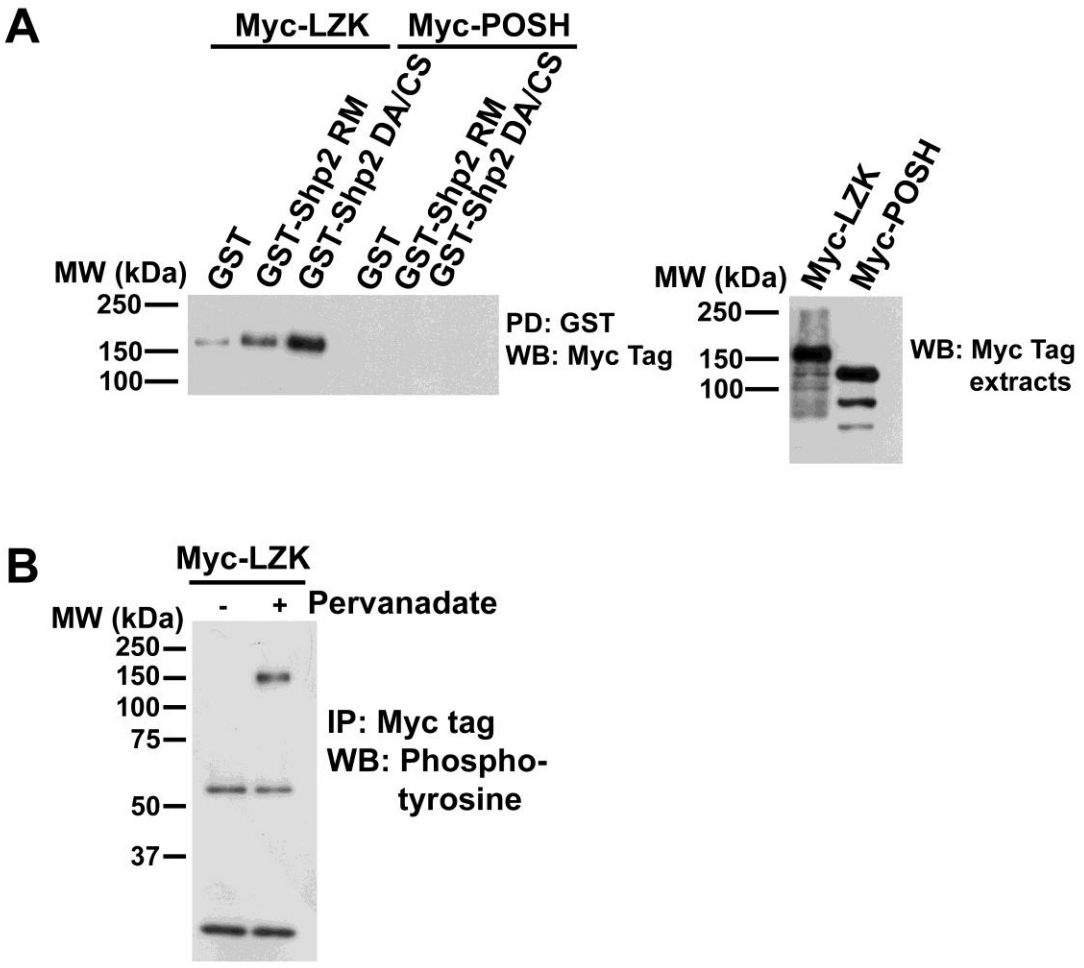

Figure 3.3 Pervanadate treatment induces Shp2 trapping and tyrosine phosphorylation of LZK

(A) HEK293 cells, transfected with Myc-LZK or Myc-POSH plasmids, were treated with pervanadate prior to pull-down analysis wirh GST, GST-Shp2 RM, or GST-Shp2 DA/CS. LZK, but not POSH, is trapped by Shp2 DA/CS. Western blot is a representative image from three independent experiments.
(B) Myc-LZK was immunoprecipitated from 293 cells treated with or without pervanadate followed by western blot analysis for the presence of phosphorylated tyrosine residues. Pervanadate treatment leads to tyrosine-phosphorylation of LZK. Western blot is a representative image from two independent experiments.

treated with pervanadate, and analyzed by western blot for the presence of phosphorylated tyrosine residues. Indeed, when phosphatases are globally inhibited, LZK is tyrosine phosphorylated (Figure 3.3B). These results, taken together with the ability of LZK to be trapped by Shp2, highlight the potential for direct regulation of LZK function by Shp2.

3.2.6 DLK, an additional MLK family member, is also a negative regulator of axon length

LZK belongs to the second subfamily of mixed lineage kinases (MLKs), which also includes dual leucine zipper kinase (DLK). The two proteins contain a kinase domain followed by two leucine-zipper motifs that are separated by a 31 amino acid spacer. LZK and DLK share 87% homology in their kinase domains and 76% homology in their zipper domains (Figure 3.4A) [28, 29]. The N and C-terminal ends are distinct, however, both proteins associate with POSH and activate JNK signaling [28-32]. Since LZK and DLK contain homology, both bind to POSH, and activate JNK, we wanted to investigate whether DLK regulates axon outgrowth. To address this question in CGNs, RNAi constructs targeting DLK were nucleofected into CGNs plated to PLL or Nogo66. Reduction of DLK function by RNAi results in enhanced process length identical to the loss of LZK function (Figure 3.4B), suggesting DLK is also a negative regulator of axon length. To determine whether DLK is downstream of Nogo66 growth inhibition, DLK RNAi-expressing neurons were plated to Nogo66. DLK RNAi neurons are refractory to growth inhibition by Nogo66 (Figure 3.4B), indicating a role for DLK as a signaling protein for myelin-associated proteins.

The above result suggested that DLK and LZK may be able to compensate for each other. To further examine this hypothesis, LZK or DLK were ectopically expressed in either DLK or LZK RNAi neurons. Expression of LZK in LZK RNAi neurons or DLK in DLK RNAi neurons reverses the long process phenotype, indicating specificity of the RNAi constructs (Figure 3.4B). Interestingly, LZK was able to complement the loss of DLK and conversely, DLK was able to complement the loss of LZK (Figure 3.4B). These results suggest

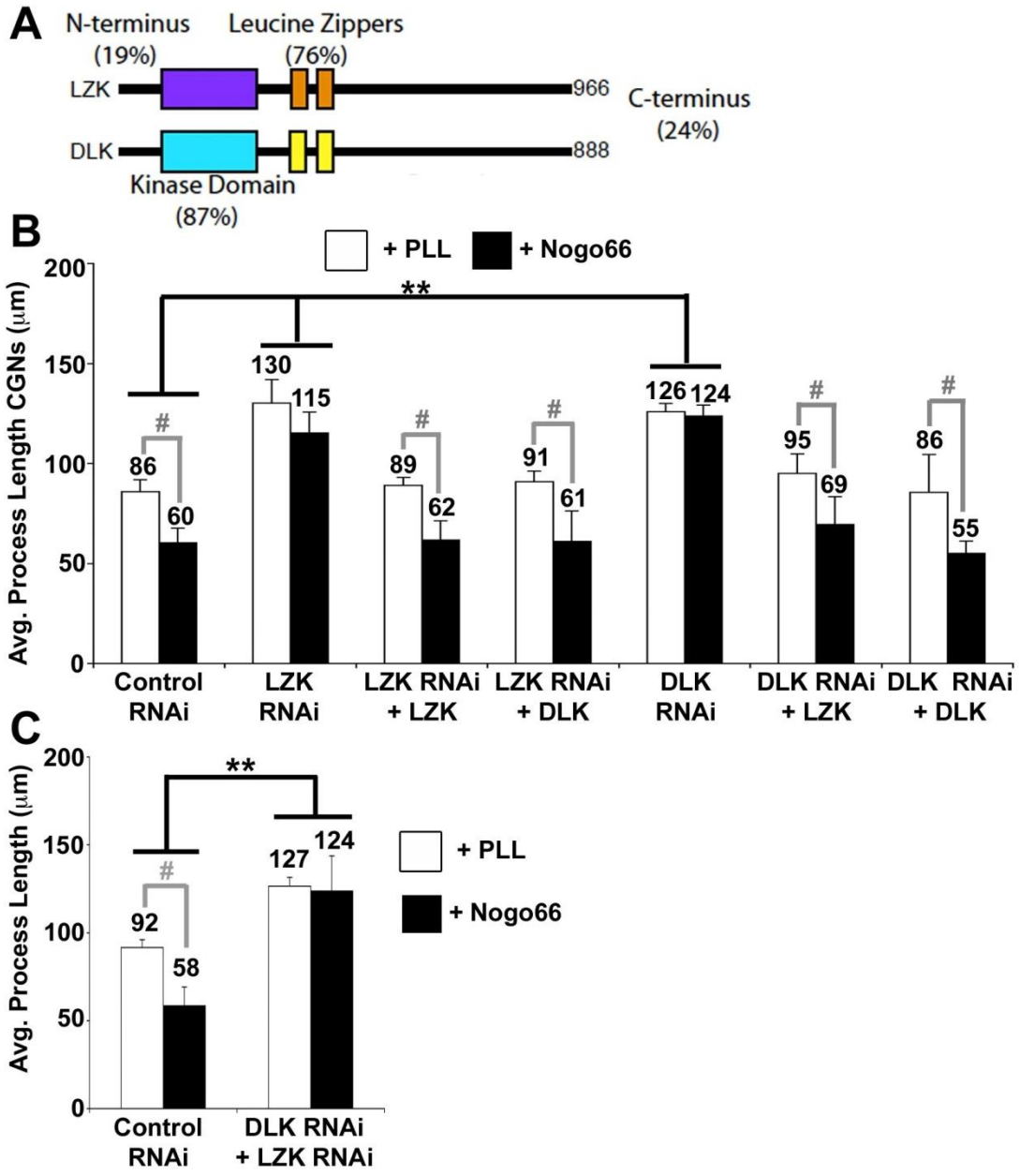

Figure 3.4 DLK, another MLK family member, is also a negative regulator of axon length

(A) Schematic of LZK and DLK homology. The family members share 87% homology in their kinase domains and 76% in their leucine zipper domains, while their N- and C- terminals are distinct.
(B) Reduction in DLK function by RNAi results in enhanced axon length. Ectopic expression of LZK or DLK is sufficient to complement the loss of either kinase by RNAi. Average process length was determined from three independent experiments, with 410-469 neurons in total measured per condition. #p,** p<0.0001, Students *t* test.
(C) Reduction in LZK and DLK function by RNAi does not lead to further enhancement of axon length. Average process length was determined from three independent experiments, with 386-422 neurons in total were measured per condition.
#p,** p<0.0001, Students *t* test.

that either kinase can function to regulate axon outgrowth and growth inhibition of Nogo66.

Since both kinases are expressed in CGNs and they both negatively regulate axon outgrowth, we hypothesized that loss of both kinases will enhance the long process phenotype. Surprisingly, removal of both DLK and LZK function by RNAi does not result in further enhancement of axon length (Figure 3.4C). This result suggests that DLK and LZK operate on the same pathway or both kinases may regulate a downstream, rate limiting step in axon outgrowth. From these studies, we conclude that DLK or LZK can modulate axon length, responsiveness to Nogo66-induced growth inhibition, and DLK or LZK are able to compensate for the loss of each other's function when overexpressed.

3.2.7 CGNs from DLK hypomorph mice display long process phenotype and are refractory to growth inhibition by Nogo66

To further examine the role of DLK in the cerebellum, DLK hypomorph mice were obtained from the Lawrence Holzman laboratory. Previous studies using DLK knockout mice demonstrated that $DLK^{-/-}$ mice progressed through embryogenesis but died soon after birth [33, 34]. Thus, the Holzman group generated a hypomorph that displayed decreased levels of DLK rather than complete removal of DLK [35]. The hypomorphs were viable and survived through adulthood. At the time of this dissertation, complete phenotypic studies of the DLK hypomorph were incomplete; however studies are ongoing in the Holzman laboratory. To determine whether constitutively decreased levels of DLK in hypomorphs behaved similar to decreasing levels of DLK in CGNs by nucleofection with RNAi constructs, CGNs from DLK hypomorph mice and wild-type litter mate controls were isolated and plated on control substrate or Nogo66. CGNs isolated from DLK hypomorph mice show enhanced process outgrowth when compared to wild-type CGNs (Figure 3.5). Additionally, DLK hypomorph CGNs were refractory to Nogo66, confirming the results seen with DLK RNAi constructs (Figure 3.4-3.5). These results suggest that DLK regulates of axon outgrowth and growth inhibition mediated by Nogo66.

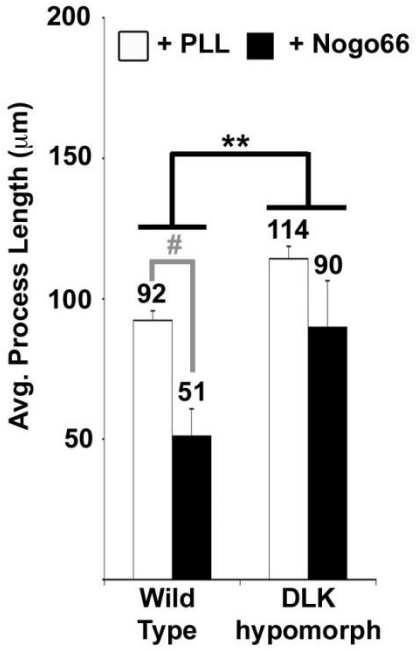

Figure 3.5 CGNs from DLK hypomorph mice show enhanced process length

CGNs were isolated from post-natal day 8 (P8) wild-type and DLK hypomorph mice and plated to PLL or Nogo66. CGNS from DLK hypomorph mice exhibit enhanced process lenth on PLL compared to wild-type and are refractory to Nogo66 growth inhibition. Average process length was determined from three independent experiments, with 372-421 neurons in total measured per condition. #p,** p<0.0001, Students *t* test.

3.2.8 Reduced DLK expression does not affect cerebellar morphology

We next wanted to assess the effect of the loss of DLK on the development of the cerebellum. The cerebellum is highly ordered, which allows for easy identification of cell types and morphology [36]. Briefly the cerebellum is organized into a molecular layer that contains the axons of the CGNs and the dendrites of the Purkinje cells, a Purkinje cell body layer, and an inner granule cell layer, containing CGN cell bodies and the axons of the Purkinje cells. The Purkinje cell axons continue into the deep nuclei, relaying further neuronal signals. Previous studies in $DLK^{-/-}$ embryos showed that loss of DLK function resulted in defects in radial migration and axon projection [34, 37, 38]. Additionally, genetic disruption of MKK4, a MAPKK which is activated by DLK, results in misalignment of the Purkinje cells of the cerebellum [39]. DLK is expressed in both the molecular layer of the cerebellum (CGN location) and in the Purkinje cells [40]. Thus, we hypothesized that loss of DLK in the cerebellum may also result in changes in granule layer formation or Purkinje cell alignment.

To examine cerebellar morphology, post-natal day 10 brains were isolated from wild-type and DLK hypomorphs and sagittal cryogenic slices were stained with calbindin (Purkinje cells) and Hematoxylin and eosin (H&E stain: general histology stain). As seen in Figure 3.6, there are no significant differences in cerebellar morphology; Purkinje cells were aligned correctly and granule layers were of comparable thicknesses in the DLK hypomorph (D-F) compared to wild-type (A-B). This was not unexpected as the mice did not exhibit any traditional cerebellar behavioral deficits such as circling or altered gait (data not shown). There may be changes in morphology at a smaller scale, such as the number of synaptic connections between CGNs and Purkinje cells and/or aberrant axon growth; however we were unable to visualize these differences with our current tools. It is also possible that LZK expression in the cerebellum is able to compensate for the loss of DLK, preventing any significant morphological differences. An inducible knock-out of DLK, LZK, and both proteins would provide

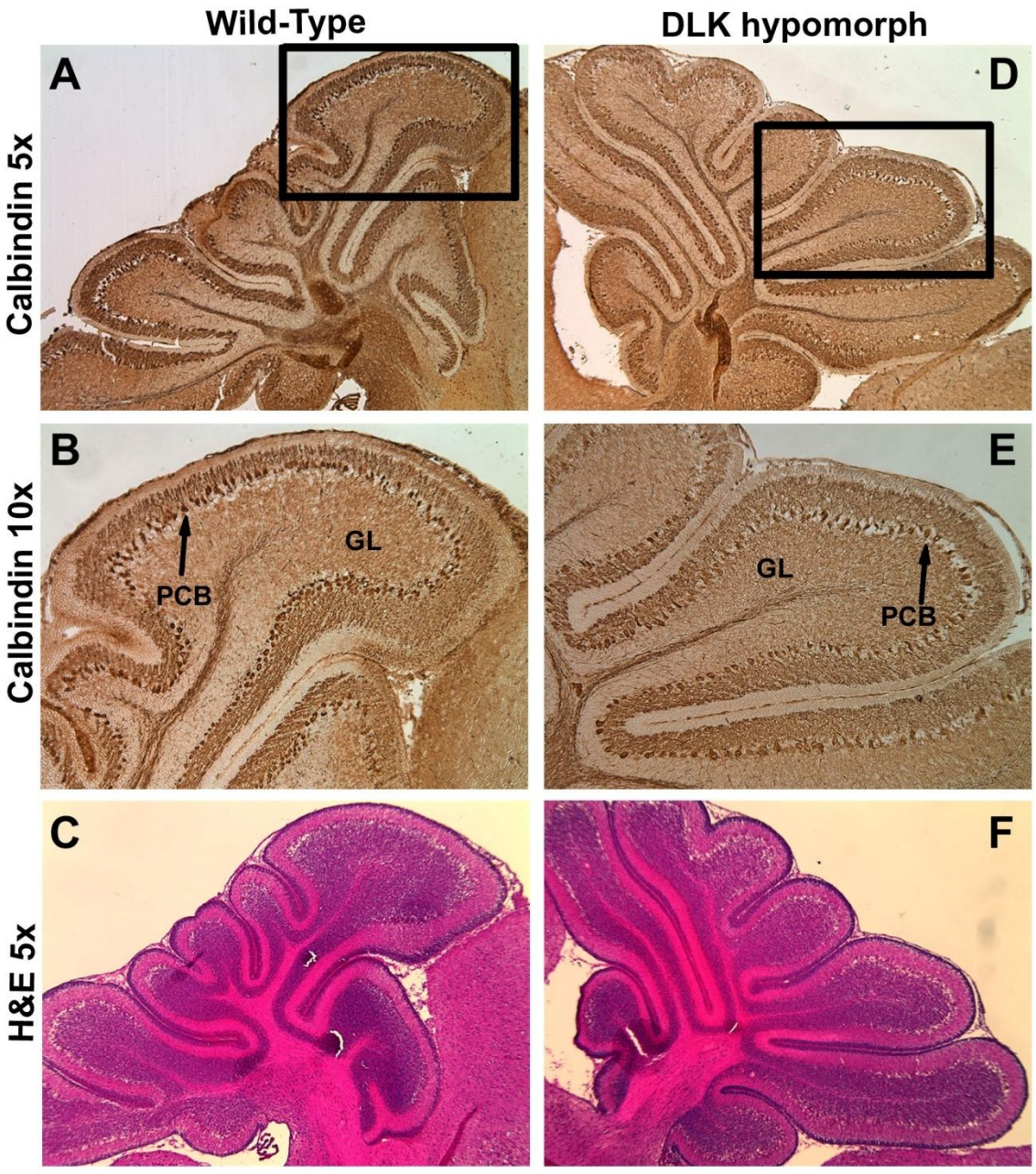

Figure 3.6 Reduced DLK expression does not affect cerebellar morphology

Post-natal day 10 (P10) brains were isolated from wild-type and DLK hypomorph mice. Following sagittal cryogenic slicing, samples were stained with calbindin (Purkinje cells) and Hematoxylin and eosin (H&E) (general histology stain). (A-C) Wildtype cerebellum display ordered Purkinje cell bodies (PCB) and thick granular layer (GL). (D-E) DLK hypomorph cerebellum do not exhibit significant morphological differences from wildtype.

valuable insight into the role of each kinase during development and after neuronal injury.

3.2.9 Unlike LZK, DLK is not able to compensate for the loss of PirB in CGNs

Our findings indicate that DLK and LZK are negative regulators of axon length and are members of the signaling pathway downstream from Nogo66-induced growth inhibition. Thus, we asked whether DLK is downstream of the Nogo66 receptor, PirB. To address this question, DLK or LZK constructs were expressed in PirB RNAi CGNs. As seen previously, overexpression of LZK in PirB RNAi expressing neurons reverses the long process phenotype observed with a loss of PirB function (Figure 3.7A). However, ectopic expression of DLK fails to complement the loss of PirB or restore growth inhibition by Nogo66 (Figure 3.7A). This result was unexpected given the previous results suggesting that either kinase can suppress the loss of the other when overexpressed in CGNs and the result that both mediate Nogo66 signaling (Figure 3.4B). It is possible that DLK is not downstream of PirB and is relaying Nogo66 signaling through a distinct signaling pathway. An alternative hypothesis is that DLK is regulated by PirB to be incorporated into the MAI signaling pathway, and therefore, a loss of PirB prevents DLK incorporation and subsequent function in regulating axon outgrowth.

3.2.10 DLK is not trapped by Shp2

LZK is trapped by Shp2 and Shp2 mediates downstream signaling from Nogo66 and PirB. Therefore, we hypothesized that DLK is regulated in a distinct method from LZK, allowing for the selection of LZK in the NogoA-PirB-POSH pathway. To assess this hypothesis, Shp2 trapping experiments with overexpressed Myc-DLK in HEK 293 cells were performed. Following pervanadate treatment, unlike LZK, DLK is not trapped by Shp2 (Figure 3.7B). This result suggests that DLK is not tyrosine phosphorylated under the same conditions as LZK, and therefore is

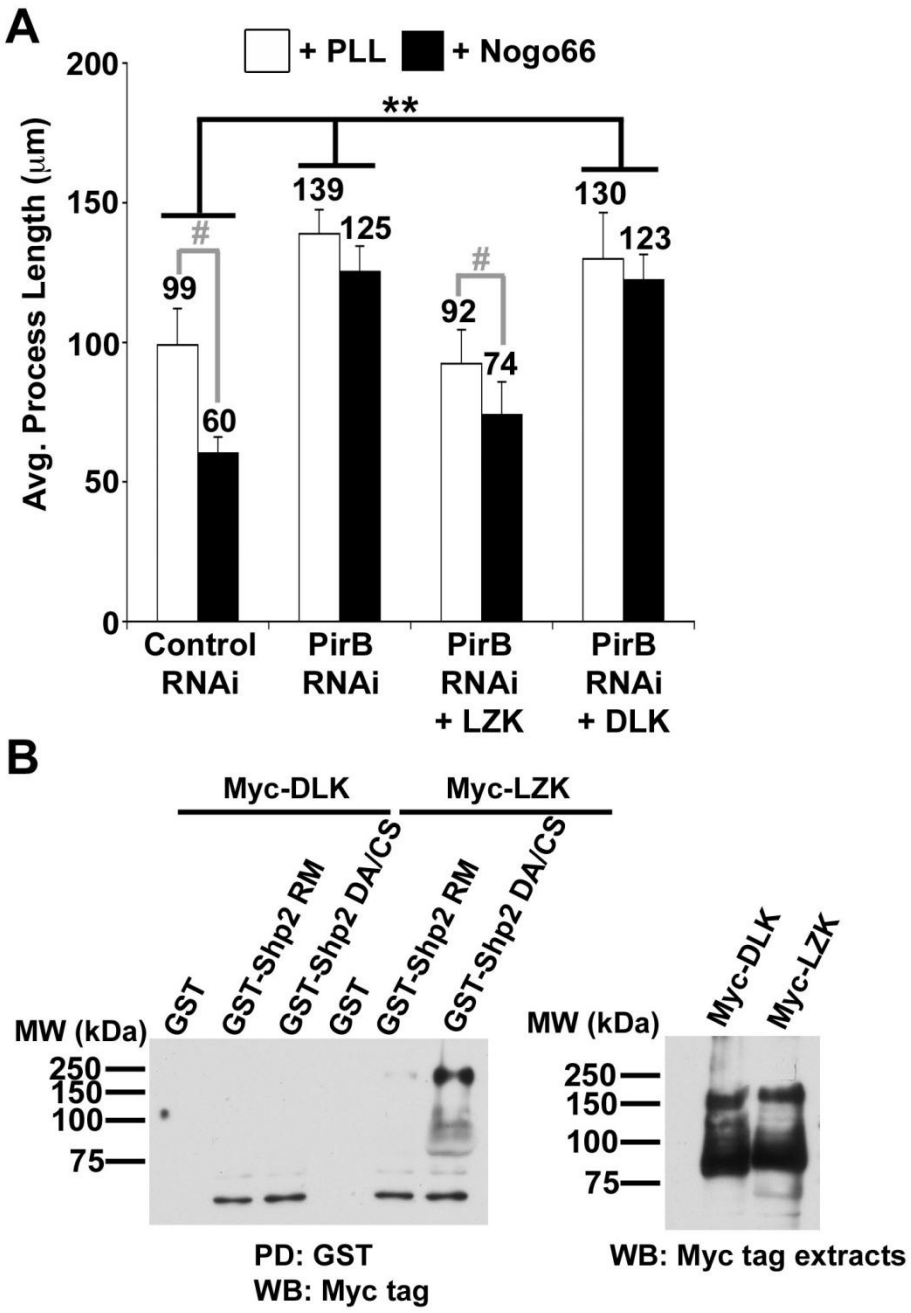

Figure 3.7 LZK, not DLK, is able to compensate for the loss of PirB and is trapped by Shp2

(A) Ectopic expression of LZK, but not DLK, is able to reverse the PirB RNAi long process phenotype and restore growth inhibtion on Nogo66 in CGNs. Average process length was determined from three independent experiments, with 348-475 neurons in total measured per condition. #p,** p<0.0001, Students *t* test.
(B) HEK293 cells, transfected with Myc-LZK or Myc-DLK plasmids, were treated with pervanadate prior to pull-down analysis wirh GST, GST-Shp2 RM, or GST-Shp2 DA/CS. Pervanadate treatment induces Shp2 trapping of LZK, but not DLK. Western blot is a representative image from three independent experiments.

not a substrate of Shp2. Collectively, these results suggest that DLK and LZK are both negative regulators of axon outgrowth, yet LZK is specific to the PirB-Shp2-POSH pathway. The mechanism of regulation of DLK/LZK function is still poorly understood and it will be interesting to determine how the neuron distinguishes between the kinases and how DLK is relaying Nogo66 inhibitory signals.

3.2.11 POSH is a convergence point for MAI signaling

The PirB receptor binds all three MAI family members, therefore we hypothesized that the POSH complex mediates inhibitory signals from MAG as well as NogoA. To address our hypothesis, CGNs were nucleofected with control, POSH, and PirB RNAi constructs and plated to PLL, Nogo66, and MAG. Loss of PirB function relieves growth inhibition mediated by MAG, similar to what we previously observed for Nogo66 (Figure 3.8). Consistent with our hypothesis, POSH RNAi expressing CGNs are also refractory to growth inhibition by MAG. This result suggests that POSH is a convergence point for MAI signaling. Collectively, the studies presented here highlight the importance in characterizing the molecular signaling mechanism of the POSH complex as targeting the POSH complex may be an efficacious strategy to enhance axonal regeneration in the damaged CNS.

3.3 Discussion

Studies from our laboratory have revealed a role for the POSH complex, composed of LZK and Shroom3, as downstream components of the NogoA-PirB pathway mediating axon growth inhibition [8, 9]. However, the signaling mechanism from PirB to the POSH complex was not known. In these studies, we define a role for Shp2 as a transmitter of NogoA mediated inhibitory signals to the POSH complex and suggest that Shp2 operates, at least in part, through the regulation of LZK function (Figure 3.9). We found that the phosphatase activity of Shp2 is required for mediating Nogo66-PirB growth inhibition, suggesting that a

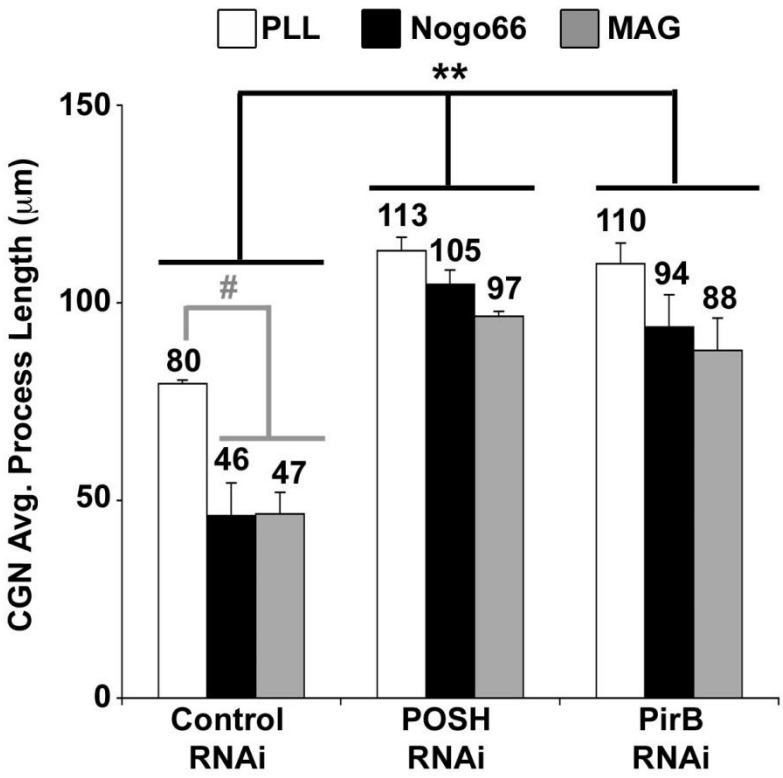

Figure 3.8 POSH is an intracellular signal transducer for Nogo66 and MAG

CGNs were nucleofected with the indicated RNAi vectors and plated to PLL, PLL+Nogo66, or PLL+MAG. Process length was scored 24 hr after nucleofection. Average process length was determined from two independent experiments, with 267-345 neurons in total measured per condition. POSH and PirB RNAi expressing neurons are refractory to growth inhibition by Nogo66 and MAG. #p, ** $p<0.0001$, Students *t* test.

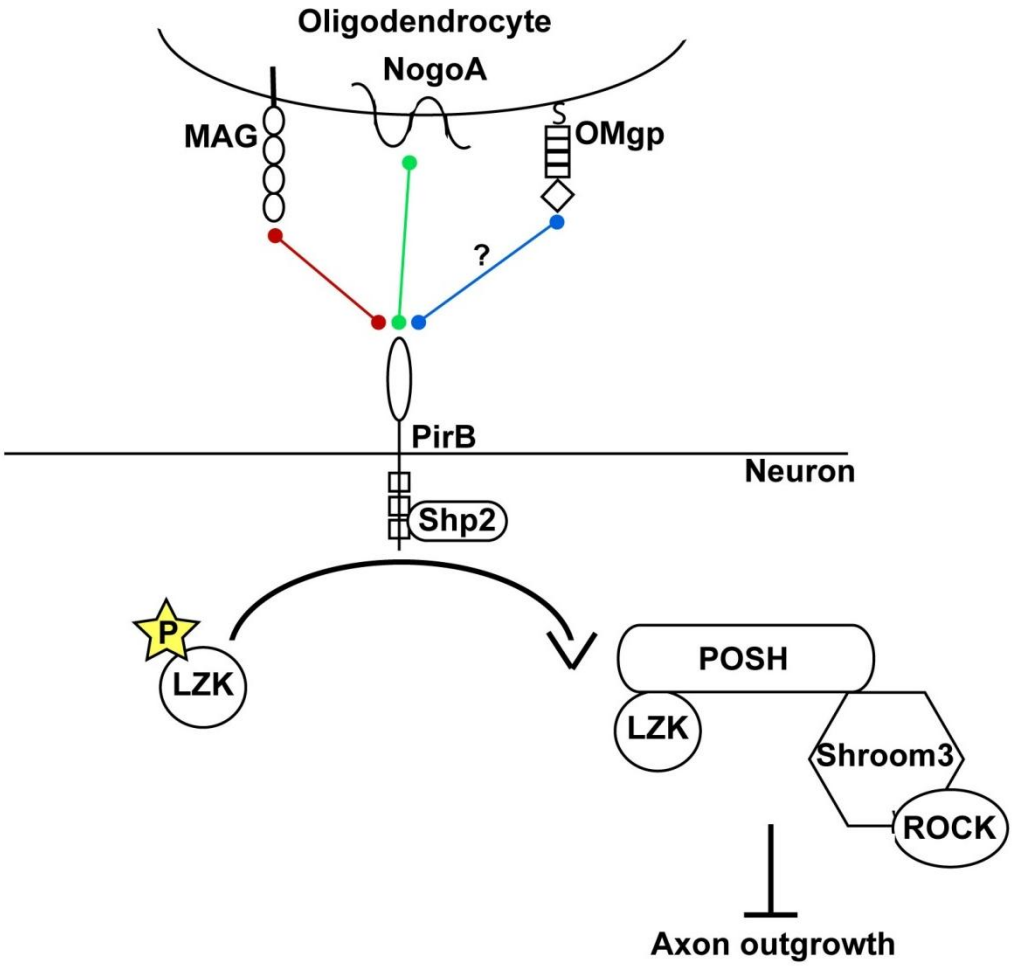

Figure 3.9 Proposed model of NogoA signaling through the POSH complex

NogoA and MAG initiate growth inhibition through association with the PirB receptor. PirB promotes the activation of Shp2 tyrosine phosphatase activity. Dephosphorylation by Shp2 promotes LZK function in an unknown mechanism. We propose that dephosphorylation facilitates LZK dimer formation and subsequent activation and/or LZK incorporation into the POSH complex composed of Shroom3 and ROCK to inhibit axon outgrowth.

downstream dephosphorylation event may be required for Nogo66 signaling. Consistent with this hypothesis, we demonstrated that upon Nogo66 stimulation of CGNs there is enhanced Shp2 trapping of tyrosine phosphorylated proteins and we identified LZK, but not POSH, as a potential Shp2 substrate. Interestingly, we show that DLK, a MLK family member, is a negative regulator of axon length and relays Nogo66-mediated growth inhibition. Additionally, ectopic expression of DLK can overcome the loss of LZK. However, DLK cannot suppress the PirB RNAi phenotype and is not trapped by Shp2, indicating DLK and LZK might undergo distinct regulation to facilitate their function. In summary, our studies suggest a model in which, in the absence of Nogo66 signaling, LZK is phosphorylated preventing its function in an unknown mechanism. Nogo66-PirB mediated inhibitory signals facilitate the dephosphorylation of LZK by Shp2 promoting LZK function to inhibit axon length. Collectively, the studies presented here further define the intracellular signaling pathway downstream from NogoA. Our studies indicate that POSH is a convergence point for MAI signaling. Reduction of POSH function by RNAi allows axonal outgrowth on Nogo66 and MAG. The PirB receptor binds all three MAIs and its function is required for growth inhibition, therefore we hypothesize that POSH is also relaying inhibitor signals from the third MAI, OMgp. There are additional receptors for MAIs and we are specifically interested in determining if the Nogo66 receptor, NgR1, is also signaling through POSH. NgR1 also binds all three MAIs and removal of NgR and PirB functions provides enhanced growth on myelin [3, 13, 17, 41]. Therefore, it is possible that they work in concert or on converging pathways to mediate inhibitory signals. If POSH is found to be a convergence point for all three MAIs and their receptors, strategies to block POSH function or complex formation could provide more efficacious regeneration of axons after injury or disease than targeting only one MAI or receptor.

The findings that Shp2 relays signals from NogoA through PirB and the requirement of its phosphatase activity suggest that Shp2 is a critical component of the NogoA signaling pathway. Additionally, these studies show that Nogo66 stimulation induces the trapping of several tyrosine phosphorylated proteins by

Shp2. This suggests that Shp2 has multiple substrates upon Nogo66 stimulation. Recently, it has been shown that upon MAG stimulation, Shp2 associates with PirB, binds to the tropomyosin receptor kinase B (TrkB) receptor, and promotes dephosphorylation of TrkB after activation by BDNF stimulation [23]. Thus, it appears that MAG may inhibit axon growth by promoting the deactivation of growth-promoting pathways. Shp2 has also been shown to dephosphorylate ROCK, promoting its activation[42]. Hence, TrkB or ROCK could be two of the proteins whose association with Shp2 is enhanced following Nogo66 stimulation. Analysis of Shp2 associated proteins by mass spectrometry from neuronal cell cultures would allow for identification of these substrates. It would also be interesting to determine whether inhibitory cues by MAG or NogoA promote Shp2 action on distinct substrates and how this links to POSH complex function.

Our studies indicate that Nogo66 stimulation promotes the trapping of LZK by Shp2. The mechanism behind LZK phosphorylation is not known. It is possible that LZK is phosphorylated by a growth promoting pathway to keep LZK from inducing growth inhibition. It is also possible that changes in phosphorylation status affect the localization or stability of LZK. LZK forms dimers to facilitate activation and requires the presence of POSH to relay axon growth inhibition [15, 28]. Therefore, we hypothesize that phosphorylation of LZK prevents dimerization or association with POSH. Experiments to map the site of phosphorylation may help determine how phosphorylation is affecting LZK function.

Our analyses of DLK and LZK reveal that both kinases are negative regulators of axon growth and can mediate growth inhibitory signals from Nogo66. Thus, it will be interesting to determine whether additional MLK family members (MLK1-4 and ZAK) can also regulate axon outgrowth. However, LZK, but not DLK, is able to complement the loss of PirB and is trapped by Shp2, indicating that there is differential regulation of MLKs promoting their function in distinct signaling pathways. Our results suggest that LZK is somehow preferentially selected over DLK to relay inhibitory signals from PirB. It is possible that association with Shp2 is sufficient to select LZK rather than DLK. DLK may

function in a distinct NogoA growth inhibitory pathway, perhaps from an unidentified Nogo66 receptor. It is also possible that DLK may require the presence of PirB to allow DLK to function, perhaps in a feed forward mechanism, and subsequently DLK would not be activated in the PirB RNAi neuron.

Finally, the DLK hypomorph studies suggest the loss of DLK does not affect Purkinje cell morphology or general cerebellar cellular organization. However, we did not examine differences in granule cell axon projection or changes in synaptic connections between granule cells and Purkinje cells. Thus, there may be differences between the DLK hypomorph and wild-type mice that we were not able to observe. Further animal studies, using conditional, double DLK/LZK knockouts along with a more in-depth phenotypic analysis would address functional redundancy of DLK or LZK and their role in development.

MAIs are a major impediment to regeneration and functional recovery of the injured CNS. The results presented by these studies demonstrate a signaling pathway downstream of NogoA composed of the receptor PirB, Shp2, LZK and POSH. Combined with our previous studies, which also showed the involvement of Shroom3 and ROCK in this signaling pathway, our studies delineate a novel intracellular signaling pathway downstream of NogoA. Additionally, these studies indicate that POSH is a convergence point for MAI signaling, highlighting the importance of POSH as an inhibitory axon outgrowth molecule. The findings presented here increase the knowledge of intracellular signaling mechanisms impeding neuronal growth in CNS. Our results also highlight that blocking the function of the POSH complex may promote enhanced axon outgrowth, plasticity, and functional recovery after injury or disease of the CNS.

3.4 Acknowledgements

We would like to thank Christin Carter-Su for providing the Shp2 plasmids which were originally from Jack Dixon. We also thank Lawrence Holzman for the generous donation of DLK hypomorph mice and Hetty Wong for her assistance with genotyping the mice. Additionally, we thank Mindy Waite and Donna Martin

for their assistance with cryogenic slicing and staining of sections, as well as for helpful discussions. We also thank Amanda Wilbur for technical assistance and Jennifer Taylor for DLK RNAi plasmid construction and characterization.

3.5 Materials and Methods

3.5.1 Antibodies and Reagents

For axon outgrowth assays, cells were stained with anti-green fluorescent protein (GFP) rabbit primary antibody (Invitrogen) and Alexa Fluor 488 goat anti-rabbit secondary antibody (Molecular Probes). For western blots the following primary antibodies were used: mouse anti-myc (9E10: purified from hybridomas), mouse anti-phosphotyrosine (Millipore), rabbit anti-actin (Sigma), rabbit anti-GFP (Invitrogen), and High Sensitivity NeutrAvidin-HRP (Pierce). Secondary antibodies used were: Goat Anti-Rabbit IgG Horseradish Peroxidase (HRP) Conjugate (BioRad) and Goat Anti-Mouse IgG Horseradish Peroxidase (HRP) Conjugate (BioRad). MAG-Fc (R&D Systems) was diluted to 100µg/mL in PBS and stored at -20°C.

3.5.2 Expression Constructs and RNAi

pUI4-SIBR-GFP is a short interfering RNA (siRNA) expression vector that co-expresses the GFP protein and a siRNA from an intronic expression cassette (the SIBR cassette) based on the miR-155 microRNA precursor [43]. For each siRNA, a pUI4-SIBR-GFP vector expressing one to four identical tandem copies of the siRNA SIBR cassette was constructed. POSH-6, luciferase (a functional control RNAi vector), PirB-874, LZK-1, LZK-2 are previously described [8, 9]. The sequence of DLK siRNA is 5’ UUAUUCGGUAAUUGGUCAGGGG 3’. CS2+MT POSH and CS2+NFLAG-LZK are described previously [8, 9, 44]. CS2+Myc-LZK was subcloned from CS2+NFLAG-LZK using BglII and EcoRI as cloning sites. CS2+NFLAG-DLK and CS2+Myc-DLK were subcloned from pcDNA3-DLK, a gift from Lawrence Holzman. CS2+3xHA-Shp2 and CS2+3xHA-Shp2 CS were

subcloned from pcDNA3+Shp2 and pcDNA3+Shp2 CS, generous gifts from Dr. Christin Carter-Su. Constitutively active CS2+3xHA-Shp2 E76K was constructed by site-directed mutagenesis, GAG being converted to AAG, substituting glutamate 76 to lysine. Phosphatase dead CS2+3xHA-Shp2 E76K/R465M and CS2+3xHA-Shp2 R465M was constructed by site-directed mutagenesis, CGG being converted to ATG, substituting arginine to methionine. The Shp2 trapping mutant D425A/C459S was constructed by site-directed mutagenesis, GAC being converted to GCC, substituting aspartate to alanine. Full length and the isolated phosphatase domain (PTP) of wild-type Shp2, the DA/CS trapping mutant, and catalytically inactive Shp2 R465M were subcloned into the bacterial expression construct pGST3. C-terminally tagged POSH-biotin binding domain was constructed by subcloning full length POSH into pEBB-cTB [45] using BamHI and NotI restriction sites.

3.5.3 Preparation of recombinant proteins

GST-Shp2 PTP WT, GST-Shp2 PTP DA/CS, GST-Shp2 RM, and GST-Shp2 DA/CS were produced in *Escherichia coli* using a pGST3 expression system. Briefly, *E.coli* cells were grown at 37°C until an OD_{600} of 0.8 was reached. Cells were induced overnight at 4°C with 0.3mM IPTG and lysed by sonication in PBS+ (PBS, 100µM PMSF, 14µg/mL aprotinin, 0.1% β-mercaptoethanol, 1µM leupeptin, 1µM pepstatin). Triton X-100 was added to the lysate at 1% of the final volume. Lysates were incubated with prewashed glutathione agarose (Pierce) for 1 hour at 4°C and washed three times in PBS+ with 300mM NaCl + 1% Triton X-100. The purified proteins, immobilized to the beads, were stored in PBS+ with 25% glycerol at -20°C. Purification of His-SUMO-conjugated Nogo66 (amino acids 1055-1079) was described previously [8].

3.5.4 Cerebellar granule neurons (CGNs)

4-well glass chamber slides or 12-well plates were coated for 4 hours with 10 µg/ml poly-L-lysine then overnight with 2µg/ml laminin (Invitrogen) or overnight at 4°C with laminin+control His-SUMO (2.5µg /cm^2), laminin+His-SUMO Nogo66 (2.5µg /cm^2), or laminin+MAG-Fc (500ng/cm^2). After overnight incubation, unbound substrates were removed by rinsing with PBS. CGNs were isolated from the cerebellum of post-natal day (P) 8 mice as described [46]. CGNs were transfected using AAD-1001 Nucleofector (Amaxa Biosystems) set to program O-03. CGNs were nucleofected with a total of 6µg of DNA: 4.5µg of pUI4 vector and 1.5µg of empty vector or CS2+3xHA-Shp2 E76K, CS2+3xHA-Shp2 E76K/RM, CS2+NFLAG-LZK, or CS2+NFLAG-DLK. CGNs isolated from wild-type and DLK hypomorph mice were plated with a final concentration of 100,000 cells/cm^2. Cells were fixed in 3.7% formaldehyde 24 hours post-nucleofection. Cells were stained with an anti-GFP primary antibody (Invitrogen) and Alexa Fluor 488 goat anti-rabbit secondary antibody (Molecular Probes).

3.5.5 Measurement of process length

Process length was measured as described previously [8, 9]. Briefly, using the box function in the MicroSuite imaging software version 5.0 (Olympus, Tokyo, Japan), the longest process per cell for all the cells within the box was measured. Results are presented as average process length, determined from three independent nucleofections with an average of 120 neurons measured per experiment per condition. Statistical significance was assessed using the Students t-test. All measurements of GFP-positive neurons from three independent nucleofections were included in the t-test, except for Figure 3.8 which was two independent nucleofections.

3.5.6 Shp2 trapping assays

In Figure 3.2A, 24 hours prior to harvest 4-10cm dishes of 100,000 CGNs/cm^2 were treated with or without 100µM pervanadate and/or 2.5µg/cm^2 Nogo66. Cells were harvested in Triton IP buffer (10mM HEPES pH 7.4, 2mM EDTA, 50mM NaF, 1% Triton X-100, 1mM PMSF, 150mM NaCl, 0.01% Aprotinin, 1mM Na_3VO_4) and incubated with 20µg of GST-Shp2 PTP WT, GST-Shp2 PTP DA/CS, GST-Shp2 RM, or GST-Shp2 DA/CS immobilized on glutathione agarose overnight at 4°C. Beads were washed 3 times with Triton IP buffer and resuspended in 40µL of 2x Sample Buffer. 10µL of sample were separated on a SDS-PAGE gel followed by western blot analysis for tyrosine phosphorylated proteins. In Figure 3.2B, 7x10^6 CGNs were nucleofected with 5µg of CS3+MT LZK and 1µg of CS2+eGFP. Each nucleofection was split onto 2-60mm dishes coated with PLL or PLL+2.5µg/cm^2 of Nogo66, for a total of 4 nucleofections and 8-60mm dishes. Prior to harvest, CGNs were treated with or without 100µM pervanadate and harvested in Triton IP Buffer. Shp2 pull downs proceeded as described above.

In HEK 293 cells, 32,000 cells/cm^2 were transfected with 3ug of DNA of CS3+MT POSH, CS3+MT LZK, or CS3+MT DLK. 24 hours after transfection, cells were treated with or without 100µM pervanadate for 30 minutes, harvested in Triton IP Buffer, and incubated with 20µg of GST-empty, GST-Shp2 RM, or GST-Shp2 DA/CS immobilized on glutathione agarose for 1 hour at 4°C. Beads were washed 3 times with Triton IP buffer and resuspended in 40µL of 2x Sample Buffer. 10µL of sample were separated on a SDS-PAGE gel followed by western blot analysis for the myc-epitope tag.

3.5.7 DLK mice/staining

All procedures involving the use of mice were approved by the University of Michigan committee on the Use and Care of Animals (UCUCA). DLK hypomorph transgenic mice were obtained from Lawrence Holzman and maintained on a C57BL/6J background (unpublished data). The DLK transgene was detected

using forward primer 5’-GGTGGTTGTTATCATAGTTCCATCATG-3’ and reverse primer 5’-GCTAGTCATGGAGTAGTAGG-3’. Whole brains from P10 mice from wild-type and DLK hypomorph mice were harvested and fixed in 4% paraformaldehyde overnight at 4°C. Brains were embedded in Optimal Cutting Temperature embedding medium (Sakura Finetek, Torrance, CA), cryosectioned (15µm) and stored at -80°C. For Calbindin staining, slides were fixed in 4% paraformaldehyde, blocked for 2 hours in Tyramide signal amplification (TSA) kit block (Invitrogen), and stained overnight at 4°C with mouse anti-Calbindin (Swant) at 1:10,000. Slides were developed using DAB reagent (Sigma), followed by mounting with mounting media. Hematoxylin and eosin stain was performed as described previously [41].

3.6 References

1. Giger, R.J., et al., Mechanisms of CNS myelin inhibition: Evidence for distinct and neuronal cell type specific receptor systems. Restorative Neurology and Neuroscience, 2008. 26(2-3): p. 97-115.
2. Gonzenbach, R.R. and M.E. Schwab, Disinhibition of neurite growth to repair the injured adult CNS: Focusing on Nogo. Cellular and Molecular Life Sciences, 2008. 65(1): p. 161-176.
3. Fournier, A.E., T. GrandPre, and S.M. Strittmatter, Identification of a receptor mediating Nogo-66 inhibition of axonal regeneration. Nature, 2001. 409(6818): p. 341-346.
4. Akbik, F., W.B.J. Cafferty, and S.M. Strittmatter, Myelin associated inhibitors: A link between injury-induced and experience-dependent plasticity. Experimental Neurology, (0).
5. Atwal, J.K., et al., PirB is a Functional Receptor for Myelin Inhibitors of Axonal Regeneration. Science, 2008. 322(5903): p. 967-970.
6. Domeniconi, M., et al., Myelin-associated glycoprotein interacts with the Nogo66 receptor to inhibit neurite outgrowth. Neuron, 2002. 35(2): p. 283-290.
7. Wang, K.C., et al., Oligodendrocyte-myelin glycoprotein is a Nogo receptor ligand that inhibits neurite outgrowth. Nature, 2002. 417(6892): p. 941-944.
8. Dickson, H.M., et al., POSH is an intracellular signal transducer for the axon outgrowth inhibitor Nogo66. J Neurosci, 2010. 30(40): p. 13319-25.
9. Taylor, J., et al., The scaffold protein POSH regulates axon outgrowth. Mol Biol Cell, 2008. 19(12): p. 5181-92.
10. Grossmann, K.S., et al., Chapter 2 - The Tyrosine Phosphatase Shp2 in Development and Cancer, in Advances in Cancer Research, F.V.W. George and K. George, Editors. 2010, Academic Press. p. 53-89.
11. Barford, D. and B.G. Neel, Revealing mechanisms for SH2 domain mediated regulation of the protein tyrosine phosphatase SHP-2. Structure, 1998. 6(3): p. 249-254.
12. Hof, P., et al., Crystal Structure of the Tyrosine Phosphatase SHP-2. Cell, 1998. 92(4): p. 441-450.
13. Neel, B.G., H. Gu, and L. Pao, The ‘Shp'ing news: SH2 domain-containing tyrosine phosphatases in cell signaling. Trends in Biochemical Sciences, 2003. 28(6): p. 284-293.
14. Chen, H.E., et al., Regulation of colony-stimulating factor 1 receptor signaling by the SH2 domain-containing tyrosine phosphatase SHPTP1. Molecular and Cellular Biology, 1996. 16(7): p. 3685-3697.
15. Timms, J.F., et al., Identification of major binding proteins and substrates for the SH2-containing protein tyrosine phosphatase SHP-1 in macrophages. Molecular and Cellular Biology, 1998. 18(7): p. 3838-3850.
16. Kubagawa, H., P.D. Burrows, and M.D. Coopers, A novel pair of immunoglobulin-like receptors expressed by B cells and myeloid cells. Proceedings of the National Academy of Sciences of the United States of America, 1997. 94(10): p. 5261-5266.
17. Burshtyn, D.N., et al., A novel phosphotyrosine motif with a critical amino acid at position-2 for the SH2 domain-mediated activation of the tyrosine phosphatase SHP-1. Journal of Biological Chemistry, 1997. 272(20): p. 13066-13072.
18. Vivier, E. and M. Daeron, Immunoreceptor tyrosine-based inhibition motifs. Immunology Today, 1997. 18(6): p. 286-291.

19. Yamashita, Y., M. Ono, and T. Takai, Inhibitory and stimulatory functions of paired Ig-like receptor (PIR) family in RBL-2H3 cells. Journal of Immunology, 1998. 161(8): p. 4042-4047.
20. Blery, M., et al., The paired Ig-like receptor PIR-B is an inhibitory receptor that recruits the protein-tyrosine phosphatase SHP-1. Proceedings of the National Academy of Sciences of the United States of America, 1998. 95(5): p. 2446-2451.
21. Maeda, A., et al., Requirement of SH2-containing protein tyrosine phosphatases SHP-1 and SHP-2 for paired immunoglobulin-like receptor B (PIR-B)-mediated inhibitory signal. Journal of Experimental Medicine, 1998. 187(8): p. 1355-1360.
22. Syken, J., et al., PirB restricts ocular-dominance plasticity in visual cortex. Science, 2006. 313(5794): p. 1795-800.
23. Fujita, Y., et al., Myelin suppresses axon regeneration by PIR-B/SHP-mediated inhibition of Trk activity. Embo Journal, 2011. 30(7): p. 1389-1401.
24. Fujita, Y., et al., The p75 receptor mediates axon growth inhibition through an association with PIR-B. Cell Death & Disease, 2011. 2.
25. Denu, J.M. and J.E. Dixon, Protein tyrosine phosphatases: mechanisms of catalysis and regulation. Current Opinion in Chemical Biology, 1998. 2(5): p. 633-641.
26. Agazie, Y.M. and M.J. Hayman, Development of an efficient "substrate-trapping" mutant of Src homology phosphotyrosine phosphatase 2 and identification of the epidermal growth factor receptor, Gab1, and three other proteins as target substrates. Journal of Biological Chemistry, 2003. 278(16): p. 13952-13958.
27. Flint, A.J., et al., Development of "substrate-trapping" mutants to identify physiological substrates of protein tyrosine phosphatases. Proceedings of the National Academy of Sciences of the United States of America, 1997. 94(5): p. 1680-1685.
28. Ikeda, A., et al., Identification and characterization of functional domains in a mixed lineage kinase LZK. Febs Letters, 2001. 488(3): p. 190-195.
29. Nihalani, D., S. Merritt, and L.B. Holzman, Identification of structural and functional domains in mixed lineage kinase dual leucine zipper-bearing kinase required for complex formation and stress-activated protein kinase activation. Journal of Biological Chemistry, 2000. 275(10): p. 7273-7279.
30. Ikeda, A., et al., Mixed lineage kinase LZK forms a functional signaling complex with JIP-1, a scaffold protein of the c-Jun NH2-terminal kinase pathway. Journal of Biochemistry, 2001. 130(6): p. 773-781.
31. Wang, C., et al., Regulation of the protein stability of POSH and MLK family. Protein & Cell, 2010. 1(9): p. 871-878.
32. Xu, Z.H., N.V. Kukekov, and L.A. Greene, POSH acts as a scaffold for a multiprotein complex that mediates JNK activation in apoptosis. Embo Journal, 2003. 22(2): p. 252-261.
33. Bloom, A.J., et al., The requirement for Phr1 in CNS axon tract formation reveals the corticostriatal boundary as a choice point for cortical axons. Genes & Development, 2007. 21(20): p. 2593-2606.
34. Hirai, S., et al., The c-Jun N-terminal kinase activator dual leucine zipper kinase regulates axon growth and neuronal migration in the developing cerebral cortex. Journal of Neuroscience, 2006. 26(46): p. 11992-12002.
35. Hofker, M.H. and J.v. Deursen, Transgenic mouse methods and protocols. Springer protocols. 2011, New York, NY: Humana Press. xi, 352 p.

36. Schilling, K., et al., Besides Purkinje cells and granule neurons: an appraisal of the cell biology of the interneurons of the cerebellar cortex. Histochem Cell Biol, 2008. 130: p. 601-615.
37. Eto, K., et al., Role of dual leucine zipper-bearing kinase (DLK/MUK/ZPK) in axonal growth. Neuroscience Research, 2010. 66(1): p. 37-45.
38. Hirai, S., et al., Axon Formation in Neocortical Neurons Depends on Stage-Specific Regulation of Microtubule Stability by the Dual Leucine Zipper Kinase-c-Jun N-Terminal Kinase Pathway. Journal of Neuroscience, 2011. 31(17): p. 6468-6480.
39. Wang, X., et al., Targeted deletion of the mitogen-activated protein kinase kinase 4 gene in the nervous system causes severe brain developmental defects and premature death. Molecular and Cellular Biology, 2007. 27(22): p. 7935-7946.
40. Suenaga, J., et al., Developmental changes in the expression pattern of the JNK activator kinase MUK/DLK/ZPK and active JNK in the mouse cerebellum. Cell and Tissue Research, 2006. 325(1): p. 189-195.
41. Sclafani, A.M., et al., Nestin-Cre mediated deletion of Pitx2 in the mouse. genesis, 2006. 44(7): p. 336-344.
42. Lee, H.H. and Z.F. Chang, Regulation of RhoA-dependent ROCKII activation by Shp2. Journal of Cell Biology, 2008. 181(6): p. 999-1012.
43. Chung, K.H., et al., Polycistronic RNA polymerase II expression vectors for RNA interference based on BIC/miR-155. Nucleic Acids Research, 2006. 34(7).
44. Figueroa, C., et al., Akt2 negatively regulates assembly of the POSH-MLK-JNK signaling complex. Journal of Biological Chemistry, 2003. 278(48): p. 47922-47927.
45. Maine, G.N., et al., A bimolecular affinity purification method under denaturing conditions for rapid isolation of a ubiquitinated protein for mass spectrometry analysis. Nature Protocols, 2010. 5(8): p. 1447-1459.
46. Bilimoria, P.M. and A. Bonni Cultures of Cerebellar Granule Neurons. Cold Spring Harbor Protocols, 2008. doi:10.1101/pdb.prot5107.

Chapter 4

Identification of Chemical Inhibitors of the Shroom3-ROCKII interaction

4.1 Introduction

The adult mammalian central nervous system (CNS) is limited in its ability to regenerate or replace the axons of neurons lost in response to injury or disease. A crucial contributor to this lack of regeneration is myelin and its three associated proteins termed myelin associated inhibitors (MAIs): Myelin-associated glycoprotein (MAG), NogoA, and Oligodendrocyte-myelin glycoprotein (OMgp) [1, 2]. Blocking the function of MAIs, with antibodies or receptor antagonists promotes axon growth and plasticity, and results in enhanced functional recovery after stroke or spinal cord injury in rodent models [3-10]. Thus, functional recovery after CNS injury is limited by MAIs, and small molecule compounds that can circumvent MAI inhibition are likely to enhance functional recovery after stroke or spinal cord injury.

A complicating factor in developing small molecules for CNS regeneration is the complexity of signaling at the neuronal cell surface. There are multiple and overlapping receptors for MAIs, and targeting individual MAIs may not fully relieve growth inhibition [11-17]. A complementary and perhaps more efficacious strategy to enhance axon growth after injury might be to target MAI intracellular signaling pathways. We have previously shown that the POSH complex consisting of LZK and Shroom3 is downstream of NogoA and its receptor PirB [18]. Loss of function of POSH, or any one of the POSH associated proteins, leads to enhanced process growth and refraction to inhibition by NogoA. POSH is also downstream of MAG (Chapter 3, Figure 3.8) suggesting that the POSH complex is a convergence point for MAI signaling. Thus, we sought to identify

chemical inhibitors that target specific protein-protein interactions of the POSH complex, and we propose that these inhibitors will circumvent NogoA or MAG-mediated growth inhibition.

Correct formation of protein-protein interactions (PPIs) is required for nearly all cellular processes and a protein's function can directly rely on its interacting protein. Indeed, the role of a signaling protein in the CNS can be distinct from its role elsewhere in the body [19]. Targeting the enzymatic activity of a protein will affect all signaling pathways in which the protein is involved, potentially leading to severe side effects. On the other hand, inhibiting the ability of an enzyme to bind a specific substrate would allow the overall activity of the enzyme to persist, but limit the downstream effects. Furthermore, specifically disrupting the interaction of an enzyme with a substrate that only occurs in the CNS would be an even more efficacious drug development strategy. Thus, there is much interest in targeting non-enzymatic, PPIs for therapeutic purposes as this strategy may limit off target side effects elsewhere in the body.

Current strategies to inhibit PPIs involve the use of antibodies, dominant negative peptides, or antisense constructs. However, all of these strategies are expensive to manufacture, lack oral bioavailability, and in the case of antibodies, are not cell permeable [20]. Therefore, strategies for treating spinal cord or stroke injury have relied on implants, which secrete antibodies, or direct injection of therapeutics into the spinal cord tract. Thus, the use of small "drug-like" compounds to target intracellular PPIs has attracted the attention of scientists both in the pharmaceutical industry and academia as tools to develop more efficient and cost effective therapies.

Development of chemical inhibitors of PPIs has proven more difficult than targeting the enzymatic activity of a protein. The major obstacle in targeting PPIs is the sheer size and geometry of the interaction interface. The contact surface involved in a PPI is typically large (~800-3,000 Å), while the contact surface of a protein-small molecule is small (~300-1000 Å) [21, 22]. Also, the interface of two interacting proteins may be flat compared to the grooves and pockets present at the active site of an enzyme or at the hydrophilic surface of a protein, thus not

providing a ideal surface for small molecule binding [21, 23, 24]. Additionally, unlike most enzymatic proteins and receptors, most PPIs do not have natural or known small molecule partners, and rational design of chemical inhibitors without structural knowledge of a PPI is difficult. Lastly, a surprisingly common inhibitory mechanism has been discovered in which small molecules inhibit the PPI without binding to the interaction site. Examples of these include: allosteric inhibitors, denaturants, or amphipathic small molecules that can form micelles around a protein, preventing the interaction from forming [25-28]. For example, DnaK is a molecular chaperone whose ATPase activity provides energy for bacterial chaperone machinery and complex formation of DnaK with DnaJ and GrpE are essential for the ATPase activity of DnaK [29, 30]. In a high-throughput screen for inhibitors of the DnaK-DnaJ interaction, myricetin was identified [31]. However, it was determined that myricetin bound to DnaK at a site 20-30Å away from the DnaJ binding region and structural studies support the hypothesis that myricetin binding may alter the confirmation of DnaK in a way that prevents DnaJ binding [31].

A breakthrough in targeting PPIs occurred when alanine scanning mutations along the interaction site of PPIs led to the discovery of 'hot spots' on protein interaction surfaces [32, 33]. Hot spots are small regions of the PPI that contribute a disproportionate amount to the binding energy of the PPI. For example, alanine scanning revealed that glutamate 62 and phenylalanine 42 on the cytokine IL-2 are critical residues for its association with its receptor IL-2Rα [34]. Small molecules were discovered which bound within this region and tethering these molecules together provided a more potent inhibitor to disrupt the cytokine-receptor interaction [35]. Thus, identifying hot spots on a protein provides knowledge for rational design of chemicals to enhance the disruption of PPIs with small molecules.

In the absence of 'hot spot' information or structural knowledge of the PPI interface, high-throughput screening (HTS) is often performed to efficiently identify chemical inhibitors. There are many approaches to the discovery of small molecule inhibitors of PPIs that are amenable to HTS. The most direct and

common method is a competitive binding assay in which one or more of the proteins is labeled, such as enzyme linked immunosorbant assay (ELISA) or Forster resonance energy transfer (FRET). In the following studies, we describe the development of a modified ELISA platform for the identification of chemical inhibitors of the POSH complex, specifically the Shroom3-ROCK interaction. Using this platform, 20,000 small molecules were screened in the Center for Chemical Genomics (CCG) at the University of Michigan. Significantly, 36 inhibitors of the Shroom3-ROCK interaction have been confirmed by dose response. Further validation and characterization of these compounds will provide valuable tools to examine the importance of PPIs in the POSH complex and their role in growth inhibition mediated by MAIs.

4.2 Results

4.2.1 The Shroom3-ROCK interaction is direct and biologically significant

The aim of this study is to identify chemical inhibitors of the POSH complex that relieve axon growth inhibition on MAIs. Thus, the chosen protein-protein interaction (PPI) must be both direct and biologically significant. The ASD2 domain of the POSH interacting protein Shroom3 is required for Shroom3 to regulate process outgrowth inhibition [36]. ROCKI and II interact with the ASD2 domain of Shroom3 through regions denoted R1C1 and R2C1, respectively [37]. In epithelial cells, ectopic expression of R1C1 or R2C1 acts in a dominant negative manner to block apical constriction by interfering with the ability of endogenous ROCK to bind Shroom3 [37]. To determine whether ROCK functions with Shroom3 to inhibit axon outgrowth, P19s were transfected with R1C1 and its effects on process length were assessed. Process length is enhanced in R1C1 expressing neurons relative to control, suggesting that Shroom3 acts through ROCK to inhibit process outgrowth (Figure 4.1A). Additionally, inhibition of ROCK with the pharmacological inhibitor Y-27632 enhances neuronal process outgrowth in control neurons, consistent with

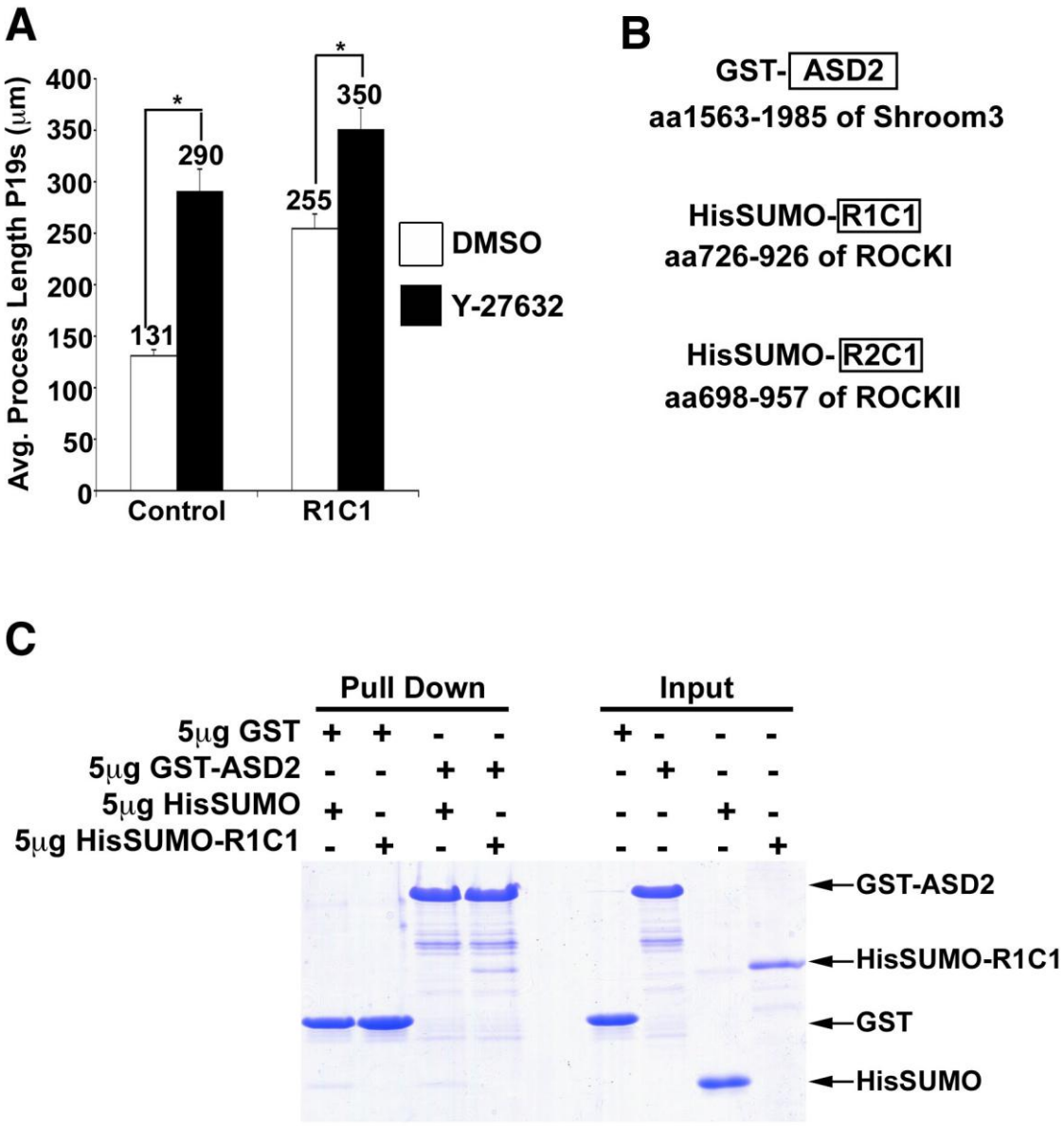

Figure 4.1 Shroom3 and ROCK interact directly and the interaction regulates axon outgrowth

(A) Ectopic expression of R1C1 acts in a dominant negative manner to inhibit the endogenous ROCK-Shroom3 interaction, resulting in enhanced process length. Treatment of P19s with the known ROCK inhibitor Y-27632 enhances process length in control neurons and further enhances the length of R1C1 neurons. Average process length was determined from two independent experiments with 224-315 total neurons measured per condition. *p<0.0001, Students *t* test.
(B) Schematic of epitope-tagged protein domains.
(C) GST-ASD2 and HisSUMO-R1C1 interact directly and the interaction is specific. 5μg of each protein were subjected to pull down analysis, followed by SDS-PAGE and detection with GelCode Blue.

previous studies that demonstrate a role for ROCK as an inhibitor of axon outgrowth and regeneration after injury [38-40]. This result also suggests that ROCK can mediate growth inhibition in both a Shroom3 dependent and independent mechanism. These results indicate process outgrowth inhibition is mediated, in part, through the Shroom3-ROCK interaction.

In order for the Shroom3-ROCK interaction to be an ideal candidate for chemical inhibition, the interaction needs to be direct. Therefore, bacterial expression constructs for the individual domains ASD2, R1C1, and R2C1 were generated (Figure 4.1B). GST-ASD2 and HisSUMO-R1C1 were purified from *Escherichia coli* and pull-down analysis was performed. HisSUMO-R1C1 bound to GST-ASD2 and the interaction was direct and specific (Figure 4.1C). Subsequent experiments with R2C1 indicate that the ASD2-R2C1 interaction is also direct and specific (data not shown). These results indicated that the ASD2-Rho kinase interaction is an attractive site for interference by a small molecule and, combined with the result that the Shroom3-ROCK interaction is biologically significant, highlights the PPI as a plausible target for chemical inhibition.

4.2.2 Development of Fluorescence Quench Assay (FQA)

To initiate a screen for potential inhibitors of the Shroom3-ROCK interaction, we investigated several high-throughput methodologies. Non-fluorescent Forster resonance energy transfer (FRET) is a common methodology to study interactions between proteins. FRET is a non-radiative energy transfer that occurs when the emission spectrum of a donor overlaps with the absorption spectrum of an acceptor [41]. As the donor and acceptor are brought within a certain distance of one another (<10nm), the interaction is characterized by a reduction in donor fluorescence and an increase in acceptor fluorescence. However, FRET is not ideal when performing binding titrations due to an overlap of the acceptor and donor fluorescence spectra [42]. Therefore, non-fluorescent acceptors have been employed to remove the need for spectral isolation, improve the sensitivity of the assay, and simplify binding experiments [31, 42].

A Fluorescence Quench Assay (FQA) which employs these non-fluorescent acceptors was initially chosen to examine the Shroom3-ROCK interaction [31, 42]. FQA was chosen based on the fact that it is highly amenable to HTS, as the assay only entails mixing of the two proteins with no wash steps or addition of detection reagents. FQA requires the labeling of one protein with a fluorescence molecule and the other with a quencher. An interaction is visualized by a quench in fluorescence. This is due to the fluorescent-tagged protein coming within distance of the protein tagged with the quencher. To develop the reagents necessary for this assay, GST-ASD2 was labeled with the fluorescent donor Alexa-488 (emission 525nm), subsequently referred to as Alexa-ASD2. Additionally, HisSUMO-R1C1 was labeled with Black Hole Quencher-10 (BHQ-10), a FRET acceptor that absorbs strongly around 507nm, henceforth referred to as BHQ-R1C1. When Alexa-ASD2 comes into contact with BHQ-R1C1, the fluorescence emission from the Alexa label should be quenched (Figure 4.2A). Inhibition of this PPI by a chemical or with unlabeled R1C1 will result in a loss of quenching (Figure 4.2A).

To characterize the Alexa-ASD2 and BHQ-R1C1 interaction, we first varied the time of incubation and monitored the percent quench in fluorescence. Using the FQA, the apparent K_d was calculated to be 1 ± 0.1μM (data not shown). However, the change in fluorescence was saturated almost immediately (less than five minutes) following the addition of the two proteins, and this signal did not change even up to two hours (Figure 4.2B). Thus, this rate of association may be too fast for identifying inhibitors effectively by HTS. Further, as there are no known chemical inhibitors of the Shroom3-ROCK interaction, unlabeled R1C1 was used as a positive control for blocking the ASD2-R1C1 interaction. A competition experiment with increasing concentrations of unlabeled R1C1 was performed to determine whether the observed quenching was due to specific ASD2-R1C1 binding. Surprisingly, unlabeled R1C1 was unable to compete with BHQ-R1C1 for association with Alexa-ASD2 (Figure 4.2C). Additionally, switching the orientation of the labels, BHQ-ASD2 and Alexa-R1C1, did not allow for competition or affect the time to saturation (data not shown). Furthermore we

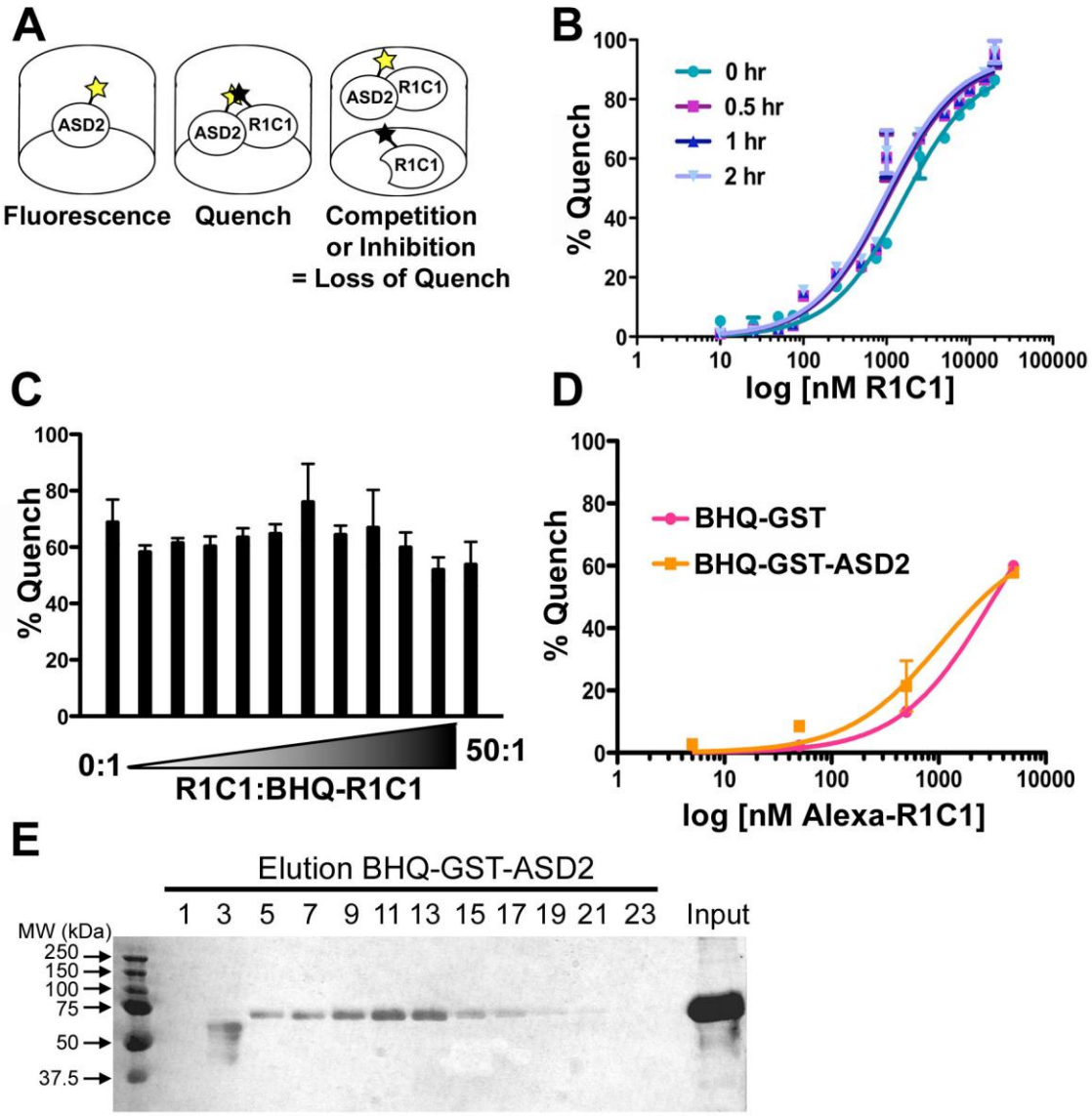

Figure 4.2 Examining ASD2-R1C1 interaction by Fluorescence Quench Assay (FQA)

(A) Schematic of FQA. 100nM of Alexa-ASD2 provides baseline fluorescence. By varying the concentrations of BHQ-R1C1, quench of fluorescence is observed as the tags come within range (<10nm) due to PPI. Competition assays using unlabeled R1C1 should release the quench, returning fluorescence to control levels.
(B) Time course of FQA reveals that the ASD2-R1C1 interaction saturates in less than 5 minutes.
(C) There is no observed competition of the ASD2-R1C1 interaction by varying concentrations of unlabeled R1C1 suggesting the interaction is non-specific.
(D) 250nM of BHQ-GST quenches the fluorescence of Alexa-R1C1 at the same level as BHQ-GST-ASD2.
(E) Size exclusion chromatography reveals that labeling of ASD2 leads to protein aggregation. BHQ-GST-ASD2 (expected molecular weight of 73 kDa) elutes from the column at 443-669 kDa (elution 5-13)

also observed quenching with labeled BHQ-GST epitope tag. BHQ-GST quenched Alexa-R1C1 fluorescence to nearly the same extent as BHQ-ASD2, suggesting that a non-specific interaction is responsible for quenching (Figure 4.2D). These results clearly indicate that the observed quench is due to non-specific association of GST, and not due to a specific ASD2-R1C1 interaction. Together with the lack of time dependent quenching, these data suggest that non-specific binding is affecting our assay.

To verify that the Alexa- or BHQ-tagged proteins were still capable of interacting, pull-down analysis was performed. Surprisingly, the proteins were no longer able to associate, suggesting that the Alexa and BHQ tags were interfering with the interaction (data not shown). Given this data, we further proposed that the addition of the tags may result in a conformational change or a decrease in solubility. To investigate this hypothesis, size exclusion chromatography was performed on BHQ-ASD2 and the fractionation pattern of protein was analyzed by SDS-PAGE. BHQ-ASD2 has an expected molecular weight of 73Kda and size exclusion chromatography showed that BHQ-ASD2 eluted off the column in fractions 5-17, with the highest amount of protein in fraction 9-13. This is consistent with a molecular weight of 400-600kda (Figure 4.2E). Similar data was seen for Alexa-R1C1, which has an expected molecular weight of 38kDa and eluted off the column in fractions 13-19, indicating a molecular weight of 150-400kDa (data not shown). These results indicate that application of the Alexa and BHQ tags to ASD2 or R1C1 results in protein aggregation. Collectively, these studies suggest that an HTS platform that requires labeling of R1C1 or ASD2 with a fluorescent tag may not be plausible for identifying chemical inhibitors of our PPI. Therefore, we next pursued an ELISA-based assay in which both proteins could be detected without the addition of fluorescent labels.

4.2.3 Development and optimization of ELISA platform

4.2.3.1 Selecting a detection method for ELISA assay

Although initial studies were carried out with ROCKI, ROCKII is the prominent isoform in the brain and displays higher affinity to Shroom3; therefore all further studies were performed with R2C1, the Shroom3 binding region of ROCKII (Figure 4.1B) [37]. The ELISA platform requires that one protein be immobilized or captured on a microplate, followed by addition of the second, interacting protein. Toward this goal, we took advantage of a high-binding polystyrene surface on clear 96 or 384-well microplates, which allowed GST-ASD2 to be directly immobilized on the surface. Briefly, our initial ELISA protocol (Figure 4.3A, left) began with immobilization of GST-ASD2 on the 96-well microplate surface, followed by addition of HisSUMO-R2C1. There are no known antibodies against ASD2 or R2C1, therefore to detect the proteins we used antibodies directed against the epitope tags. Thus, binding of HisSUMO-R2C1 was detected using an anti-SUMO antibody, followed by application of an HRP-conjugated secondary antibody. Detection of HRP was carried out using turnover of the HRP substrate tetramethylbenzidine (TMB, absorbance at 450 nm). HisSUMO-R2C1 bound to GST-ASD2 in a promising dose-dependent manner (Figure 4.3B). However, even at a 20:1 ratio of ASD2:R2C1, the maximum signal was < 1 absorbance units at 450nm, suggesting the need for a more sensitive detection system.

In order to enhance efficiency and improve the signal-to-noise ratio of the ELISA, HisSUMO-R2C1 was biotinylated and detected with NeutrAvidin-HRP (Figure 4.3C). The advantage of this detection system is three-fold: first, the biotin label is smaller than the fluorescent labels (589 Da to 703-885 Da, respectively) and, second, the polyethylene glycol (PEG) linker on the biotin label enhances solubility of the protein, preventing the aggregation that was seen when the proteins were labeled with the fluorescent tags. Third, the high-affinity biotin-avidin interaction is extremely sensitive and efficient relative to the use of primary and secondary antibodies (Figure 4.3B). Further, this approach reduces

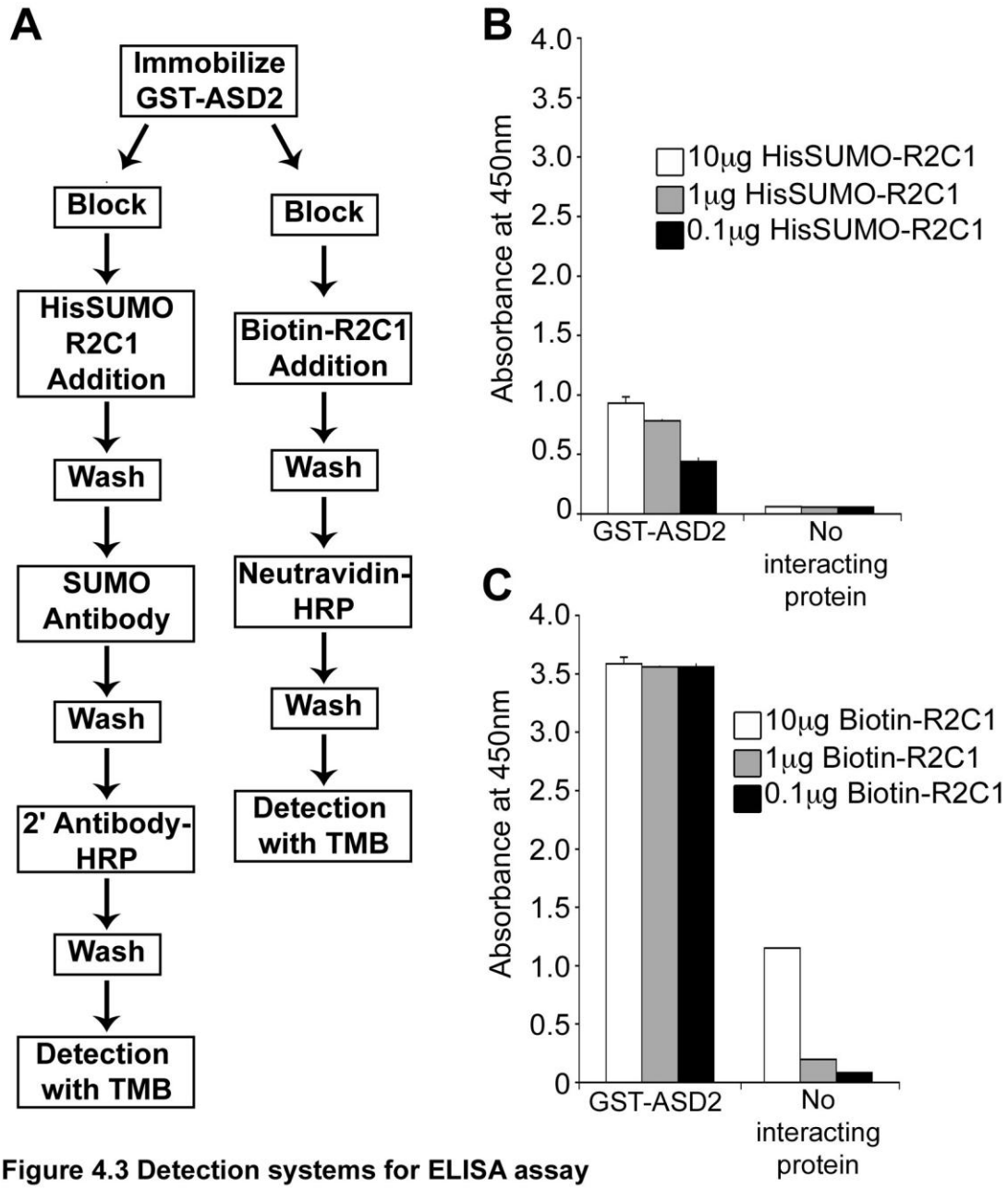

Figure 4.3 Detection systems for ELISA assay

(A) Comparison of ELISA protocol using HisSUMO-R2C1 detected with anti-SUMO antibody or Biotin-R2C1 detected with NeutrAvidin-HRP.
(B-C) Detection of ASD2-R2C1 interaction with anti-SUMO antibody followed by 2'Antibody-HRP yields low absorbance signal (B) when compared to detection of Biotin-R2C1 with NeutrAvidin-HRP (C). Detection with NeutrAvidin also increases the efficiency of the ELISA assay and enhances the signal to noise ratio.

the number of steps necessary for detection, making the assay more amenable for HTS. As expected, detection using NeutrAvidin-HRP increased the absorbance signal over 3-fold, allowing for an enhanced signal-to-noise ratio of 3.5:0.1 (Figure 4.3A, left). Therefore, all further optimization was performed with Biotin-HisSUMO-R2C1 (termed Biotin-R2C1) and was detected with NeutrAvidin-HRP.

4.2.3.2 Removal of GST epitope tag and affinity determination

As previously observed in the FQA assay, non-specific binding between epitope tags was again observed, despite improvements in signal-to-noise. Using the ELISA platform, we determined the apparent K_d for GST-ASD2 and Biotin-R2C1 using 0.5µg immobilized GST-ASD2 and varying concentrations of Biotin-R2C1. The apparent K_d was calculated to be 3.2 ± 0.2 nM (Figure 4.4A). However, interaction of Biotin-R2C1 with the same amount of isolated GST immobilized on the plate resulted in an apparent of K_d of 290 ± 19 nM (Figure 4.5A). Additionally, untagged R2C1 was unable to compete with 100ng of Biotin-R2C1 for binding 0.5µg GST-ASD2 (Figure 4.4B). Together, these data indicate that non-specific binding between GST and HisSUMO-R2C1 is contributing to the interaction. As a first attempt to remedy this, the concentrations of salt and detergent in the wash buffers were varied. We varied Tris, Phosphate, and HEPES buffers with amounts of salt, detergent, and carrier protein (data not shown). However, no significant reduction in non-specific binding was observed. The HTS screen could be run at protein concentrations just at the K_d of the specific ASD2-R2C1 interaction (3.2 nM). At this concentration, we do not observe non-specific binding of R2C1 to GST (Figure 4.4A). However, the fact that we are not able to compete with the ASD2-R2C1 interaction using unlabeled R2C1 is more problematic. Collectively, these results necessitate the removal of the GST tag altogether.

Removal of the GST tag by TEV protease digestion did not significantly alter the apparent K_d of the ASD2 interaction with Biotin-R2C1 (7.9 ± 0.9 nM) (Figure

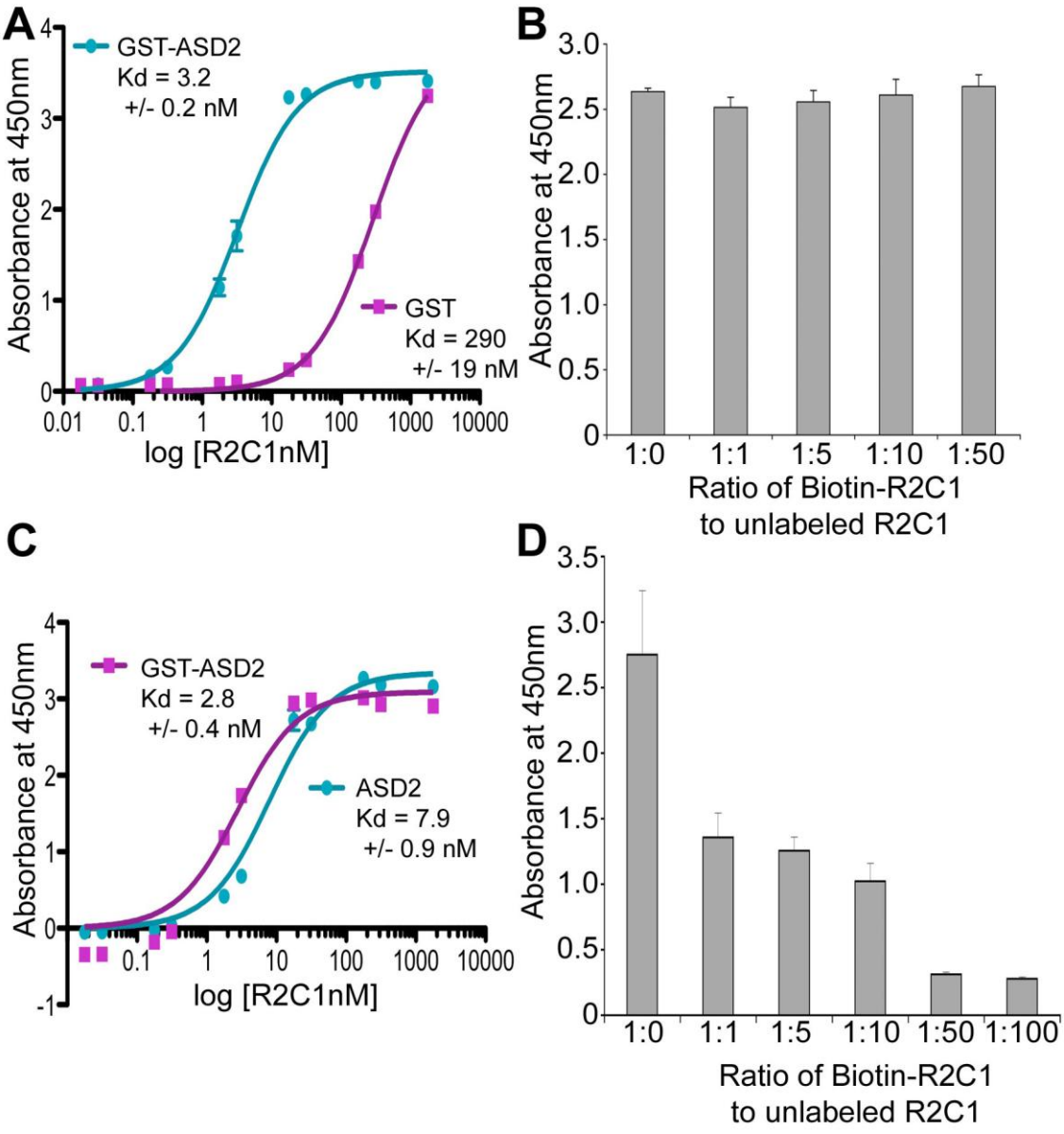

Figure 4.4 Removal of GST tag and binding affinity determination

(A) Apparent Kd of GST-ASD2 was calculated to be 3.2 +/- 0.2 nM. GST tag causes non-specific binding of Biotin-R2C1 resulting in a Kd of 290 +/- 19 nM.
(B) Unlabeled R2C1 was not able to compete with 100ng Biotin-R2C1 for binding with 250ng GST-ASD2.
(C) Removal of GST tag from ASD2 resulted in an apparent Kd of 7.9 +/- 0.9 nM for interaction with Biotin-R2C1.
(D) Removal of GST tag allowed unlabeled R2C1 to compete with 100ng Biotin-R2C1 for association with 500ng ASD2.

4.4C). Importantly, removal of the GST tag allowed unlabeled R2C1 to compete with Biotin-R2C1 for association with ASD2 (Figure 4.4D). Significantly, this is the first interaction between ASD2 and R2C1 that could specifically be disrupted by titration of an unlabeled competitor. Thus, the ELISA platform using Biotin-R2C1 and untagged ASD2 is appropriate for screening for chemical inhibitors.

4.2.3.3 Optimization of ELISA platform for 384-well HTS

Prior to optimization of assay conditions and HTS protocol, it is necessary to first transition a 96-well assay to a 384-well microplate format for efficient HTS. In order to achieve the highest signal-to-noise ratio, we varied concentrations of salt, detergent, and carrier proteins in the interaction and wash buffers (Figure 4.5A). It was determined that the signal resulting from the ASD2-R2C1 interaction was highest when in Tris- buffered saline (TBS) supplemented with 0.05% Triton X-100, 150mM KCl, and 0.5% BSA. The wash buffer that removed any remaining background binding was TBS with 300mM KCl and 0.5% Triton X-100 (Figure 4.5A).

The stability of a PPI in the presence of DMSO must also be known, as the diverse chemical libraries in the CCG are stored in DMSO. For our screen and subsequent dose response confirmation, the highest amount of compound that may be added to a sample is 2µL, which in our assay volume of 30µL is 6.7% DMSO. For the desired compound concentration of 10µM in the primary screen, 200nL of compound will be added to each well, which is 0.7% DMSO. Therefore, the ASD2-R2C1 interaction was monitored in 0-10% DMSO. The ASD2-R2C1 interaction is unaffected by the presence of DMSO up to a concentration of 10% of the final volume of the assay and this lies within the range of our assay (Figure 4.5B).

To finalize the screening protocol, the stability of ASD2 immobilized on the 384-well microplate was determined, as the duration of the assay in screening centers such as the CCG is often driven by the rate of compound addition by robotics. Further, during compound addition and incubation, it is not feasible to

A

Detergents	Salts	Carrier Protein
2% NP40	500mM NaCl	1% BSA
1% NP40	150mM NaCl	**0.5% BSA**
2% Triton X-100	500mM KCl	
1% Triton X-100	**300mM KCl**	
0.5% Triton X-100	**150mM KCl**	
0.05% Triton X-100		

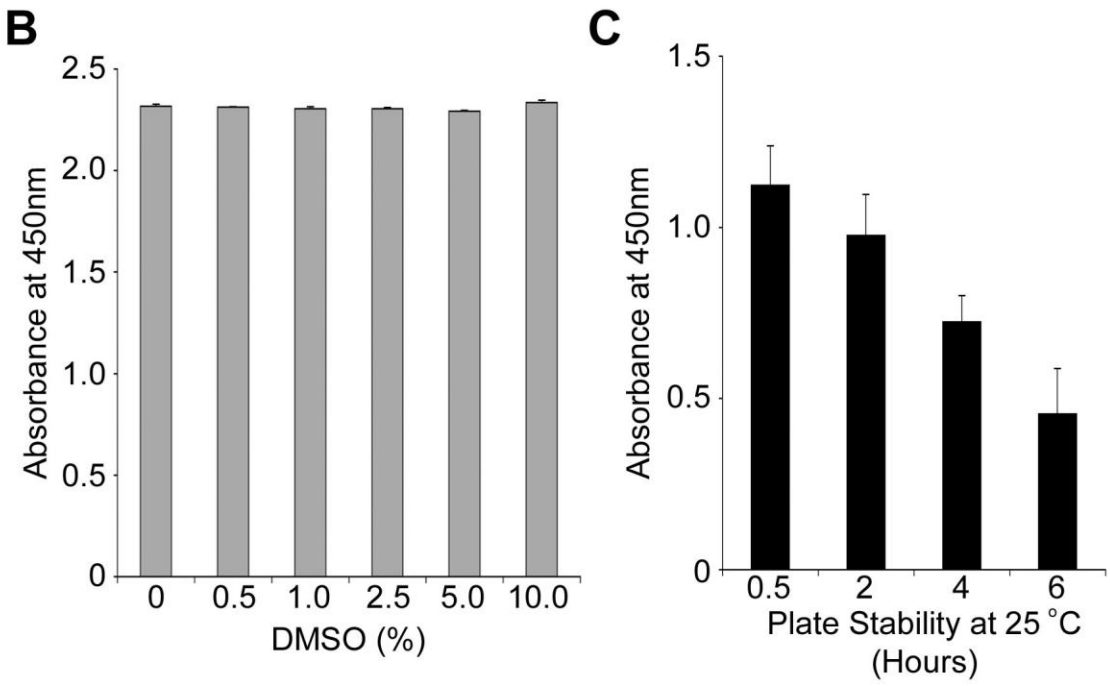

Figure 4.5 Optimization of ELISA platform for chemical screening

(A) Concentrations of detergent, salt, and carrier protein were varied to achieve the highest signal to noise ratio. It was determined that Tris Buffer with 0.05% Triton X-100, 150mM KCl, and 0.5% BSA (green text) is ideal for the PPI and wash buffer with Tris Buffer with 0.5% Triton X-100 and 300mM KCl (bold, black text) removes unbound protein.
(B) The ASD2-R2C1 interaction is stable in up to 10% DMSO.
(C) Immobilized ASD2 is stable at 25'C for 2 hours.

store plates at 4°C. Thus, the stability of immobilized ASD2 was determined at 25°C from 0.5-6 hours. Immobilized ASD2 is stable at 25°C for up to 2 hours without significant loss of signal (Figure 4.5C). After 2 hours, the signal is nearly halved, indicating that compound addition followed by R2C1 addition must occur within 2 hours. The ASD2-R2C1 interaction is stable up to 8 hours (data not shown). Fully optimized conditions and protein concentrations based on these collective data are described in detail in the Materials and Methods.

4.2.4 Primary Screen for inhibitors of Shroom3-ROCKII interaction

The Chem Div 20,000 compound collection from the CCG at the University of Michigan was used as the source of the small molecules for the primary screen. The collection was chosen based on the availability of compounds for potential follow-up and the structural diversity of the compounds. Since our target is a protein-protein interaction with no known inhibitors to use as reference, it was especially important to screen a library that sampled a large amount of chemical space to increase the probability of hits.

Briefly, 150ng of ASD2 was immobilized on 384-well high-binding plates for 16 hours at 4°C prior to the screen. Plates were washed, blocked, and then 200 nL of chemical compound was added to columns 3-22 for a final concentration of 10μM. One compound is added per well with no replicates for the primary screen. The concentration of Biotin-R2C1 used in the screen was chosen to be 7nM (10ng) which is at the apparent K_d of 7.9 nM. This concentration of Biotin-R2C1 was chosen as it yielded an adequate signal for detection (~ 1-1.5 absorbance units at 450nm). Also, it is important to screen at concentrations at or below the K_d, as an excess of ASD2 or R2C1 in the assay could raise the IC_{50} values of the chemicals above the threshold used to identify active compounds, therefore preventing them from being identified as hits [43]. Biotin-R2C1 was added to all columns (1-24). The negative control for inhibition by a compound, located in columns 1 and 2, was defined as the absorbance signal from ASD2 with 10ng Biotin-R2C1 in 0.67% DMSO. As a positive control

for inhibition we used unlabeled HisSUMO-R2C1. Thus, in columns 23 and 24, the positive control was defined as the absorbance signal with 5μM HisSUMO-R2C1 and 10ng Biotin-R2C1 (Figure 4.6A-B).

As an official gauge of signal-to-noise in HTS, a Z-factor (Z') is calculated using both the positive and negative control terms and the error associated with these terms. A Z' value between 0.5-1 is considered an excellent assay [44]. In our primary screen, the negative and positive controls displayed average signals of 1.25 and 0.14 respectively, resulting in an overall average Z-factor of approximately 0.74. Data is fit at percentage change in signal relative to the negative control (Figure 4.6C). Hits were defined as showing a signal that is greater than or equal to 3 standard deviations (3SD) away from the mean negative control per individual plate, roughly greater than 20- 30% inhibition (red line in Figure 4.6C). In Figure 4.6D, a sample plate is shown as a 'heat map,' where the negative controls (columns 1-2) show no signal (0% inhibition, blue) and the positive controls (columns 23-24) represent 100% inhibition (red). A representative hit is observed in well A11, yielding inhibition of 53.3% (yellow square). Of the 20,000 compounds tested, 180 compounds were identified as hits using the 3SD cutoff (hit rate = 0.9%) (Figure 4.6E). The ELISA assay was developed to be highly stringent, and non-enzymatic protein-protein interactions have proven difficult to inhibit, therefore the low hit-rate was not unexpected.

4.2.5 Confirmation by dose response

To analyze and further rank initial hits, a primary screen is often followed by dose-response characterization. Thus, our 180 compounds proceeded to a round of confirmation by dose-response. Briefly, compounds were titrated from stock plates of 5mM to concentrations of 3-100μM using the Mosquito X1 in the CCG. For the dose-response round of HTS, we used more stringent criteria to define compounds as active. Two requirements were used: (1) compounds with inhibition greater than 30% compared to the negative control and (2) pAC_{50} of greater than 3.5 (IC_{50} < 300 μM) (Figure 4.7A). The CCG uses pAC_{50} values as

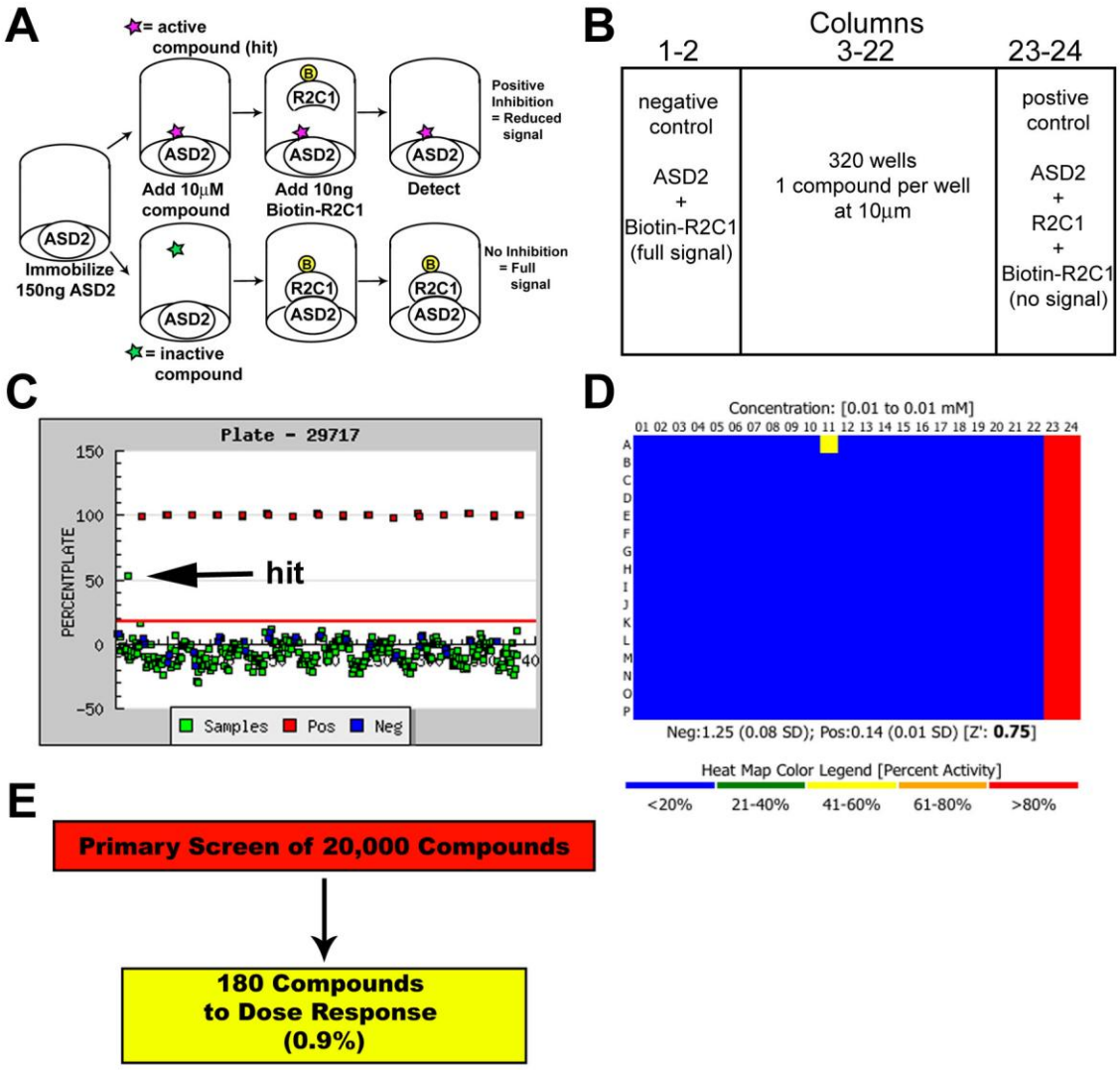

Figure 4.6 Primary Screen of 20,000 Chemical Diversity Library yielded 180 active compounds

(A-B) Schematic of HTS ELISA (A) and plate layout (B). A positive hit will have decreased absorbance signal (pink stars). A negative hit will have full absorbance signal when compared to controls in columns 1 and 2 (green stars).
(C) Representative plate out of 64 in primary screen. Red squares represent positive control for inhibition (competition of unlabeled R2C1 with Biotin-R2C1 = 100% inhibition, ~0.14 absorbance units). Blue squares are negative controls for inhibition (maximum absorbance signal = 0% inhibition, ~1.25 absorbance units). Green squares are samples with 10µm chemical molecules. Red line represents 3 standard deviations from the mean of the negative controls. The arrow on graph shows a hit with 53.3% inhibition.
(D) Heat map of B. Yellow square on heat map shows a hit with 53.3% inhibition. Average Z-factor for the assay was 0.74.
(E) The primary screen yielded 180 compounds (3 standard deviations above the mean of the negative controls) that proceeded to dose response confirmation (hit rate of 0.9%).

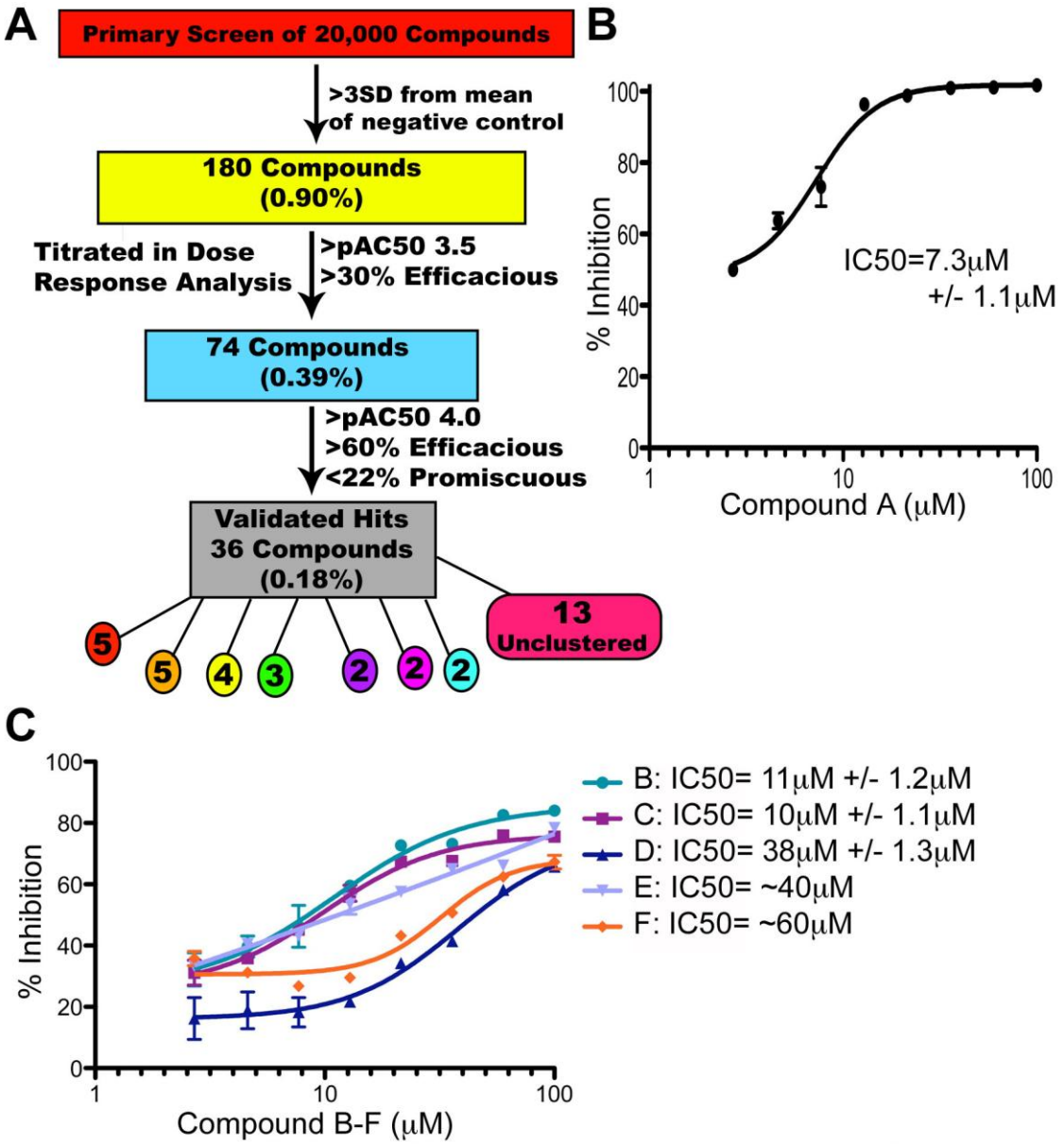

Figure 4.7 Dose response confirmation results in 36 hits for a final hit rate of 0.18%

(A) Screen of 20,000 compounds yielded 180 compounds that proceeded to confirmation by dose response. Of these 74 were confirmed as active compounds as they had pAC50 values greater than 3.5 and were greater than 30% efficacious. Compounds were further restricted: >pAC50 of 4, >60% efficacious, and <22% promiscuous, resulting in 36 validated compounds. The 36 validated hits were clustered based on 65% structural homology. Clusters were: 2 clusters of 5, 1 cluster of 4, 1 cluster of 3, 3 clusters of 2, and 13 unclustered compounds.
(B) Compound A is the highest rated compound by our selection criteria. It has an IC50 of 7.3μM +/- 1/1μM and reaches 100% efficacy by 20μm.
(C) IC50 values of a representative cluster of 5 compounds. Compounds B and C were the 3rd and 4th rated compounds of the 36 confirmed hits.

an estimate of the IC_{50} value (pAC_{50} = -log (IC_{50})). From the 180 compounds, 74 chemicals were identified as active using these dual criteria (Figure 4.7A).

Additional selection criteria were applied to prioritize the pool of hits. Small molecules that yielded less than 60% maximum efficacy (defined as inhibition at the highest concentration screened, 100 μM) were eliminated, reducing positive hits to a collection of 52 compounds. Next, we used additional data available in the CCG to eliminate potentially promiscuous compounds. Briefly, we defined the number of other protein targets that a compound has hit from previous screens as the promiscuity index. Thus, compounds that were identified as hits in greater than 22% of screens performed at the CCG were eliminated as promiscuous inhibitors of PPIs. Promiscuous molecules may be general inhibitors of PPIs such as denaturants or hydrophobic molecules, which form micelles to inhibit PPIs. Application of these criteria resulted in 36 chemical inhibitors of the ASD2-R2C1 interaction (Figure 4.7A). The highest rated compound by our criteria, termed Compound A, displayed an IC_{50} value of 7.3 ± 1.1 μM with a maximum efficacy of 100% at 35.9 μM (Figure 4.7B). Further, compound A hit only 3.2% of other targets screened in the CCG.

Finally, DataMiner software using Tripos algorithm OptiSim software was used to structurally classify and cluster the remaining 36 hits. Interestingly, clustering of compounds with 65% structural similarity in scaffold structure yielded: 2 clusters of 5, 1 cluster of 4, 1 cluster of 3, 3 clusters of 2, and 13 unique compounds (Figure 4.7A). Significantly, if a scaffold is found multiple times within a screen, it strongly indicates a real disruption to the PPI, rather than an artifact. Further, it offers initial data for structure-activity analysis, the next step in analyzing a class of small molecule inhibitors. However, a cluster is not indicative of equivalent efficacy or potency, as one of these clusters of 5 compounds yields a range of IC_{50} values from 11-60 μM (Figure 4.7C). Additionally, we only screened 20,000 compounds which is a small collection of chemicals and the collection is structurally diverse to begin with; therefore, the fact that 13 of the hits did not cluster does not imply that they are less ideal inhibitors than those which cluster.

4.3 Discussion

In summary, these studies describe a modified ELISA platform that is amenable for screening chemical libraries to identify small molecule inhibitors of the Shroom3-ROCK interaction. Screening of the 20,000 ChemDiv library in the Center for Chemical Genomics (CCG) at the University of Michigan yielded 180 active compounds of which 74 titrated in dose response. A total of 36 inhibitors of the Shroom3-ROCK interaction were selected to proceed to the next stages of development through the application of the following criteria: greater than 60% efficacy and less than 22% promiscuity (Figure 4.7A). The next step is to establish confidence in the structural identity, purity, and activity of our confirmed active compounds by repeating the dose-response using fresh powder samples with a larger titration, as not all compounds reached maximum/minimum inhibition. Compounds that are re-confirmed in dose-response with fresh sample will proceed to secondary assay confirmation to ensure that inhibition was not due to general interference in the ELISA assay rather than inhibiting the ASD2-R2C1 interaction. Lastly, active compounds will then proceed to functional assays in primary neuronal cells.

The modified ELISA assay yields an average Z-factor of 0.74. The Z-factor is a measure of statistical effect size and is used in high-throughput screening to judge whether the response in an assay is large enough to proceed, and also to assess the quality of an assay. The Z-factor is determined from the means and standard deviations of both the positive and negative controls. An ideal Z-factor is 1, 1-0.5 is defined as an excellent assay, 0.5-0 a marginal assay, and anything less than 0 suggests there is too much overlap between the positive and negative controls to be useful. A Z-factor of 0.74 indicates that our ELISA platform is statistically an ideal assay.

However, relative to more current methods, an ELISA is not an ideal platform for high-throughput screening. The ELISA is highly labor intensive with multiple additions, incubations, and wash steps. The protocol limits the amount of compounds that can be tested per day to 5,000. NIH defines a high-throughput

screening platform as one that is capable of 10,000 compounds per day and recent advances in technology have allowed for 100,000 compounds per day [45]. Therefore, our assay is not considered high-throughput by industry standards. Finally, one of our proteins is immobilized on polystyrene. This could influence the conformation of the protein and the interaction site. Indeed, there is precedent for a difference in affinity between two proteins, depending upon whether the interaction is measured on solid-phase or in solution [46]. Therefore, inhibitors identified in this platform may not necessarily translate in solution. A secondary confirmation assay in solution is discussed below.

Despite these disadvantages, there exist several benefits of performing an ELISA for HTS. The requirement for multiple wash steps removes chemicals with low affinity or non-specific binding, creating a highly stringent assay. The wash steps also allow for the removal of compound prior to TMB addition, preventing potential oxidation by the compound, and as a result, removing potential false-positive hits. Removal of the compound prior to detection further reduces the possibility of false-positive hits because the compound is absent when absorbance is read. Thus, any compounds that absorb light at 450 nm will not interfere with detection, unlike an assay without wash steps, which would require an additional round of hit confirmation to screen for false-positives. In our assay, the only potential false-positive hit could occur from a chemical that inhibits the biotin-avidin interaction.

The apparent K_d for the ASD2-R2C1 interaction using the ELISA platform was determined to be 7.9 ± 0.9 nM. This is the first time the binding affinity for the ASD2-R2C1 interaction has been defined and, surprisingly, this is a high affinity interaction. However, several interactions between signaling proteins have been calculated in the nanomolar range. For example, the K_d for the Ras-Raf interaction is 50nM [47]. The K_d for Shroom3-ROCK was determined using the isolated interacting domains and it will be necessary to determine the affinity of the full length proteins. Additionally, as mentioned, the apparent K_d could also be affected by immobilization of ASD2 on the plate and could be different in solution.

The ELISA platform was developed after attempts at labeling ASD2 and R1C1/R2C1 resulted in changes in protein solubility and conformation. Labeling R2C1 with biotin did not affect solubility, which is likely due to the presence of a polyethylene glycol (PEG) linker on the biotin molecule, which can facilitate solubility. Current applications for non-enzymatic high-throughput screening require either that one protein be labeled with a tag, or that primary antibodies are available for at least one of the proteins of interest. Our results with epitope-tagged ASD2 and R1C1/R2C1, coupled with the lack of primary antibodies to the individual protein domains, significantly limit techniques we can employ to further examine the Shroom3-ROCK interaction in an efficient way. In addition, there are an additional 130,000 purified compounds and 25,000 natural product extracts available in the CCG for screening. Therefore, we are currently developing an AlphaLISA platform (Perkin Elmer) as a secondary assay for use in confirmation of our hits from the primary screen and for further primary screening of these additional libraries.

AlphaLISA is a bead-based technology that uses luminescent oxygen-channeling chemistry [48]. Donor and acceptor beads with various epitope tags are used and the formation of the PPI brings the beads into proximity. Laser irradiation of the donor beads generates a flow of singlet oxygen which results in chemical events in the nearby acceptor beads resulting in a chemiluminescent emission [49]. The AlphaLISA assay provides an assay that is more amenable for high-throughput screening, will allow for secondary confirmation of our current hits, and additional screening of chemical libraries [50].

The aim of HTS-assay development was to identify chemical inhibitors of the Shroom3-ROCK interaction that will be used as probes to examine PPIs in the POSH complex regulating axon outgrowth. Following confirmation in the AlphaLISA, primary neuronal cells will be treated with the validated hits and changes in axon outgrowth will be examined. An inhibitor of the Shroom3-ROCK interaction should yield neurons with enhanced axon length, similar to results seen with ectopic expression of the isolated R1C1 domain (Figure 4.1A). The Shroom3-ROCK interaction is crucial for growth inhibition mediated by myelin

associated inhibitors (MAIs); therefore a validated chemical inhibitor should also relieve growth inhibition on MAIs. Following confirmation in the functional axon length assays, identified compounds could be translated for use in stroke models to determine whether inhibition of the Shroom3-ROCK interaction is sufficient to support functional recovery after stroke.

4.4 Acknowledgements

We thank: Jason Gestwicki for helpful discussions and technical assistance, Lyra Chang and Matthew Smith for assistance in developing the FQA assay, Martha Larsen for HTS consultation and guidance, Steven Swaney for technical assistance and HTS development, Thomas McQuade for HTS technical advice, Paul Kirchhoff for medicinal chemistry support, Amanda Wilbur for technical assistance and preparation of protein, and finally Ashley Reinke for technical advice, helpful discussions, and critical reading of the manuscript. Portions of Figure 4.1A have been previously published in Molecular Biology of the Cell [36].

4.5 Materials and Methods

4.5.1 Antibodies and reagents

Primary antibodies used were neuronal β-III-tubulin (Covance Research Products), green fluorescent protein (GFP) (Invitrogen), and SUMO from yeast (Rockland). Secondary antibodies included Alexa 488 and 594-conjugated antibodies (Invitrogen) and Goat anti-rabbit IgG Horseradish peroxidase conjugate (BioRad). For the ELISA assays, High Sensitivity NeutrAvidin-HRP (Pierce) was used. The ROCK1/2 inhibitor, Y-27632, was purchased from Calbiochem. For the FQA assays, proteins were labeled with BHQ-10 carboxylic acid, succinimidyl ester (BHQ-10S) (Biosearch Technologies) and Alexa Fluor 488 Carboxylic Acid, 2,3,5,6 Tetrafluorophenyl ester (Invitrogen). For biotin labeling, Pierce EZ-Link NHS-PEO4-Biotinylation Kit (#21455) was used.

4.5.2 Expression Constructs

pUI4-SIBR-GFP luciferase (a functional control RNAi) sequence is described previously [36]. pUS2-R2C1 expressing the Shroom3 binding domain of human Rock1 (amino acids 726-926) was cloned from human ROCKI. pGST1-ASD2 (1563-1986aa) was cloned from human Shroom3. ppSUMO-R1C1 was subcloned from pUS2-R1C1 using BamHI and NotI as cloning sites. ppSUMO-R2C1 (698-957aa) was cloned by RT-PCR with RNA isolated from mouse brain.

4.5.3 Axon outgrowth experiments

P19 cells, grown in minimal essential medium-α supplemented with 7.5% calf serum, 2.5% fetal bovine serum, and penicillin-streptomycin were plated the day before transfection to a density of 9 X 10^3 cells/well of a 12-well dish and transfected the next day with 2µg of total DNA (0.75µg of Ngn2, 1.25µg of pUI4/UI5 RNAi expression vector). pUS2-R1C1 was transfected at 850ng/12-well. 4-6 hours after transfection, cells were resplit 1:5 or 1:6 on laminin-coated dishes. 18-20 hours later, the cells were transferred into Opti-mem supplemented with 1% FBS and penicillin-streptomycin. 72 hours after transfection, cells were fixed in 3.7% formaldehyde in PBS and stained for GFP or neuronal markers of differentiation.

4.5.4 Measurement of Process Length

To measure process length, photographs of fixed, stained neurons were captured with a digital camera, and the length of the longest process per cell was measured using the polyline function in MicroSuite Special Edition imaging software version 5.0. Processes 50µm or greater were measured: 50µm is ~3 times the length of the cell body. Process length is determined in two or more independent experiments for a total of 224-315 neurons measured per condition. Similar results for process length measurements are obtained if neurons are fixed and stained for GFP or for neuronal markers of differentiation (β-III-tubulin).

4.5.5 Preparation of recombinant proteins

GST-ASD2, HisSUMO-R1C1, and HisSUMO-R2C1 were produced in *Escherichia coli*. Briefly, *E.coli* were lysed by sonication in PBS+ buffer (GST purification: PBS with 0.1mM phenylmethylsulfonyl fluoride, 14µg/mL aprotinin, 0.1% β-mercaptoethanol, 1µM leupeptin, 1µM pepstatin) (His purification: PBS with 0.1mM phenylmethylsulfonyl fluoride, 14µg/mL aprotinin, 0.1% β-mercaptoethanol, 1µM leupeptin, 1µM pepstatin, 25mM Imidazole). Triton X-100 was added to the lysate at 1% of the final volume. Lysates were incubated with prewashed glutathione agarose or HisPur Ni-NTA resin (Thermo Scientific) for 1 hour at 25°C. Purified protein was eluted 3 times with 1mL of GST elution buffer (50mM Tris buffer with 100mM reduced glutathione, pH 8) or His elution buffer (PBS+ with 250mM Imidazole). HisSUMO-R1C1 and R2C1 were dialyzed overnight at 4°C in PBS and stored in 25% glycerol at -20°C. GST-ASD2 was dialyzed for 3 hours at 4°C in PBS with 3 buffer changes. The GST epitope tag was removed using His-TeV (S219V)-Arg Protease overnight at a concentration of 1µg TeV per 100µg of GST-ASD2. TeV and free GST was removed from purified ASD2 by incubation overnight at 4°C with prewashed glutathione agarose and HisPur Ni-NTA resin. ASD2 was stored at -20°C in 25% glycerol.

4.5.6 Labeling with AlexaFluor 488 5-TFP and BHQ-10 carboxylic acid

Labeling of GST-ASD2 or HisSUMO-R1C1 with BHQ-10 carboxylic acid (Biosearch Technologies) or AlexaFluor 488 5-TFP (Invitrogen) was performed as per manufacturer's instructions. Briefly, labeling reactions were carried out at a 10:1 molar ratio of dye to protein in bicarbonate buffer (100mM $NaHCO_3$, 5mM $MgCl_2$, 10mM KCl, pH 9.5). Proteins were labeled for 1 hour at 25°C under a constant low vortex. After the incubation, the unreacted dye was removed and the buffer was exchanged to PBS (pH 7.4) using Zeba^{TM} Desalt Spin Columns (2mL, MWCO= 7000Da) (Pierce). The average extent of labeling for GST-ASD2 and HisSUMO-R1C1 was determined to be approximately 6.5 fluorophore/dye

per protein, respectively, using the ε_{495}= 71,000 $M^{-1}cm^{-1}$ (Alexa Fluor 488) and ε_{507}= 30,000 $M^{-1}cm^{-1}$ (BHQ-10). Labeled proteins were stored at -80°C.

4.5.7 Biotinylation of HisSUMO-R2C1

HisSUMO-R2C1 was biotinylated as described with the NHS-PEO_4-Biotinylation Kit (Pierce). Briefly, biotinylation reactions were carried out at a 20:1 molar ratio of NHS-PEO_4-biotin to HisSUMO-R2C1 in PBS (pH 7.4). HisSUMO-R2C1 was labeled for 2 hours at 4°C. After the incubation, the unreacted NHS-PEO_4-biotin was removed with buffer exchange in PBS (pH 7.4) using Zeba™ Desalt Spin Columns (2mL, MWCO= 7000Da) (Pierce). The average extent of labeling for HisSUMO-R2C1 was estimated to be 4 biotin molecules per 1 mole of protein using the HABA assay, a measurement of the extent of biotinylation, as per the manufacturer's protocol. Biotin-R2C1 was stored at -20°C in 25% glycerol.

4.5.8 Pull down assay

5µg of GST or GST-ASD2 and 5µg of HisSUMO or HisSUMO-R1C1 were incubated for 1 hour in 10µL prewashed glutathione agarose. Pull-downs were washed 2 times in PBS+0.1% Triton X-100 and 1 time with PBS. Proteins were eluted from beads with 20µL of sample buffer and 15µL of samples were analyzed by SDS-PAGE followed by staining with GelCode Blue (Pierce).

4.5.9 Fluorescence Quench Assay (FQA)

To determine the K_d (Figure 4.2B and C), 250nM of Alexa-ASD2, diluted in PBS (pH 7.4), was added to 384-well, black round bottom plates (Corning). BHQ-R1C1 (20nM-60µM) was added in triplicate to appropriate wells and the samples were incubated for 30 minutes, 1 hour, or 2 hours. After incubation, the fluorescence at 525nm (excite 480nm, cut-off 515nm) was measured using a SpectraMax M5 microplate reader. The results were analyzed by GraphPad

Prism 4.0 using a hyperbolic fit with a non-zero intercept ($\Delta F=\Delta F_{max}*[R1C1]/(K_{app}+[R1C1])+b$). ΔF= fluorescence change; ΔF_{max}= maximum fluorescence change; K_{app}= apparent K_d; [R1C1] = R1C1 concentration. For competition assays, 100nM of BHQ-R1C1 and varying concentrations of unlabeled HisSUMO-R1C1 were added to 250nM Alexa-ASD2. Samples were incubated for 1 hour and then read at 525nm (Figure 4.2D). To determine if non-specific quenching was being observed, 250nm of BHQ-GST or BHQ-ASD2 was incubated for an hour with varying concentrations of Alexa 488-HisSUMO or Alexa-R1C1 (Figure 4.3A and B).

4.5.10 Size exclusion chromatography

BHQ-ASD2 and Alexa 488-R1C1 were fractionated by size exclusion chromatography over a Superose 6 HR10/30 column (GE Healthcare) equilibrated and run in PBS with 300mM NaCl. Eluted fractions containing the protein peak were subjected to SDS-PAGE followed by detection using GelCode Blue (Pierce).

4.5.11 ELISA assay, detection methods, and affinity determination

For the anti-SUMO detection system (Figure 4.3B), 1µg of GST or GST-ASD2 diluted in 75µL PBS was immobilized for 16 hours at 4°C on 96-well Immulon 2B high binding plates (Thermo Scientific). Plates were blocked for 1 hour at 25°C in 200µL SuperBlock T20 (TBS) Blocking buffer (Thermo Scientific). 0.1µg, 1µg, and 10µg HisSUMO-R2C1 was added to wells in 40µL TBS-1 (20mM Tris HCl, 150mM KCl, 0.5% Triton X-100, pH 7.9) with 0.5% Bovine Serum Albumin (BSA) for 1 hour at 25°C. Unbound protein was removed with 4 washes in TBS-2 (20mM Tris HCl, 300mM KCl, 0.5% Triton X-100, pH 7.9). Anti-SUMO antibody was added at a dilution of 1:1000 in 40µL TBS-3 (25mM Tris HCl, 8.25mM Tris Base, 154mM NaCl, 2% BSA, 0.05% Tween-20) for 1 hour at 25°C. Excess SUMO antibody was removed with 2 washes in TBS-T (25mM Tris HCl, 137mM NaCl, 2.7mM KCl, 0.1% Tween-20). Goat anti-rabbit IgG HRP (BioRad)

was added at a dilution of 1:1000 in 40µL TBS-3 for 1 hour at 25°C. Following 2 washes in TBST, 40µL TMB substrate (Pierce) was added for 15 minutes and quenched with 40µL 0.18 M H_2SO_4. Absorbance was measured at 450 nm using a SpectraMax M5 microplate reader.

For the biotin-avidin detection system (Figure 4.3C), the ELISA assay was performed as just described except that Biotin-R2C1 was used in place of HisSUMO-R2C1 and High Sensitive NeutrAvidin-HRP was added at a dilution of 1:40,000 for 1 hour in TBS-3, followed by detection using TMB substrate.

Apparent binding affinity (K_d) was determined by immobilizing 0.5 µg of GST-ASD2 or ASD2 on 96-well plates. Concentrations of Biotin-R2C1 were added from 0-1778 nM for a total of 11 concentration points. ELISA was performed as described for the biotin-avidin detection system. The K_d was calculated using GraphPad Prism 4.0 using a hyperbolic fit with a non-zero intercept ($\Delta A=\Delta A_{max}*[R2C1]/(K_d+[R2C1])$. ΔA= absorbance change; ΔA_{max}= maximum absorbance change; [R2C1]= R2C1 concentration. Competition ELISAs were performed as described above with 100 ng of Biotin-R2C1 being combined with varying concentrations of unlabeled R2C1 (0-10µg) followed by incubation on plates for 1 hour at 25°C.

4.5.12 High-throughput primary screen and dose-response in the CCG

The 20,000 Chemical Diversity Library (ChemDiv) was screened in the Center for Chemical Genomics at the University of Michigan. All reagent additions were performed using Thermo Labsystems Multidrop and plate washes were performed using Bio Tek EL406 washer/aspirator. 150 ng of ASD2 diluted in 20 µL PBS (pH, 7.4) was immobilized for 16 hours at 4°C on 384-well high-binding plates (Perkin Elmer). Unbound protein was removed with 2-80µL washes of PBS (pH, 7.4). Plates were blocked for 1 hour at 25°C in 80µL SuperBlock T20 (TBS) Blocking buffer (Thermo Scientific), followed by 2-80µL washes of PBS (pH, 7.4). 20 µL of Buffer A (20mM Tris HCl, 150mM KCl, 0.05% Triton X-100, 0.5% BSA, pH 7.9) was added to all wells. 200 nL of compounds

were pin-tooled (one per well) into columns 3-22 resulting in a final concentration of 10 µM using the Biomex FX (Beckman). 200nL of DMSO was added to control columns 1-2 (negative control) and 23-24 (positive control). 5 µg of unlabeled R2C1 in 20µL of Buffer A was added to columns 23-24 as a positive control for inhibition. After 30 minutes at 25°C, 10 ng of Biotin-R2C1 in 10µL of Buffer A was added to all wells and incubated for 1 hour at 25°C. Unbound protein was removed with 3 washes in 80µL wash buffer (Buffer A supplemented with 300mM KCl and 0.5% Triton X-100). 40µL of 1:40,000 NeutrAvidin-HRP diluted in TBS-3 was added to all wells and incubated for 45 minutes at 25°C. Plates were washed 3 times in 80µL TBS-T, followed by the addition of 20 µL of TMB substrate for 5 minutes. The TMB reaction was quenched with 20 µL 0.18 M H_2SO_4. Absorbance was measured at 450 nm using an automated PHERAstar plate reader (BMG Labs). Positive hits were defined as having a percent inhibition greater than 3 standard deviations (3SD) away from the mean of the negative control for inhibition.

4.5.13 Dose response and hit selection criteria

Dose-response confirmation (180 compounds) was performed following the ELISA screening platform. Compound dilutions of 100µM, 59.8µM, 35.9µM, 21.5µM, 12.9µM, 7.69µM, 4.61µM, and 2.70µM were delivered using the Mosquito X1 (TTP Labtech) in duplicate. Compounds with at least 30% inhibition and a pAC50 of 3.5 were considered active (74 compounds). Compounds with greater than 22% promiscuity and less than 60% efficacy were removed. The application of these selection criteria resulted in 36 compounds. The IC_{50} values for Compounds A-F were calculated using GraphPad Prism 4.0 using nonlinear regression and the log (inhibitor) vs. response, variable slope equation. Clustering was performed using DataMiner by the Tripos algorithm OptiSim under the criteria of 65% or greater similarity.

4.6 References

1. Filbin, M.T., Myelin-associated inhibitors of axonal regeneration in the adult mammalian CNS. Nature Reviews Neuroscience, 2003. 4(9): p. 703-713.
2. Giger, R.J., et al., Mechanisms of CNS myelin inhibition: Evidence for distinct and neuronal cell type specific receptor systems. Restorative Neurology and Neuroscience, 2008. 26(2-3): p. 97-115.
3. Benowitz, L.I. and S.T. Carmichael, Promoting axonal rewiring to improve outcome after stroke. Neurobiology of Disease, 2010. 37(2): p. 259-266.
4. Freund, P., et al., Nogo-A-specific antibody treatment enhances sprouting and functional recovery after cervical lesion in adult primates. Nature Medicine, 2006. 12(7): p. 790-792.
5. Freund, P., et al., Anti-Nogo-A antibody treatment promotes recovery of manual dexterity after unilateral cervical lesion in adult primates - re-examination and extension of behavioral data. European Journal of Neuroscience, 2009. 29(5): p. 983-996.
6. GrandPre, T., S.X. Li, and S.M. Strittmatter, Nogo-66 receptor antagonist peptide promotes axonal regeneration. Nature, 2002. 417(6888): p. 547-551.
7. Li, S.X., et al., Blockade of Nogo-66, myelin-associated glycoprotein, and oligodendrocyte myelin glycoprotein by soluble Nogo-66 receptor promotes axonal sprouting and recovery after spinal injury. Journal of Neuroscience, 2004. 24(46): p. 10511-10520.
8. MacDermid, V.E., et al., A soluble Nogo receptor differentially affects plasticity of spinally projecting axons. European Journal of Neuroscience, 2004. 20(10): p. 2567-2579.
9. Papadopoulos, C.M., et al., Functional recovery and neuroanatomical plasticity following middle cerebral artery occlusion and IN-1 antibody treatment in the adult rat. Annals of Neurology, 2002. 51(4): p. 433-441.
10. Papadopoulos, C.M., et al., Dendritic plasticity in the adult rat following middle cerebral artery occlusion and Nogo-A neutralization. Cerebral Cortex, 2006. 16(4): p. 529-536.
11. Atwal, J.K., et al., PirB is a Functional Receptor for Myelin Inhibitors of Axonal Regeneration. Science, 2008. 322(5903): p. 967-970.
12. Domeniconi, M., et al., Myelin-associated glycoprotein interacts with the Nogo66 receptor to inhibit neurite outgrowth. Neuron, 2002. 35(2): p. 283-290.
13. Fournier, A.E., T. GrandPre, and S.M. Strittmatter, Identification of a receptor mediating Nogo-66 inhibition of axonal regeneration. Nature, 2001. 409(6818): p. 341-346.
14. Mi, S., et al., LINGO-1 is a component of the Nogo-66 receptor/p75 signaling complex. Nature Neuroscience, 2004. 7(3): p. 221-228.
15. Park, J.B., et al., A TNF receptor family member, TROY, is a coreceptor with Nogo receptor in mediating the inhibitory activity of myelin inhibitors. Neuron, 2005. 45(3): p. 345-351.
16. Wang, K.C., et al., p75 interacts with the Nogo receptor as a co-receptor for Nogo, MAG and OMgp. Nature, 2002. 420(6911): p. 74-78.

17. Wang, K.C., et al., Oligodendrocyte-myelin glycoprotein is a Nogo receptor ligand that inhibits neurite outgrowth. Nature, 2002. 417(6892): p. 941-944.
18. Dickson, H.M., et al., POSH is an intracellular signal transducer for the axon outgrowth inhibitor Nogo66. J Neurosci, 2010. 30(40): p. 13319-25.
19. Goodman, L.S., et al., Goodman & Gilman's the pharmacological basis of therapeutics. Pharmacological basis of therapeutics. 2006, New York: McGraw-Hill. xxiii, 2021 p.
20. Arkin, M.R. and J.A. Wells, Small-molecule inhibitors of protein-protein interactions: Progressing towards the dream. Nature Reviews Drug Discovery, 2004. 3(4): p. 301-317.
21. Jones, S. and J.M. Thornton, Principles of protein-protein interactions. Proceedings of the National Academy of Sciences of the United States of America, 1996. 93(1): p. 13-20.
22. Wells, J.A. and C.L. McClendon, Reaching for high-hanging fruit in drug discovery at protein-protein interfaces. Nature, 2007. 450(7172): p. 1001-1009.
23. Hopkins, A.L. and C.R. Groom, The druggable genome. Nature Reviews Drug Discovery, 2002. 1(9): p. 727-730.
24. Toogood, P.L., Inhibition of Protein−Protein Association by Small Molecules: Approaches and Progress†. Journal of Medicinal Chemistry, 2002. 45(8): p. 1543-1558.
25. McGovern, S.L., et al., A common mechanism underlying promiscuous inhibitors from virtual and high-throughput screening. Journal of Medicinal Chemistry, 2002. 45(8): p. 1712-1722.
26. McGovern, S.L., et al., A specific mechanism of nonspecific inhibition. Journal of Medicinal Chemistry, 2003. 46(20): p. 4265-4272.
27. Seidler, J., et al., Identification and prediction of promiscuous aggregating inhibitors among known drugs. Journal of Medicinal Chemistry, 2003. 46(21): p. 4477-4486.
28. Way, J.C., Covalent modification as a strategy to block protein-protein interactions with small-molecule drugs. Current Opinion in Chemical Biology, 2000. 4(1): p. 40-46.
29. Genevaux, P., C. Georgopoulos, and W.L. Kelley, The Hsp70 chaperone machines of Escherichia coli: a paradigm for the repartition of chaperone functions. Molecular Microbiology, 2007. 66(4): p. 840-857.
30. Harrison, C.J., et al., Crystal structure of the nucleotide exchange factor GrpE bound to the ATPase domain of the molecular chaperone DnaK. Science, 1997. 276(5311): p. 431-435.
31. Chang, L., et al., Chemical Screens against a Reconstituted Multiprotein Complex: Myricetin Blocks DnaJ Regulation of DnaK through an Allosteric Mechanism. Chemistry & Biology, 2011. 18(2): p. 210-221.
32. Bogan, A.A. and K.S. Thorn, Anatomy of hot spots in protein interfaces. Journal of Molecular Biology, 1998. 280(1): p. 1-9.
33. Wells, J.A., SYSTEMATIC MUTATIONAL ANALYSES OF PROTEIN PROTEIN INTERFACES. Methods in Enzymology, 1991. 202: p. 390-411.
34. Bazan, J.F. and D.B. McKay, Unraveling the Structure of IL-2. Science, 1992. 257(5068): p. 410-413.
35. Thanos, C.D., M. Randal, and J.A. Wells, Potent Small-Molecule Binding to a Dynamic Hot Spot on IL-2. Journal of the American Chemical Society, 2003. 125(50): p. 15280-15281.
36. Taylor, J., et al., The scaffold protein POSH regulates axon outgrowth. Mol Biol Cell, 2008. 19(12): p. 5181-92.

37. Nishimura, T. and M. Takeichi, Shroom3-mediated recruitment of Rho kinases to the apical cell junctions regulates epithelial and neuroepithelial planar remodeling. Development, 2008. 135(8): p. 1493-1502.
38. Alabed, Y.Z., et al., Neuronal responses to myelin are mediated by rho kinase. Journal of Neurochemistry, 2006. 96(6): p. 1616-1625.
39. Duffy, P., et al., Rho-Associated Kinase II (ROCKII) Limits Axonal Growth after Trauma within the Adult Mouse Spinal Cord. Journal of Neuroscience, 2009. 29(48): p. 15266-15276.
40. Fournier, A.E., B.T. Takizawa, and S.M. Strittmatter, Rho kinase inhibition enhances axonal regeneration in the injured CNS. Journal of Neuroscience, 2003. 23(4): p. 1416-1423.
41. Clegg, R.M., Fluorescence resonance energy transfer. Current Opinion in Biotechnology, 1995. 6(1): p. 103-110.
42. Ruan, Q., J.P. Skinner, and S.Y. Tetin, Using nonfluorescent Förster resonance energy transfer acceptors in protein binding studies. Analytical Biochemistry, 2009. 393(2): p. 196-204.
43. Inglese, J., et al., High-throughput screening assays for the identification of chemical probes. Nat Chem Biol, 2007. 3(8): p. 466-479.
44. Zhang, J.H., T.D.Y. Chung, and K.R. Oldenburg, A simple statistical parameter for use in evaluation and validation of high throughput screening assays. Journal of Biomolecular Screening, 1999. 4(2): p. 67-73.
45. Martis E.A., R.R., Badve R.R High-Throughput Screening: The Hits and Leads of Drug Discovery- An Overview Journal of Applied Pharmaceutical Science, 2011. 1(1): p. 2-10.
46. Lawrence, D.A., et al., Characterization of the binding of different conformational forms of plasminogen activator inhibitor-1 to vitronectin - Implications for the regulation of pericellular proteolysis. Journal of Biological Chemistry, 1997. 272(12): p. 7676-7680.
47. Warne, P.H., P.R. Viciana, and J. Downward, DIRECT INTERACTION OF RAS AND THE AMINO-TERMINAL REGION OF RAF-1 IN-VITRO. Nature, 1993. 364(6435): p. 352-355.
48. McGiven, J.A., et al., A new homogeneous assay for high throughput serological diagnosis of brucellosis in ruminants. Journal of Immunological Methods, 2008. 337(1): p. 7-15.
49. Ullman, E.F., et al., Luminescent oxygen channeling immunoassay: measurement of particle binding kinetics by chemiluminescence. Proceedings of the National Academy of Sciences, 1994. 91(12): p. 5426-5430.
50. Szekeres, P.G., et al., Development of Homogeneous 384-Well High-Throughput Screening Assays for Aβ1-40 and Aβ1-42 Using AlphaScreen™ Technology. Journal of Biomolecular Screening, 2008. 13(2): p. 101-111.

Chapter 5

Conclusion

5.1 Background and Significance

The regenerative capacity in the injured adult mammalian CNS is limited, in part, by an inhibitory extracellular environment in which myelin associated inhibitors (MAIs) contribute. The primary focus of this body of work has been the identification of a signaling pathway downstream of MAIs organized by the scaffold protein POSH. Further, high-throughput screening was performed to identify chemicals with the potential to inhibit POSH complex function to promote axonal growth in the presence of MAIs.

In this dissertation, we have defined a signaling pathway downstream of the PirB receptor upon activation by the MAIs, Nogo66 and MAG. The activity of the PirB associated phosphatase Shp2 is required to inhibit axon length and LZK was identified as a potential Shp2 substrate. LZK co-associates with POSH and, together with Shroom3 and ROCK, relays MAI-mediated growth inhibition. The identification of the POSH complex as a signaling component of MAI pathways has provided insight into MAI intracellular signaling mechanisms. The POSH complex provides novel targets for therapeutics to enhance regeneration after injury or disease in the CNS. Additionally, by selectively inhibiting the function of the POSH complex, axon growth in the CNS may be promoted without disrupting other inhibitory signaling pathways, allowing for regeneration and maintenance of intact neuronal connections.

5.2 The POSH complex mediates MAI growth inhibition

Our studies define a central role for the POSH complex in relaying process growth inhibition downstream of MAG and NogoA and their receptor PirB (Chapter 3, Figure 3.8). MAG and NogoA, along with OMgp have been termed prototypic myelin inhibitors as they are highly expressed and have been well characterized as inhibitory proteins within myelin [1]. All three MAIs associate with the receptor PirB and the POSH complex relays NogoA signaling through PirB (Chapter 2 and [2]. We demonstrated that POSH is downstream of MAG and NogoA, thus we predict OMgp is also signaling through the POSH complex. There are additional receptors for MAIs including NgR1 and NgR2, as well as the integrin receptors [3-5]. NgR1 is a high affinity receptor for all three MAIs, while NgR2 has only been shown to bind MAG [3, 5, 6]. The question can then be raised: Is the POSH complex only a scaffold for MAI signaling through the receptor PirB or is POSH a convergence point for all MAI receptors?

NgR1 does not contain an intracellular domain and must associate with a co-receptor to mediate intracellular signaling (p75, LINGO1, or Taj/TROY) [7-9]. PirB has been shown to complex with p75 upon MAG stimulation to promote activation of Shp2 function [10]. As we have linked Shp2 to the POSH complex, it is possible that POSH may be also be downstream of p75 signaling and thus POSH could also mediate signals emanating from NgR1 when it is coupled to p75. Interestingly, studies in NgR1 null mice have shown that a combinatorial approach of removing NgR1and PirB facilitates more robust axon extension in the presence of crude myelin in cell culture [2]. Therefore, if POSH is indeed a convergence point for MAIs, blocking POSH function may be more productive than targeting multiple MAI receptors for enhancement of axon outgrowth after injury.

In addition to the prototypical MAIs, there are other classes of growth inhibitory proteins present in the CNS: canonical axon guidance molecules (ex. semaphorins, ephrins, netrins) and chondroitin sulfate proteoglycans (CSPGs) [11]. Our laboratory has previously determined that reduction of Robo1 and

EphrinB2 function in P19 neurons results in enhanced axon length indicative of their function as negative regulators of axon length and our data suggests that they do not signal through the POSH complex [12]. Given these results, it is unlikely that POSH is functioning in all pathways. Rather, we propose that POSH is a convergence point for MAIs.

5.3 The role of POSH as a scaffold protein

POSH is a multi-domain scaffold protein [13]. As a scaffold POSH regulates many diverse biological functions from apoptosis, to membrane trafficking, and our studies define a role for POSH as a negative regulator of axon outgrowth [12, 14-20]. Complex formation by scaffold proteins can regulate selectivity in pathways, shape signaling outputs, and achieve new functions for preexisting signaling proteins [21]. Thus, examining the role of POSH as a scaffold protein may provide additional insight into MAI signaling and regulation.

One function of a scaffold protein is to promote spatial organization of a signaling complex to the desired location in the cell [21]. For example, in differentiated PC12 cells, POSH exhibits a widespread punctate pattern in neurites and the cell body [22]. Upon growth factor deprivation or camptothecin treatment to induce apoptosis, POSH localizes to the perinuclear region of the neuron to promote JNK followed by cJun activation [22]. The change in localization of POSH to the perinuclear region is hypothesized to facilitate the translocation of JNK into the nucleus to activate cJun. The same rationale can be applied to the role of POSH as a mediator of growth inhibition. In the axon of neurons, the growth cone responds to extracellular cues and relays these signals to cytoskeletal components to promote or inhibit growth [23]. Thus, a model could be proposed where upon stimulation by a MAI, the POSH complex becomes localized at the growth cone and promotes cytoskeletal rearrangements leading to inhibition of growth. Furthermore, the POSH-associated protein Shroom3 associates with actin, and promotes the localization of ROCK to sites of apical constriction in epithelial cells [24]. Therefore, it is possible that MAI stimulus

leads to Shroom3 promoting localization of POSH at the growth cone through Shroom's association with the actin-myosin cytoskeleton. This dissertation did not address spatial organization of the POSH complex, and it will be of interest to determine if MAI signaling promotes changes in sub-cellular location of POSH and/or its associated proteins to facilitate its role as a negative regulator of axon length. Another hypothesis that was not addressed is whether MAIs induce changes in expression of POSH complex proteins, and this could be examined by looking at changes in mRNA or protein expression over time in the presence of MAIs.

The formation of distinct protein complexes by POSH also suggests that regulation of POSH function via post-translational modifications may promote or inhibit complex formation, and subsequent biological pathways. For example, Akt regulates POSH's apoptotic function. Akt2 associates with POSH through its third SH3 domain and disassembles the complex through phosphorylation of MLK3 [25]. Additionally, Akt1 and Akt2 have been shown to promote phosphorylation of POSH in the Rac-binding domain preventing Rac association and subsequent activation of JNK [26]. Inactivation of PTEN and, subsequent activation of PI3K and Akt, promotes axon growth and facilitates regeneration after injury in retinal ganglion cells [27, 28]. Collectively, these studies raise the hypothesis that Akt may regulate the POSH complex by promoting disassembly. Therefore, the stimulation of Akt activity may promote axon regeneration on multiple levels: (1) directly regulating the POSH complex and (2) through its role in other growth-promoting pathways.

5.4 The role of POSH as an E3 ubiquitin ligase

POSH contains six domains promoting protein-protein interaction: a RING domain, 4-SH3 domains, and an activated Rac binding domain. Truncation mutations in POSH removing the RING domain and the 3rd and 4th SH3 domain reveal that these domains are crucial for mediating axon length regulation [12]. Consistent with this, Shroom3 associates with POSH through the 3rd SH3. The

necessity of the RING domain is interesting. The RING domain gives POSH a function as an E3 ligase. E3 ligases promote ubiquitination by bringing E2 ubiquitin conjugating enzymes in contact with substrates [29]. Ubiquitination results in the formation of an isopeptide bond between ubiquitin's C-terminal glycine residue (G76) with a lysine residue on the target protein [30]. Ubiquitin can form poly-ubiquitin chains with diverse structures through G76-K linkages with one of seven lysine residues present in ubiquitin. K48 linkages have been typically associated with targeting substrates for degradation by the proteasome, while K63 linkages regulate protein-protein interactions, kinase activation, and protein trafficking[31]. In other biological systems, there is evidence that POSH is able to mediate ubiquitination of substrates, using both K48 and K63 linked ubiquitination [14, 17, 19, 20]. K63 ubiquitination of the protein Herp causes a change in localization from the *trans* Golgi network to the endoplasmic reticulum[20]. Collectively, these studies, together with our finding that the RING domain of POSH is required for regulating axon outgrowth, support the hypothesis that ubiquitination events are playing a role in MAI growth inhibition.

There is no precedent in the literature for ubiquitination events regulating the current known POSH complex members supporting axon outgrowth inhibition, Shroom3, ROCK, or LZK. Performing in vitro ubiquitination experiments in the presence of POSH would address their potential for ubiquitination. However, a more biologically relevant question is whether MAI stimulation promotes K63 or K48 ubiquitination on POSH complex members. POSH-mediated ubiquitination may facilitate protein-protein interactions or target a substrate for proteosomal degradation to inhibit axon length.

Recently, it has been shown that upon MAG stimulation, PirB and Shp2 along with p75 bind to the tropomyosin receptor kinase B (TrkB) receptor and promote the dephosphorylation of TrkB after activation by BDNF stimulation. This study proposes a model where growth inhibition by MAG is due, in part, to the inactivation of growth-promoting pathways. It is unknown whether Nogo66 also induces association with and dephosphorylation of TrkB. However, TrkB receptors have been shown to be regulated by ubiquitination and the E3 ligase

responsible for TrkB ubiquitination has yet to be identified. The E3 ligase activity of POSH is required for the negative regulation of axon outgrowth, and therefore it raises the hypothesis that POSH could be facilitating ubiquitination of TrkB following activation by NogoA-PirB [12]. It would be interesting if inhibitory cues were regulating TrkB on multiple levels, dephosphorylation and ubiquitination, and further studies will need to be performed to investigate this hypothesis.

5.5 Shp2 and ROCK function downstream of MAIs

Our results suggest that Nogo66 activation of CGNs results in an enhanced Shp2 trapping of multiple tyrosine phosphorylated proteins (Chapter 3, Figure 3.2). The identity of these proteins has yet to be determined, although as stated above Shp2 is linked to TrkB regulation, therefore TrkB is likely to be trapped by Shp2 in response to MAIs. Additionally, Shp2 also dephosphorylates ROCK, providing another link from Shp2 to the POSH complex. In a myeloid leukemia cell line, ROCKII is negatively regulated by tyrosine phosphorylation to promote cell adhesion. Shp2 dephosphorylates ROCKII, promoting its activation, and the deadhesion of cells [32]. Further, ROCK has previously been linked to MAI signaling as the ROCK antagonist, Y-27632, can promote neurite growth on MAI substrates in vitro and enhanced regeneration in rats subjected to corticospinal tract transection [33-35]. Additionally, our studies show that the association of ROCK and Shroom3 is crucial for axon length regulation. Collectively, these studies raise the hypothesis that Shp2 dephosphorylation of ROCK may be regulating its activity or association into the POSH-Shroom3 complex downstream of MAI activation.

Investigation into the molecular mechanism of ROCK signaling downstream of MAIs revealed that upon NogoA stimulation ROCK translocates to the cellular membrane and phosphorylation of myosin light chain is enhanced [36]. As stated previously, phosphorylation of MLC regulates myosin II function by promoting its interaction with actin, thereby activating myosin ATPase and enhancing cell contractility [37-39]. Additionally, ROCK can regulate actin

dynamics and microtubule stability through activation of LIM kinases and collapsing response mediator protein-2 (CRMP2), a neuronal protein that is involved in growth cone collapse [40, 41]. Therefore, it will be interesting to determine if association with POSH and Shroom3 promote ROCK's activity on these substrates. Shroom3 associates with F-actin through its ASD1 domain and regulates myosin II function through its ASD2 domain [24, 42]. Thus, it is possible that Shroom3 may act as a scaffold protein tethering together the actin-myosin cytoskeleton with ROCK to promote efficient MAI signaling.

Lastly, ROCK and RhoA, the upstream activator of ROCK, have been implicated in multiple inhibitory pathways such as chondroitin sulfate proteoglycans, semaphorin, ephrin, and repulsive guidance molecule (RGMa) [33, 34, 36, 43-45]. These findings highlight the complexity and redundancy of signaling molecules downstream of inhibitory cues. Thus, regulation or blocking unique protein-protein interactions, distinct for each signaling pathway, such as scaffold proteins, may provide more selective regeneration in the CNS.

5.6 The role of Shp2 in POSH dependent MAI-mediated growth inhibition

In these studies, we show that the phosphatase activity of Shp2 is required to regulate axonal outgrowth and mediate inhibitory signals from Nogo66 downstream of the receptor PirB (Chapter 3, Figure 3.1). Ectopic expression of Shp2 is not able to suppress the POSH and LZK RNAi phenotype, suggesting that Shp2 is upstream of the POSH complex or it is regulating a protein at the same level as the complex (Figure 3.1). Collectively, these results indicated that Shp2 may be dephosphorylating a member of the POSH complex to inhibit axon outgrowth. Consistent with this hypothesis, we found that LZK is trapped by Shp2 and Nogo66 stimulation promotes this association (Chapter 3, Figure 3.2).

LZK is a member of the mixed-lineage kinase family whose activity is facilitated by dimerization and association with POSH. To our knowledge, regulation of LZK activity by phosphorylation has not been shown and these results raised several hypotheses as to the effect of phosphorylation events on

LZK in axon outgrowth regulation. Phosphorylation of LZK may be preventing dimer formation and thereby impeding its activation. Additionally, phosphorylation may prevent LZK association with POSH, preventing an active POSH signaling module. Therefore, our proposed model is that NogoA activation of the receptor PirB facilitates Shp2 phosphatase activity on LZK allowing correct formation of the POSH complex and/or promotes LZK kinase activity to mediate axon growth inhibition. This hypothesis also supports a secondary theory that growth-promoting pathways induce phosphorylation of LZK, thereby negatively regulating the function of LZK as an inhibitor of axon length.

5.7 The DLK conundrum

Our studies suggest a role for DLK as a negative regulator of axon length and a mediator of NogoA growth inhibition (Chapter 3, Figure 3.4B). However, only LZK is trapped by Shp2 and signals downstream from PirB (Chapter 3, Figure 7). One hypothesis for this distinction between the kinases is that Shp2 regulation is promoting the selection of LZK rather than DLK to relay Nogo66 signaling through PirB. Elucidation of the mechanisms promoting phosphorylation events of LZK may provide insight into the differences between the kinases. Another possibility is that DLK is relaying MAI signaling through another receptor, such as NgR1.

5.8 Promoting regeneration through POSH complex inhibition

In these studies, we have shown that the POSH complex is downstream of NogoA, MAG, and PirB-mediated growth inhibition (Chapter 3, Figure 3.8). Thus, we hypothesized that small molecule inhibitors of the POSH complex formation would circumvent NogoA or MAG-mediated growth inhibition to promote regeneration of the injured CNS. To begin to address this hypothesis we performed a high-throughput screen to identify chemical inhibitors of the Shroom3-ROCK interaction. We have identified 36 potentially active molecules

and will test these molecules in primary neuronal cells for their ability to promote growth over NogoA or MAG (Chapter 4, Figure 4.7A). Due to POSH promoting the formation of a multi-protein complex, there are additional protein-protein interactions that could be tested. Inhibiting the direct association of Shroom3 and POSH was decided against due to the binding occurring through an SH3 domain, which may be of low affinity and contain a large, flat binding surface which may be difficult to inhibit with small molecules. However, blocking LZK function may be an ideal target for inhibition. Our laboratory has shown its kinase activity and association with POSH is required for process length and MAI growth inhibition (Chapter 2, Figures 2.1 and 2.7 and [15]). Thus, chemical inhibitors which block the ability of LZK to dimerize and subsequently activate or associate with POSH could be valuable tools to investigate growth inhibition mediated by the POSH complex.

Extrinsic inhibitory proteins are only one factor limiting regeneration of the CNS, as a lack of intrinsic growth-promoting factors and a robust immunological response after injury also impedes CNS recovery [11, 46, 47]. Chondroitin sulfate proteoglycans (CSPGs) are basally present and upregulated by astrocytes after CNS damage and are both membrane bound and secreted into the extracellular space [48-50]. CSPGs can be cleaved with the bacterial enzyme Chondroitinase ABC and administering this enzyme promotes growth in the presence of CSPGs in cell culture and enhances functional recovery after spinal cord injury [51, 52]. Therefore, using a combination of chemical inhibitors which target MAI signaling and block CSPG function may be more efficacious. Additionally, chemicals that promote intrinsic growth, such as inhibitors of PTEN to promote mTOR activation, might also be beneficial in combination with MAIs [27, 53, 54]. As we continue to characterize the adult mammalian CNS, new and enhanced strategies for treatment after injury or disease can be developed and tested.

5.9 Concluding remarks

In the past thirty years, there has been an explosion in our understanding of brain plasticity. The canonical model of the CNS as a stable and static structure has been modified to one that is more dynamic, but yet more controlled when compared directly to the developing CNS. It is now acknowledged that to robustly regenerate the injured CNS a combinatorial strategy will need to be employed to target extrinsic inhibitory molecules and enhance intrinsic growth properties of neurons. Additionally, a goal of therapeutics for CNS injury is to promote the correct amount of regeneration without disrupting the connectivity of uninjured brain regions. Towards this aim, this dissertation has identified the POSH complex as a novel target for therapeutics downstream of MAIs. By selectively inhibiting the POSH complex, axon outgrowth in the CNS may be promoted without disrupting other inhibitory signaling pathways, such as those required for maintaining uninjured neuronal connections, suggesting that fully characterizing inhibitory signaling pathways in the intact CNS is important for effective drug and therapeutic design.

5.10 References

1. Giger, R.J., et al., Mechanisms of CNS myelin inhibition: Evidence for distinct and neuronal cell type specific receptor systems. Restorative Neurology and Neuroscience, 2008. 26(2-3): p. 97-115.
2. Atwal, J.K., et al., PirB is a Functional Receptor for Myelin Inhibitors of Axonal Regeneration. Science, 2008. 322(5903): p. 967-970.
3. Domeniconi, M., et al., Myelin-associated glycoprotein interacts with the Nogo66 receptor to inhibit neurite outgrowth. Neuron, 2002. 35(2): p. 283-290.
4. Fournier, A.E., T. GrandPre, and S.M. Strittmatter, Identification of a receptor mediating Nogo-66 inhibition of axonal regeneration. Nature, 2001. 409(6818): p. 341-346.
5. Wang, K.C., et al., Oligodendrocyte-myelin glycoprotein is a Nogo receptor ligand that inhibits neurite outgrowth. Nature, 2002. 417(6892): p. 941-944.
6. Venkatesh, K., et al., The Nogo-66 receptor homolog NgR2 is a sialic acid-dependent receptor selective for myelin-associated glycoprotein. Journal of Neuroscience, 2005. 25(4): p. 808-822.
7. Mi, S., et al., LINGO-1 is a component of the Nogo-66 receptor/p75 signaling complex. Nature Neuroscience, 2004. 7(3): p. 221-228.
8. Park, J.B., et al., A TNF receptor family member, TROY, is a coreceptor with Nogo receptor in mediating the inhibitory activity of myelin inhibitors. Neuron, 2005. 45(3): p. 345-351.
9. Wang, K.C., et al., p75 interacts with the Nogo receptor as a co-receptor for Nogo, MAG and OMgp. Nature, 2002. 420(6911): p. 74-78.
10. Fujita, Y., et al., The p75 receptor mediates axon growth inhibition through an association with PIR-B. Cell Death & Disease, 2011. 2.
11. Giger, R.J., E.R. Hollis, and M.H. Tuszynski, Guidance Molecules in Axon Regeneration. Cold Spring Harbor Perspectives in Biology, 2010. 2(7).
12. Taylor, J., et al., The scaffold protein POSH regulates axon outgrowth. Mol Biol Cell, 2008. 19(12): p. 5181-92.
13. Tapon, N., et al., A new Rac target POSH is an SHS-containing scaffold protein involved in the JNK and NF-kappa B signalling pathways. Embo Journal, 1998. 17(5): p. 1395-1404.
14. Alroy, I., et al., The trans-Golgi network-associated human ubiquitin-protein ligase POSH is essential for HIV Woe 1 production. Proceedings of the National Academy of Sciences of the United States of America, 2005. 102(5): p. 1478-1483.
15. Dickson, H.M., et al., POSH is an intracellular signal transducer for the axon outgrowth inhibitor Nogo66. J Neurosci, 2010. 30(40): p. 13319-25.
16. Kim, G.H., E. Park, and J.K. Han, The assembly of POSH-JNK regulates Xenopus anterior neural development. Developmental Biology, 2005. 286(1): p. 256-269.
17. Kim, G.H., et al., Novel function of POSH, a JNK scaffold, as an E3 ubiquitin ligase for the Hrs stability on early endosornes. Cellular Signalling, 2006. 18(4): p. 553-563.
18. Schnorr, J.D., et al., Ras1 interacts with multiple new signaling and cytoskeletal loci in Drosophila eggshell patterning and morphogenesis. Genetics, 2001. 159(2): p. 609-622.

19. Tsuda, M., et al., The RING-finger scaffold protein Plenty of SH3s targets TAK1 to control immunity signalling in Drosophila. Embo Reports, 2005. 6(11): p. 1082-1087.
20. Tuvia, S., et al., The ubiquitin E3 ligase POSH regulates calcium homeostasis through spatial control of Herp. Journal of Cell Biology, 2007. 177(1): p. 51-61.
21. Good, M.C., J.G. Zalatan, and W.A. Lim, Scaffold Proteins: Hubs for Controlling the Flow of Cellular Information. Science, 2011. 332(6030): p. 680-686.
22. Kukekov, N.V., Z. Xu, and L.A. Greene, Direct Interaction of the Molecular Scaffolds POSH and JIP Is Required for Apoptotic Activation of JNKs. Journal of Biological Chemistry, 2006. 281(22): p. 15517-15524.
23. Huber, A.B., et al., Signaling at the growth cone: Ligand-receptor complexes and the control of axon growth and guidance. Annual Review of Neuroscience, 2003. 26: p. 509-563.
24. Nishimura, T. and M. Takeichi, Shroom3-mediated recruitment of Rho kinases to the apical cell junctions regulates epithelial and neuroepithelial planar remodeling. Development, 2008. 135(8): p. 1493-1502.
25. Figueroa, C., et al., Akt2 negatively regulates assembly of the POSH-MLK-JNK signaling complex. Journal of Biological Chemistry, 2003. 278(48): p. 47922-47927.
26. Lyons, T.R., et al., Regulation of the pro-apoptotic scaffolding protein POSH by Akt. Journal of Biological Chemistry, 2007. 282(30): p. 21987-21997.
27. Park, K.K., et al., Promoting Axon Regeneration in the Adult CNS by Modulation of the PTEN/mTOR Pathway. Science, 2008. 322(5903): p. 963-966.
28. Song, G., G.L. Ouyang, and S.D. Bao, The activation of Akt/PKB signaling pathway and cell survival. Journal of Cellular and Molecular Medicine, 2005. 9(1): p. 59-71.
29. Joazeiro, C.A.P. and A.M. Weissman, RING finger proteins: Mediators of ubiquitin ligase activity. Cell, 2000. 102(5): p. 549-552.
30. Kerscher, O., R. Felberbaum, and M. Hochstrasser, Modification of proteins by ubiquitin and ubiquitin-like proteins, in Annual Review of Cell and Developmental Biology. 2006. p. 159-180.
31. Pickart, C.M. and D. Fushman, Polyubiquitin chains: polymeric protein signals. Current Opinion in Chemical Biology, 2004. 8(6): p. 610-616.
32. Lee, H.H. and Z.F. Chang, Regulation of RhoA-dependent ROCKII activation by Shp2. Journal of Cell Biology, 2008. 181(6): p. 999-1012.
33. Dergham, P., et al., Rho signaling pathway targeted to promote spinal cord repair. Journal of Neuroscience, 2002. 22(15): p. 6570-6577.
34. Fournier, A.E., B.T. Takizawa, and S.M. Strittmatter, Rho kinase inhibition enhances axonal regeneration in the injured CNS. Journal of Neuroscience, 2003. 23(4): p. 1416-1423.
35. Niederost, B., et al., Nogo-A and myelin-associated glycoprotein mediate neurite growth inhibition by antagonistic regulation of RhoA and Rac1. Journal of Neuroscience, 2002. 22(23): p. 10368-10376.
36. Alabed, Y.Z., et al., Neuronal responses to myelin are mediated by rho kinase. Journal of Neurochemistry, 2006. 96(6): p. 1616-1625.
37. Amano, M., et al., Myosin II activation promotes neurite retraction during the action of Rho and Rho-kinase. Genes to Cells, 1998. 3(3): p. 177-188.
38. Amano, M., et al., Phosphorylation and activation of myosin by Rho-associated kinase (Rho-kinase). Journal of Biological Chemistry, 1996. 271(34): p. 20246-20249.

39. Chihara, K., et al., Cytoskeletal rearrangements and transcriptional activation of c-fos serum response element by Rho-kinase. Journal of Biological Chemistry, 1997. 272(40): p. 25121-25127.
40. Arimura, N., et al., Phosphorylation of collapsin response mediator protein-2 by Rho-kinase - Evidence for two separate signaling pathways for growth cone collapse. Journal of Biological Chemistry, 2000. 275(31): p. 23973-23980.
41. Goshima, Y., et al., COLLAPSIN-INDUCED GROWTH CONE COLLAPSE MEDIATED BY AN INTRACELLULAR PROTEIN RELATED TO UNC-33. Nature, 1995. 376(6540): p. 509-514.
42. Yoder, M., et al., The Shroom Family of Actin-binding Proteins as Evolutionarily Conserved Determinants of Cellular Architecture and Epithelial Morphogenesis. Mol Biol Cell, 2006. 17.
43. Bito, H., et al., A critical role for a Rho-associated kinase, p160ROCK, in determining axon outgrowth in mammalian CNS neurons. Neuron, 2000. 26(2): p. 431-441.
44. Lingor, P., et al., Inhibition of Rho kinase (ROCK) increases neurite outgrowth on chondroitin sulphate proteoglycan in vitro and axonal regeneration in the adult optic nerve in vivo. Journal of Neurochemistry, 2007. 103(1): p. 181-189.
45. Gallo, G. and P.C. Letourneau, Regulation of growth cone actin filaments by guidance cues. Journal of Neurobiology, 2004. 58(1): p. 92-102.
46. Benowitz, L.I. and S.T. Carmichael, Promoting axonal rewiring to improve outcome after stroke. Neurobiology of Disease, 2010. 37(2): p. 259-266.
47. Carmichael, S.T., Translating the frontiers of brain repair to treatments: Starting not to break the rules. Neurobiology of Disease, 2010. 37(2): p. 237-242.
48. Jones, L.L., D. Sajed, and M.H. Tuszynski, Axonal regeneration through regions of chondroitin sulfate proteoglycan deposition after spinal cord injury: A balance of permissiveness and inhibition. Journal of Neuroscience, 2003. 23(28): p. 9276-9288.
49. Jones, L.L., et al., NG2 is a major chondroitin sulfate proteoglycan produced after spinal cord injury and is expressed by macrophages and oligodendrocyte progenitors. Journal of Neuroscience, 2002. 22(7): p. 2792-2803.
50. Morgenstern, D.A., R.A. Asher, and J.W. Fawcett, Chondroitin sulphate proteoglycans in the CNS injury response, in Spinal Cord Trauma: Regeneration, Neural Repair and Functional Recovery, L. McKerracher, G. Doucet, and S. Rossignol, Editors. 2002, Elsevier Science Bv: Amsterdam. p. 313-332.
51. Garcia-Alias, G., et al., Chondroitinase ABC treatment opens a window of opportunity for task-specific rehabilitation. Nature Neuroscience, 2009. 12(9): p. 1145-U16.
52. McKeon, R.J., A. Hoke, and J. Silver, INJURY-INDUCED PROTEOGLYCANS INHIBIT THE POTENTIAL FOR LAMININ-MEDIATED AXON GROWTH ON ASTROCYTIC SCARS. Experimental Neurology, 1995. 136(1): p. 32-43.
53. McKerracher, L., et al., IDENTIFICATION OF MYELIN-ASSOCIATED GLYCOPROTEIN AS A MAJOR MYELIN-DERIVED INHIBITOR OF NEURITE GROWTH. Neuron, 1994. 13(4): p. 805-811.
54. Park, K.K., et al., PTEN/mTOR and axon regeneration. Experimental Neurology, 2010. 223(1): p. 45-50.